NUREG/IA-0415

International Agreement Report

TRACE (V 5.0 Patch 2) Validation Based on the RELAP5-Calculation of FIX-III LOCA Experiments NO. 5052, 4011, 3051

Prepared by:
S. ChunHong Sheng

Studsvik Nuclear AB
SE-61182 Nyköping Sweden

K. Tien, NRC Project Manager

Division of Systems Analysis
Office of Nuclear Regulatory Research
U.S. Nuclear Regulatory Commission
Washington, DC 20555-0001

Manuscript Completed: February 2013
Date Published: October 2014

Prepared as part of
The Agreement on Research Participation and Technical Exchange
Under the Thermal-Hydraulic Code Applications and Maintenance Program (CAMP)

Published by
U.S. Nuclear Regulatory Commission

AVAILABILITY OF REFERENCE MATERIALS IN NRC PUBLICATIONS

NRC Reference Material

As of November 1999, you may electronically access NUREG-series publications and other NRC records at NRC's Public Electronic Reading Room at http://www.nrc.gov/reading-rm.html. Publicly released records include, to name a few, NUREG-series publications; *Federal Register* notices; applicant, licensee, and vendor documents and correspondence; NRC correspondence and internal memoranda; bulletins and information notices; inspection and investigative reports; licensee event reports; and Commission papers and their attachments.

NRC publications in the NUREG series, NRC regulations, and Title 10, "Energy," in the *Code of Federal Regulations* may also be purchased from one of these two sources.

1. The Superintendent of Documents
   U.S. Government Printing Office
   Mail Stop SSOP
   Washington, DC 20402–0001
   Internet: bookstore.gpo.gov
   Telephone: 202-512-1800
   Fax: 202-512-2250
2. The National Technical Information Service
   Springfield, VA 22161–0002
   www.ntis.gov
   1–800–553–6847 or, locally, 703–605–6000

A single copy of each NRC draft report for comment is available free, to the extent of supply, upon written request as follows:

Address: U.S. Nuclear Regulatory Commission
Office of Administration
Publications Branch
Washington, DC 20555-0001
E-mail: DISTRIBUTION.RESOURCE@NRC.GOV
Facsimile: 301–415–2289

Some publications in the NUREG series that are posted at NRC's Web site address http://www.nrc.gov/reading-rm/doc-collections/nuregs are updated periodically and may differ from the last printed version. Although references to material found on a Web site bear the date the material was accessed, the material available on the date cited may subsequently be removed from the site.

Non-NRC Reference Material

Documents available from public and special technical libraries include all open literature items, such as books, journal articles, transactions, *Federal Register* notices, Federal and State legislation, and congressional reports. Such documents as theses, dissertations, foreign reports and translations, and non-NRC conference proceedings may be purchased from their sponsoring organization.

Copies of industry codes and standards used in a substantive manner in the NRC regulatory process are maintained at—

The NRC Technical Library
Two White Flint North
11545 Rockville Pike
Rockville, MD 20852–2738

These standards are available in the library for reference use by the public. Codes and standards are usually copyrighted and may be purchased from the originating organization or, if they are American National Standards, from—

American National Standards Institute
11 West 42nd Street
New York, NY 10036–8002
www.ansi.org
212–642–4900

Legally binding regulatory requirements are stated only in laws; NRC regulations; licenses, including technical specifications; or orders, not in NUREG-series publications. The views expressed in contractor-prepared publications in this series are not necessarily those of the NRC.

The NUREG series comprises (1) technical and administrative reports and books prepared by the staff (NUREG-XXXX) or agency contractors (NUREG/CR-XXXX), (2) proceedings of conferences (NUREG/CP-XXXX), (3) reports resulting from international agreements (NUREG/IA-XXXX), (4) brochures (NUREG/BR-XXXX), and (5) compilations of legal decisions and orders of the Commission and Atomic and Safety Licensing Boards and of Directors' decisions under Section 2.206 of NRC's regulations (NUREG-0750).

NUREG/IA-0415

International Agreement Report

TRACE (V 5.0 Patch 2) Validation Based on the RELAP5-Calculation of FIX-III LOCA Experiments NO. 5052, 4011, 3051

Prepared by:
S. ChunHong Sheng

Studsvik Nuclear AB
SE-61182 Nyköping Sweden

K. Tien, NRC Project Manager

Division of Systems Analysis
Office of Nuclear Regulatory Research
U.S. Nuclear Regulatory Commission
Washington, DC 20555-0001

Manuscript Completed: February 2013
Date Published: October 2014

Prepared as part of
The Agreement on Research Participation and Technical Exchange
Under the Thermal-Hydraulic Code Applications and Maintenance Program (CAMP)

Published by
U.S. Nuclear Regulatory Commission

ABSTRACT

The purpose of this project is to (i) evaluate the functionality of the SNAP capability to convert RELAP5 input files to corresponding TRACE input, and (ii) to validate the TRACE code against selected FIX-II experiments where the blowdown phase of large and small break LOCA is the main focus.

More specifically, the TRACE Version 5.0 Patch 2 code is validated against the FIX-II experiments, where the input is obtained by converting a legacy RELAP5 FIX-II model by means of SNAP, possibly accompanied by additional manual adjustments. All FIX-II components in the RELAP5 model are retained after being converted to TRACE. Three transients (FIX 5052, 4011 and 3051) are analyzed. The TRACE analysis results are compared with experimental data and with previously obtained results from analyses made with the RELAP5/MOD3.3 Patch 03 model.

This work has been performed with financial support from the Swedish Radiation Safety Authority.

TABLE OF CONTENTS

LIST OF FIGURES

Page

LIST OF TABLES

Page

EXECUTIVE SUMMARY

The SSM and the USNRC have an agreement (SSM 2008/158) regarding participation and work effort within the Code Applications and Maintenance Program (CAMP). The agreement grants Sweden the access to thermal-hydraulic and neutronics codes developed within CAMP, such as the RELAP5- and TRACE-codes, but also requires Sweden to contribute to CAMP with code calculations and assessments.

Within the current project, the TRACE thermal hydraulic system code, Version 5.0 Patch 2, is validated against some FIX-II experiments, where the associated FIX-II input is obtained by converting previously used legacy RELAP5 FIX-II models by means of the SNAP utility. The TRACE analysis results are compared with the corresponding experimental data but also with the results from the used RELAP5/MOD3.3 Patch 03 model.

The BWR integral test program FIX-II was performed at Studsvik during years 1979–1986, with the Swedish BWR Oskarshamn 2 as the reference reactor unit. FIX-II capability included the simulation of double ended breaks in the main recirculation pipe for a non-jet pump external recirculation loop BWR, but also simulations of split breaks and pump trip transients.

The SNAP model editor should ideally be capable to convert any RELAP5 input model into corresponding TRACE input. This functionality of SNAP however does not work to a full extent and consequently some user effort had to be spent to complete the TRACE model into an acceptable level. After the manual corrections the TRACE analyses could nevertheless be accomplished with the same boundary condition as in RELAP5.

Three FIX-II transients (5052, 4011 and 3051) were analyzed. The performed TRACE analyses revealed in general quite good comparisons with RELAP5 results and corresponding measured parameters, however, not quite as good as the RELAP5 results when it comes to the system depressurization rate and the rod PCT and dryout predictions. It was specifically noted that:

- The various differential pressures around the test facility loops were well simulated indicating an overall favorable simulation of the liquid inventory distribution. Also the loop pressure decrease as a result of the flow expelled through the break was acceptably calculated although the rate of the decrease was somewhat exaggerated especially in the TRACE analyses. This exaggeration could have been made less pronounced by more careful tuning of the break conditions, i.e. basically tuning of the discharge coefficients associated with the used break flow model but also adjustments of the loss coefficients at and close to the break location.

- For the large break LOCA tests 5052 and 4011, the TRACE analyses could predict almost as well as the RELAP5 analyses on the dryout and the flow reversal in the test section bundle, with about 50 ^{o}C lower PCT in comparison to measurements from the tests 5052 (716 ^{o}C) and 4011 (520 ^{o}C).
- For the small break LOCA test 3051, where forced steam blow down occurred, the RELAP5 model well predicted the transient sequences in which no dryout occurred in the test section bundle due to the small loss of mass through the break; while the TRACE predicted a dryout in the later period of the transient due to larger loss of mass through the break and higher void distribution in the core.

ACKNOWLEDGMENTS

The author acknowledges the financial support from the SSM.

The author is also very grateful to the OKG AB utility for providing access to the RELAP5 input for the FIX-II experiments.

Finally, the author also thanks the colleague Anders Sjöberg for his kind support and valuable guidance during the work.

ABBREVIATIONS

BWR	boiling water reactor
LOCA	loss of coolant accident
LP	lower plenum
O2	Oskarshamn 2 nuclear power plant
PLEX	plant life extension
RCL	recirculation line
SNAP	Symbolic Nuclear Analysis Package
SRV	steam relief valve
SSM	the Swedish Radiation Safety Authority
TH	thermal-hydraulic
UP	upper plenum
USNRC	the United States Nuclear Regulatory Commission

1. INTRODUCTION

The SSM and the USNRC have an agreement (SSM 2008/158) regarding participation and work effort within the Code Applications and Maintenance Program (CAMP). The CAMP comprises different activities including international partners' exchange of information on thermal-hydraulic safety issues related to nuclear reactor and plant systems, and analysis work activities within associated code development and assessments. The agreement grants Sweden the access to thermal-hydraulic and neutronics codes developed within CAMP, such as the RELAP5- and TRACE-codes, but also requires Sweden to contribute to CAMP with code calculations and assessments on a regularly basis.

Within the current project, the TRACE thermal hydraulic system code, Version 5.0 Patch 2, is validated against some FIX-II experiments, where the associated FIX-II input is obtained by converting previously used legacy RELAP5 FIX-II models by means of the SNAP utility. The TRACE analysis results are compared with the corresponding experimental data but also with the results from the used RELAP5/MOD3.3 Patch 03 model. Thus the purpose of the project is twofold: (i) to evaluate the functionality of the SNAP capability to convert RELAP5 input files to corresponding TRACE input, and (ii) to validate the TRACE code.

The extensive BWR integral test program FIX-II was performed at Studsvik during years 1979–1986, with the Swedish BWR Oskarshamn 2 as the reference reactor unit. FIX-II had been widely used as validation data base for e.g. the Westinghouse vendor codes BISON and GOBLIN. FIX-II is the only test program available with the capability to simulate the double ended break in the main recirculation pipe for a non-jet pump external recirculation loop BWR.

Studsvik Nuclear AB has contributed to the LOCA analyses made within the Oskarshamn 2 modernization and power uprate project PLEX. Those analyses were made with the RELAP5/MOD3.3, Patch 03, and as part of the analysis effort some validation of the RELAP5 and used input models was performed against selected FIX-II experiments.

This TRACE validation project comprises three main recirculation pipe break experiments from the FIX-II test program, which are the very same as included in the mentioned RELAP5 validation:

- Experiment 5052 is a double ended break test in the main recirculation pipe. The test facility core heating power corresponds to 2 500 MW for the real plant, which is about the power after PLEX project finalization.
- Experiment 4011 is also a double ended break test in the main recirculation pipe. The test facility core heating power corresponds to 1 800 MW for the real plant, which represents the current Oskarshamn 2 full power.

- Experiment 3051 is a 10 % (in area) split break in the main recirculation pipe, where the forced blowdown occurs at 40 s, and this will greatly influence the LOCA transient sequences. The test facility core heating power corresponds to current 1 800 MW for the real plant.

2. FACILITY AND TEST DESCRIPTION

The FIX-II project was an extensive BWR LOCA blowdown and pump trip test program carried out during the years 1979–1986. The reference nuclear power plant was the Oskarshamn 2 BWR equipped with external recirculation loops. FIX-II was carried out by Studsvik Energiteknik AB in cooperation with Asea-Atom AB, and with support from the Swedish Nuclear Power Inspectorate.

The FIX-II experiments were very well documented, and some of the experimental data are available in modern electronic form. The experiments have been widely used as validation data base for the Westinghouse vendor codes BISON and GOBLIN. The FIX-II is the only test series available related to the double ended break in the main recirculation pipe of an external circulation pump type BWR like the Oskarshamn 2 nuclear power plant.

The aim of the project was to increase the knowledge of and improve the data base for calculations of certain accident transients for Swedish BWRs. The transients studied were those which provided a reduced circulation of coolant in the reactor core, caused by a break in a main recirculation loop (LOCA) for external pump type reactors, or by a loss of power supply to the pumps (pump trip).

2.1 Test Facility

The test facility layout is shown in Figure 2-1. FIX-II was designed with a volume scaling of 1:777, relative to the reference reactor. A detail description of the FIX-II test facility is provided in [1], therefore, only some fundamental aspects of the facility are presented here.

The test facility mainly includes the following components in representing the reactor pressure vessel internals and the main recirculation pipe lines:

1 Steam condenser with internal steam separator

2 Downcomer

3 Two main recirculation pipe lines: one representing the three intact loops and the other one representing the broken loop.

4 Lower plenum

5 Rod channel (6×6 rod simulators electrically heated, 12.25 mm OD, full length 3.68 m)

6 Bypass channel with heating simulating the heat transfer from fuel assemblies

7 Upper plenum

8 Spray lines

9 Feed water line

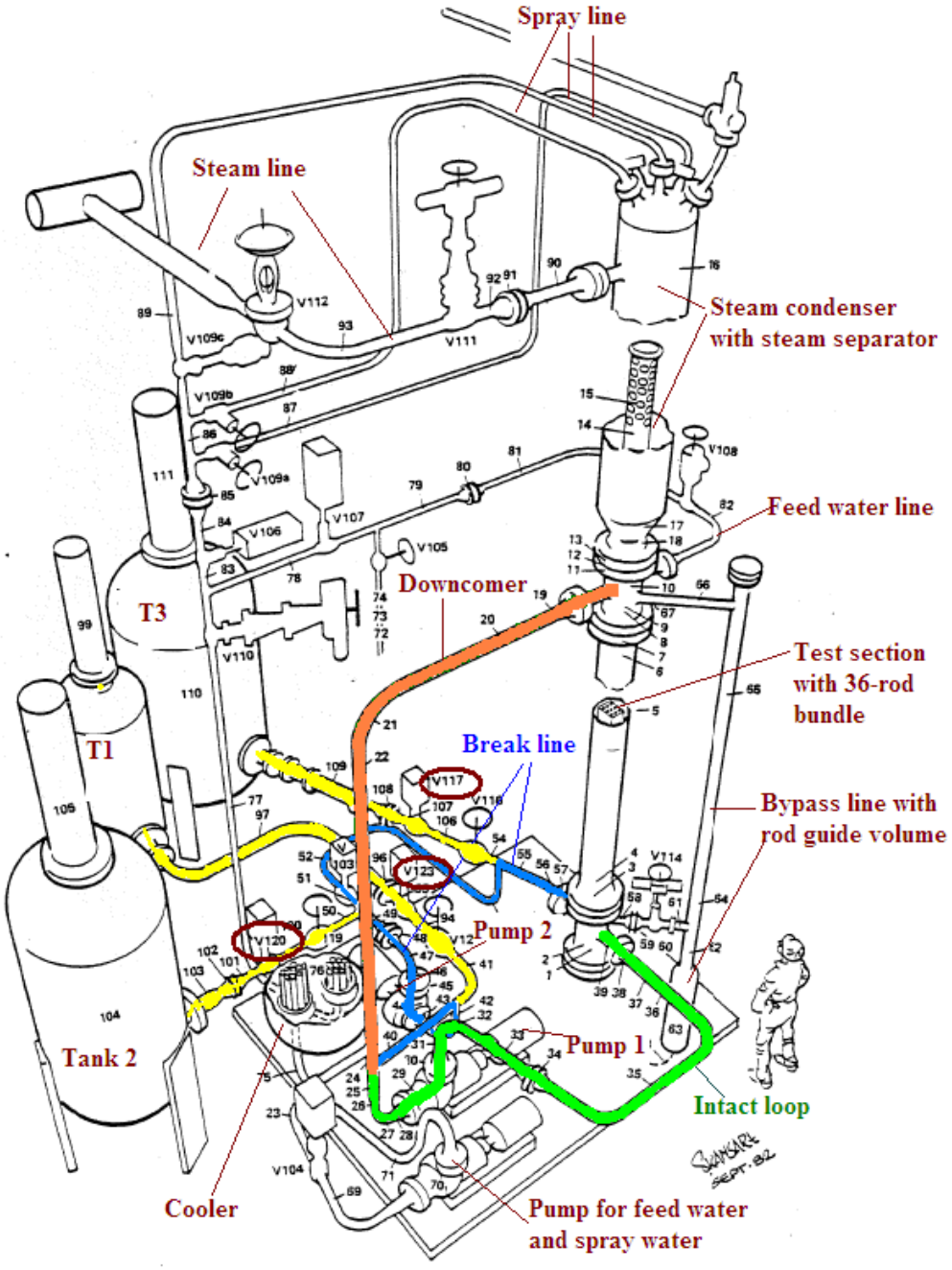

Figure 2-1. General view of the FIX-II facility.

The test section comprises a lower plenum with connections to the two recirculation lines, a middle part with the heated rod bundle, and an upper plenum (Figure 2-1). A spray condenser is placed on top of the test section. A simplified steam separator is located in the lower part of the condenser, and the upper part is used as a steam dome. The steam relief line is connected to the steam dome. During steady state operation the main steam outlet line is closed.

The external downcomer line represents the actual power plant downcomer annulus surrounding the core. An external pipe connects the downcomer and the recirculation lines. The turbine power associated condenser effects are modeled by the partial circulation of water from the downcomer through an external 6 MW cooler with feedback to three spray lines and feed water line. The flow rate in the two branches with cooled water is adjusted to control the condenser pressure, the liquid level and the core inlet subcooling. The flow through the cooler is shut off immediately after the initiation of the break.

The remaining downcomer flow representing the recirculation coolant flow splits at the lower downcomer end into two loops (both loops have its own recirculation pump):

- One loop representing three intact recirculation lines of the reference reactor.
- The other loop representing the fourth recirculation line, with break devices.

In order to simulate both the double ended break and the split break, the break recirculation line was varied by a combination of three break locations, i.e. the valves V117, V120 and V123. The size of the break is determined by the flow area in the break restriction nozzle. The break flow is discharged into the water filled tanks, designed to provide an efficient condensation of steam. Three different configurations A, B and C were used as shown in Figure 2-2.

The core channel is equipped with a full length rod bundle (3.68 m), which is closely adhered to the fuel assembly of Oskarshamn 2 in geometry. However, there are only 6×6 rod simulators (12.25 mm O.D.) instead of 8×8 rods in the typical fuel element of that time period. Figure 3-5 shows an assembly drawing of the test section. The cross section of the heated part of the bundle is shown in Figure 2-3. The 36 fuel rods were directly heated by electric current through the cladding material (Inconel 600). The cladding is filled with MgO_2 which has about the same heat capacity as the referenced reactor fuel rod. A mercury rheostat was used for power regulation; this allows simulating both the decay heat and the latent heat stored in the fuel rods.

As mentioned above FIX-II has as part of the core model an external bypass simulator. Through this bypass about 12 % of the recirculation mass flow is diverted through a control valve. This bypass is heated separately to represent the channel wall heat transfer. At the lower end of the bypass, Figure 2-1, there is a stagnant water volume to simulate the reference reactor space for the control rod guide tubes.

Since the FIX-II facility has been designed only for blowdown experiments, no emergency core cooling equipment is installed.

Data from the comprehensive data measurement acquisition system (Figure 2-4) includes:

- Pressure (PT)
- Several differential pressures (dPT) measurement points along the loop which provide information of the flow distribution during the course of the transient sequences
- Fluid temperature (TE)
- Cladding temperature (about 100 thermocouples distributed at 16 axial levels of the 36 rods)

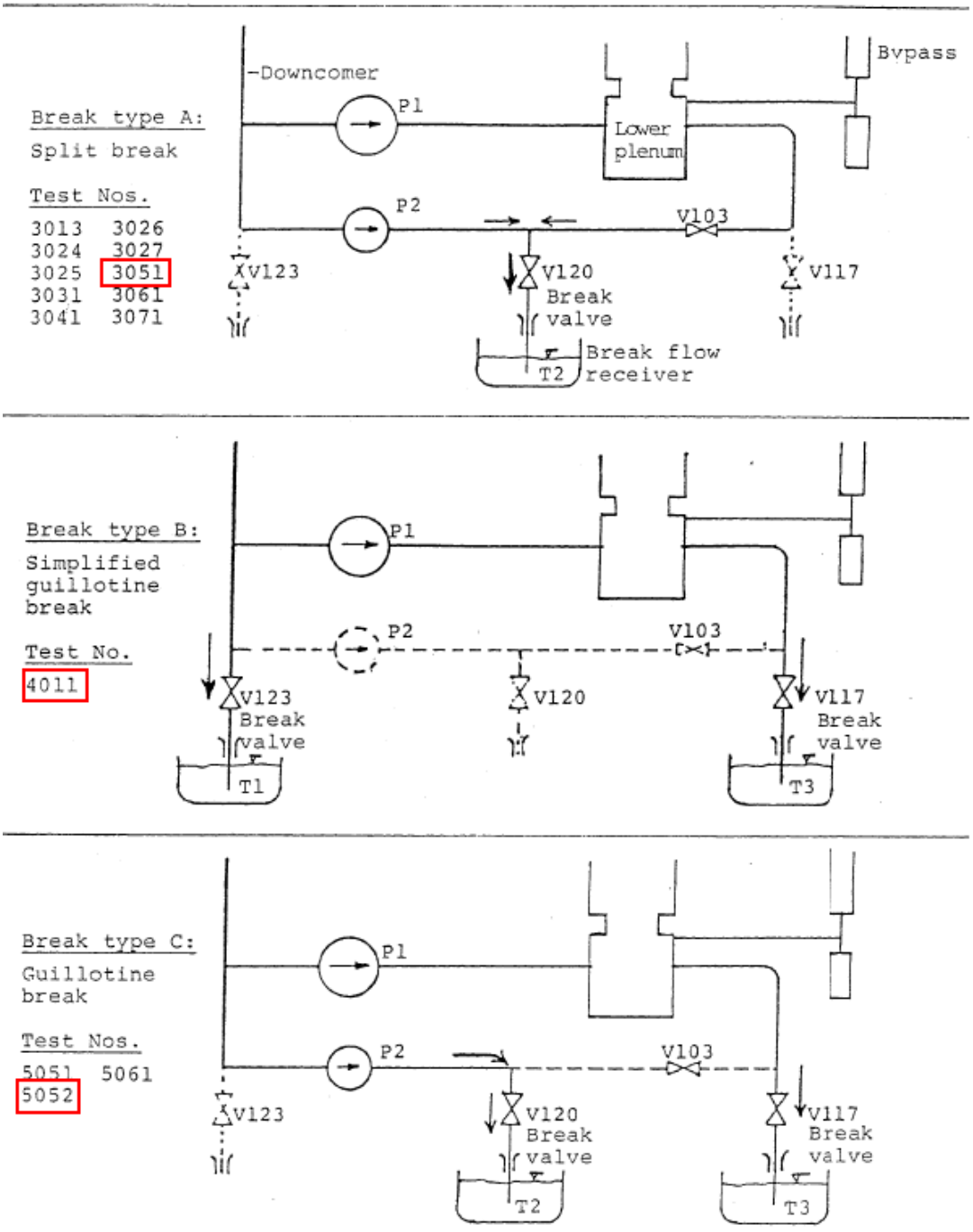

Figure 2-2. Options of break simulations in FIX-II facility.

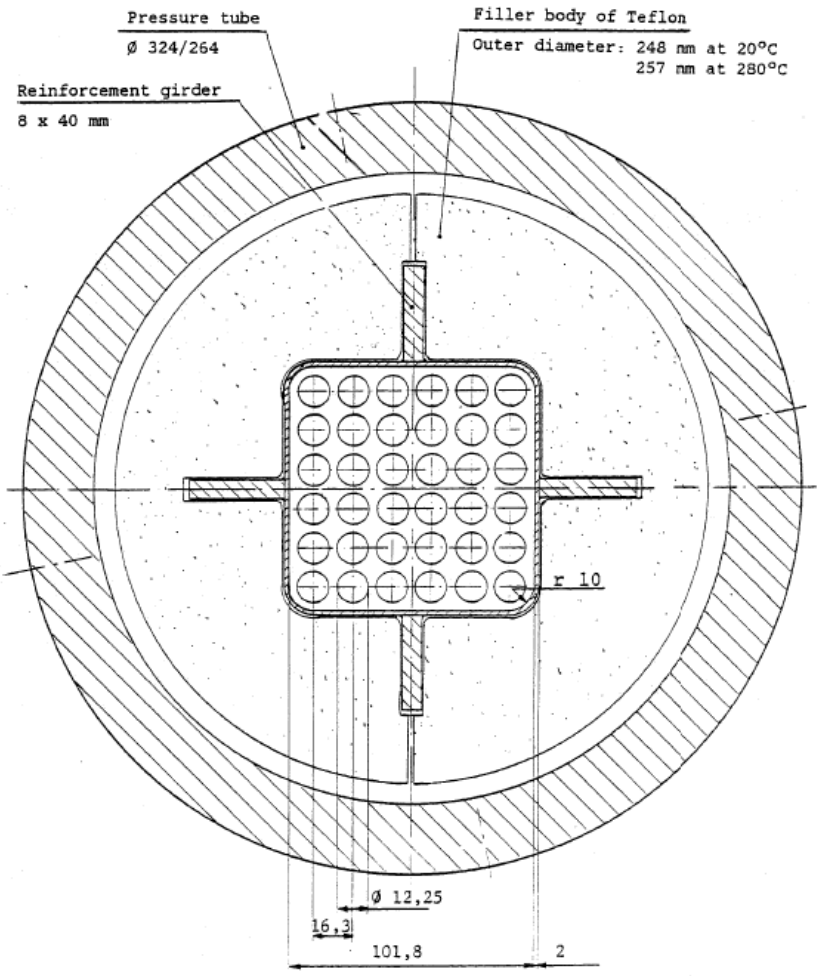

Figure 2-3. Cross section of heated part of bundle.

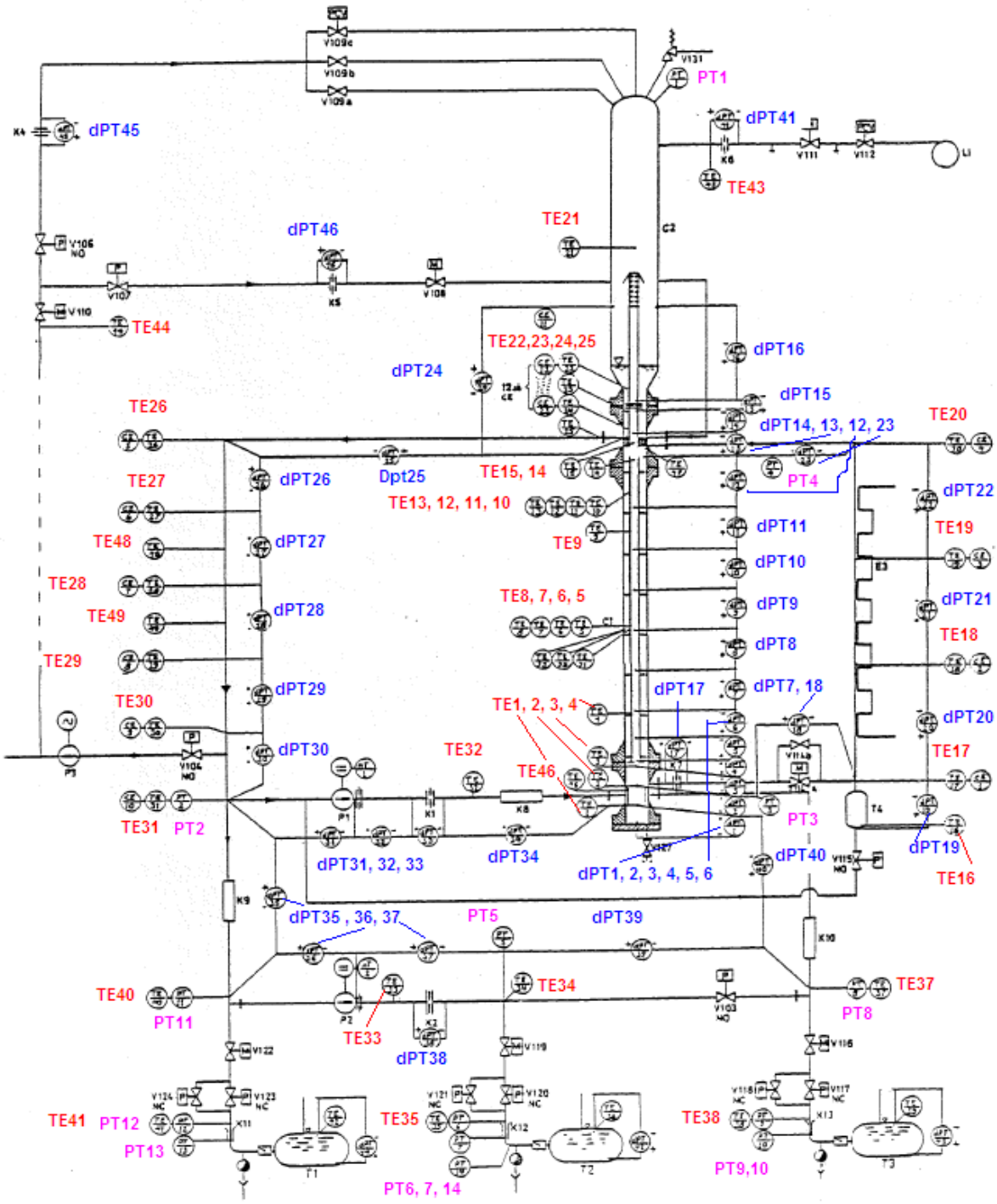

Figure 2-4. Measurement points in the circuit.

2.2 Selected Test Cases

This validation project comprises three main recirculation pipe break experiments from the FIX-II test program with break simulations according to Figure 2-2:

- Experiment 5052 is a double ended break test in the main recirculation pipe. The test heating power is corresponding to 2 500 MW core power of the real plant, which is about the power after PLEX.
- Experiment 4011 is also a double ended break test in the main recirculation pipe. The test heating power is corresponding to 1 800 MW core power of the real plant, which represents the present O2 full power.
- Experiment 3051 is a 10 % (in area) split break in the main recirculation pipe, where the forced blowdown occurs at 40 s, and this will greatly influence the LOCA transient sequences. The test heating power is corresponding to 1 800 MW core power of the real plant.

Table 2-1 provides short information about the different FIX-II experiments.

Table 2-1. The test matrix for the first FIX-II LOCA experimental period.

Break classification	Split breaks							Guillotine		
Type of simulation (see Figure 2-2)	A							B	C	
Relative break area (%)	10	31		48	100	150	200	155	200	
Break I.D. (mm)	6.8	12.0		15.0	21.6	26.4	30.5	16.0+21.6	21.6+21.6	
Initial bundle power (MW) -hot channel -average	2.35	2.35	3.35	3.35	2.35	2.35	2.35	2.35	2.35	3.35
LOCA test ident. No.	**3051**	3013	3024 3025 3026 3027	3031	3061	3071	3041	**4011**	5061	5051 **5052**

3. CODE AND MODEL DESCRIPTION

3.1 Used Code Version

The analyses of the FIX-II experiment 5052, 4011 and 3051 are performed with the TRACE code, which is available for safety analyses through the agreement between the SSM and the USNRC. The version being used is TRACE Version 5.0 Patch 2 with the associated code manual [2].

3.2 The TRACE Model

Previous RELAP5 models of FIX-II 5052, 4011 and 3051 experiments were converted to TRACE Version 5.0, Patch 2 by means of SNAP (note that the RELAP5 input model of FIX-II was developed in ASCII, i.e. without SNAP, and is described in chapter 3.3). All FIX-II components in RELAP5 are retained after converted to TRACE.

For the conversion the latest SNAP-version was used as available at the time when the project activities were pursued, i.e. the SNAP version 1.2.6 was used. Importing of the RELAP5 ASCII input file into SNAP resulted in a little bit unstructured mask as shown in Figure 3-1. The user had to spend some time in rearranging the objects, changing the "Width Scale Factor" and "Pixel per Meter" and making other changes to obtain a more clearly arranged SNAP mask (See Figure 3-2).

Ideally the SNAP model editor should be capable to convert any RELAP5 input model into corresponding TRACE input. This functionality of SNAP however does not work to a full extent and consequently some user effort was necessary to complete the model into a "runable" status. A conversion report is generated by running the "convert to TRACE" tool in SNAP and an excerpt of the report is shown in Table 3-1, in this report table corresponding components in RELAP5 and TRACE are listed. Table 3-3 shows some nodalization information.

The problems encountered during the RELAP5 to TRACE conversion are listed in Table 3-2, in which also is shown the corrective action by the code user to handle the problem and revise the model.

After the manual corrections the TRACE calculations could be run with the same boundary conditions as previous calculations with RELAP5:

- The same core and bypass power.
- The same boundary flow including spray, feed water and cooling flow.
- The same pump characteristics.

- The same trip time to activate the break flow, the steam flow, the decay power, the pump coast down, and the time to close the spray, feed water and cooling water flow.

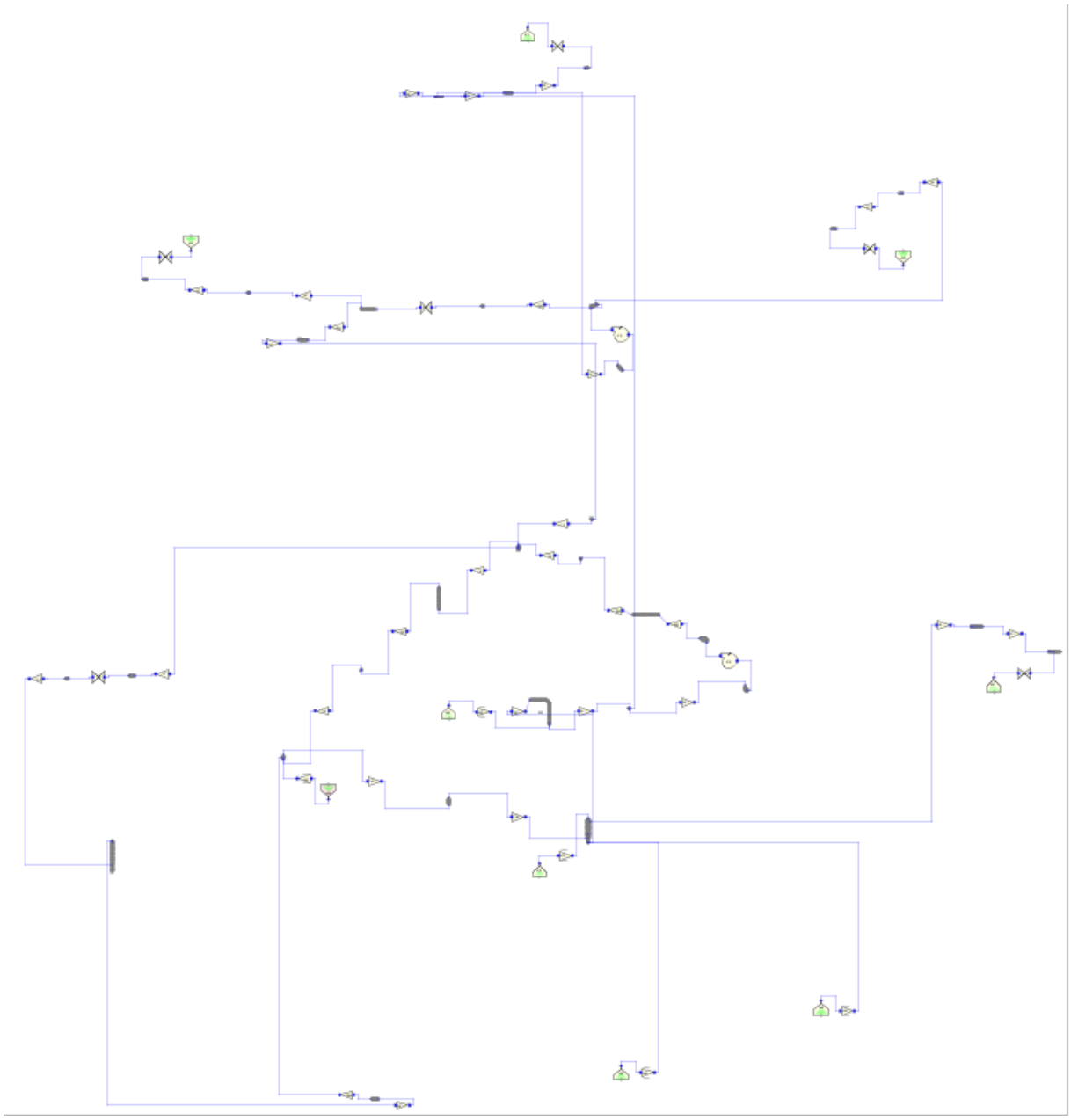

Figure 3-1. Display of SNAP Model Editor with imported RELAP5 model of FIX-II.

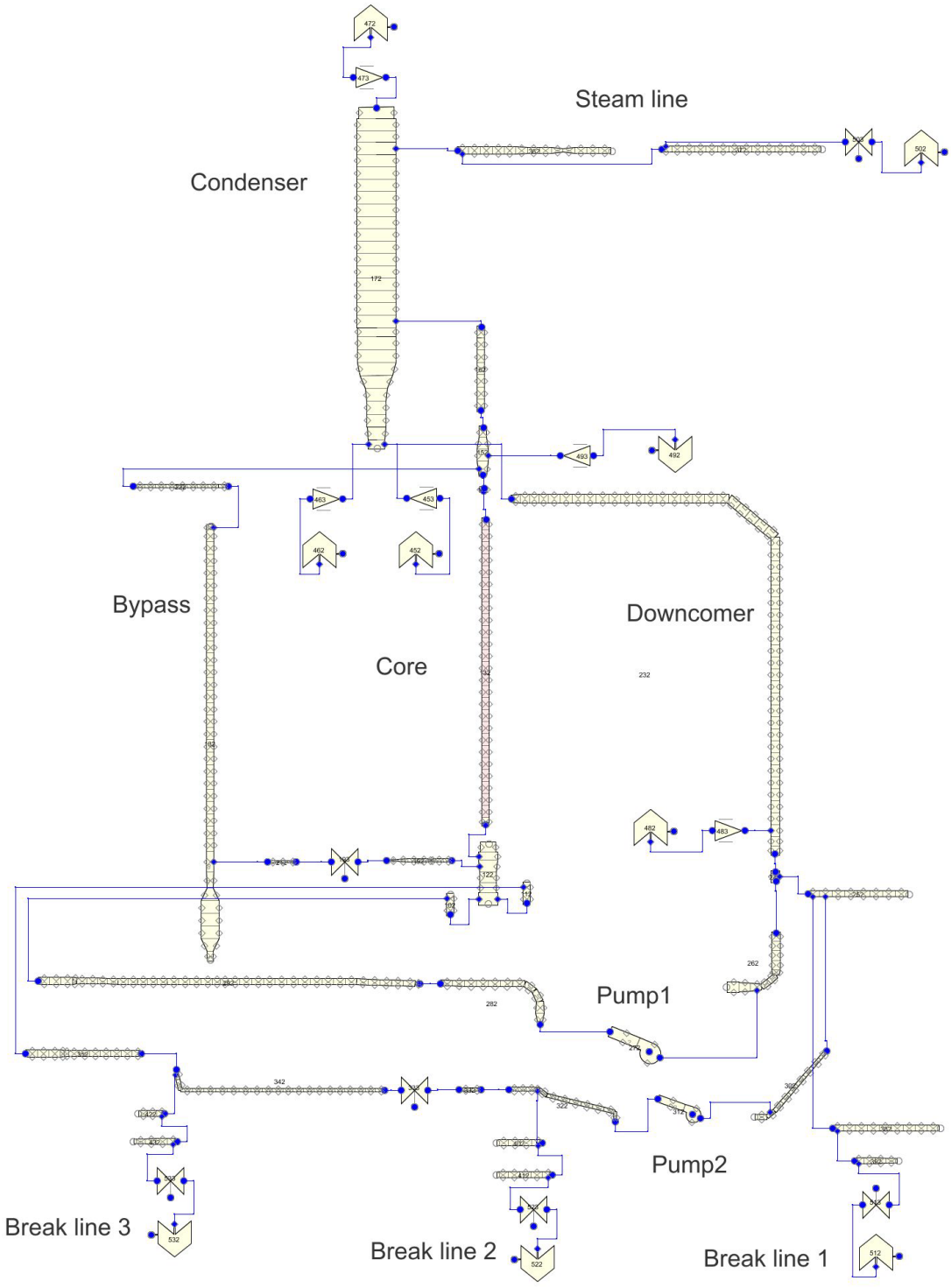

Figure 3-2. TRACE input model of FIX-II in SNAP Model Editor after rearrangement.

Table 3-1. Excerpt of conversion report from RELAP5 to TRACE.

Original RELAP5 component	Resulting TRACE component
CB 10 tripunit (ssunit)	Trip -10 (ssunit)
CB 20 sum (fd1)	Sum -20 (fd1)
CB 30 mult (ssmul1)	Multiply -30 (ssmul1)
CB 40 integral (integ1)	Integrate -40 (integ1)
CB 50 function (p1sptab)	Function -50 (p1sptab)
CB 60 mult (p1vel)	Multiply -60 (p1vel)
CB 70 sum (fd2)	Sum -70 (fd2)
CB 80 mult (ssmul2)	Multiply -80 (ssmul2)
CB 90 integral (integ2)	Integrate -90 (integ2)
CB 100 function (p2sptab)	Function -100 (p2sptab)
CB 190 mult (p2vel)	Multiply -190 (p2vel)
CB 200 function (srvtab)	Function -200 (srvtab)
CB 320 sum (bpdf)	Sum -320 (bpdf)
CB 330 mult (ssmulbp)	Multiply -330 (ssmulbp)
CB 340 integral (integbp)	Integrate -340 (integbp)
CB 500 sum (tot-pow)	Sum -500 (tot-pow)
CB 501 function (cor-pow)	Function -501 (cor-pow)
CB 502 function (bp-pow)	Function -502 (bp-pow)
CB 1181 constant (romeslin)	Constant -1181 (romeslin)
CB 1183 sum (dpcnd)	Sum -1183 (dpcnd)
CB 1184 sum (xp)	Sum -1184 (xp)
CB 1185 stdfnctn-sqrt (sqxp)	Square Root -1185 (sqxp)
CB 1186 sum (xdro)	Sum -1186 (xdro)
CB 1187 sum (nomin)	Sum -1187 (nomin)
CB 1188 div (zofcnd)	Divide -1188 (zofcnd)
CB 1189 lag (zxcnd)	First Order Lag -1189 (zxcnd)
CB 1199 sum (zcnd)	Sum -1199 (zcnd)
CB 3001 sum (p_dp0)	Sum -3001 (p_dp0)
CB 3002 sum (p_dp1)	Sum -3002 (p_dp1)
CB 3003 sum (p_dp2)	Sum -3003 (p_dp2)
CB 3004 sum (p_dp3)	Sum -3004 (p_dp3)
CB 3005 sum (p_dp4)	Sum -3005 (p_dp4)
CB 3006 sum (p_dp5)	Sum -3006 (p_dp5)
CB 3007 sum (p_dp6)	Sum -3007 (p_dp6)
CB 3008 sum (p_dp7)	Sum -3008 (p_dp7)

Table 3-1. Excerpt of conversion report…….(continued)

CB 3009 sum (p_dp8)	Sum -3009 (p_dp8)
errmax 0	Generic Signal Variable (R5:errmax) 147
systms 1	Generic Signal Variable (R5:systms) 148
time 0	Problem Time 149
timeof 501	Trip Time -3
timeof 504	Trip Time -4
General Table 1	GeneralTable 1
General Table 2	GeneralTable 2
General Table 3	GeneralTable 3
General Table 5	GeneralTable 5
General Table 201	GeneralTable 201
General Table 202	GeneralTable 202
httemp 132202505	Slab/Rod Temperature 152
httemp 132202405	Slab/Rod Temperature 153
httemp 132202305	Slab/Rod Temperature 154
httemp 132202205	Slab/Rod Temperature 155
httemp 132202105	Slab/Rod Temperature 156
httemp 132202005	Slab/Rod Temperature 157
httemp 132201905	Slab/Rod Temperature 158
Heatstructure 1021	Heat Structure 1021
Heatstructure 1022	Heat Structure 1022
Heatstructure 1121	Heat Structure 1121
Heatstructure 1122	Heat Structure 1122
Heatstructure 1221	Heat Structure 1221
Heatstructure 1222	Heat Structure 1222
Heatstructure 1223	Heat Structure 1223
Heatstructure 1224	Heat Structure 1224
Heatstructure 1225	Heat Structure 1225
Heatstructure 1226	Heat Structure 1226
Heatstructure 1227	Heat Structure 1227
Heatstructure 1228	Heat Structure 1228
Heatstructure 1321	Heat Structure 1321
Heatstructure 1322	Heat Structure 1322
	Power 11
Heatstructure 1323	Heat Structure 1323
	Power 21
Heatstructure 1324	Heat Structure 1324
	Power 31
Heatstructure 1325	Heat Structure 1325
Heatstructure 1421	Heat Structure 1421

Table 3-1. Excerpt of conversion report…..(continued)

Heatstructure 1422	Heat Structure 1422
Heatstructure 1521	Heat Structure 1521
Heatstructure 1522	Heat Structure 1522
Heatstructure 1523	Heat Structure 1523
Heatstructure 1524	Heat Structure 1524
Heatstructure 1525	Heat Structure 1525
Heatstructure 1526	Heat Structure 1526
Heatstructure 1527	Heat Structure 1527
Heatstructure 1528	Heat Structure 1528
Heatstructure 1621	Heat Structure 1621
Heatstructure 1721	Heat Structure 1721
Heatstructure 1722	Heat Structure 1722
Heatstructure 1723	Heat Structure 1723
Heatstructure 1724	Heat Structure 1724
Heatstructure 1725	Heat Structure 1725
Heatstructure 1726	Heat Structure 1726
Heatstructure 1727	Heat Structure 1727
mflowj 272020000	Mix Mass Flow Across the X Axis 51
mflowj 312020000	Mix Mass Flow Across the X Axis 52
mflowj 193000000	Mix Mass Flow Across the X Axis 53
Logical Trip 601	Trip -601
	Trip Set Status Value 202
	Trip Set Status Value 203
	Logical AND -7
Logical Trip 604	Trip -604
	Trip Set Status Value 204
	Trip Set Status Value 205
	Logical AND -11
Logical Trip 606	Trip -606
	Trip Set Status Value 206
	Trip Set Status Value 207
	Logical AND -12
Logical Trip 607	Trip -607
	Trip Set Status Value 208
	Trip Set Status Value 209
	Logical AND -13
Logical Trip 608	Trip -608
	Trip Set Status Value 210
	Trip Set Status Value 211
	Logical AND -14

Table 3-1. Excerpt of conversion report…(continued)

Logical Trip 609	Trip -609
	Trip Set Status Value 212
	Trip Set Status Value 213
	Logical AND -16
Logical Trip 610	Trip -610
	Trip Set Status Value 214
	Trip Set Status Value 215
	Logical AND -18
Material 1	Material 50
Material 2	Material 51
Material 3	Material 52
Material 4	Material 53
Material 5	Material 54
PIPE 102 (dskri)	Pipe 102 (dskri)
PIPE 112 (dskrb)	Pipe 112 (dskrb)
PIPE 122 (lp)	Pipe 122 (lp)
PIPE 132 (core)	Pipe 132 (core)
PIPE 142 (core_ut)	Pipe 142 (core_ut)
PIPE 152 (up)	Pipe 152 (up)
PIPE 162 (ss)	Pipe 162 (ss)
PIPE 172 (cnd)	Pipe 172 (cnd)
PIPE 182 (bp)	Pipe 182 (bp)
PIPE 192 (bpin1)	Pipe 192 (bpin1)
PIPE 212 (bpin2)	Pipe 212 (bpin2)
PIPE 222 (bput)	Pipe 222 (bput)
PIPE 232 (dc)	Pipe 232 (dc)
PIPE 242 (dco)	Pipe 242 (dco)
PIPE 252 (dc1)	Pipe 252 (dc1)
PIPE 262 (hci_in)	Pipe 262 (hci_in)
PIPE 282 (hci_u1)	Pipe 282 (hci_u1)
PIPE 292 (hci_u2)	Pipe 292 (hci_u2)
PIPE 302 (hcb_in)	Pipe 302 (hcb_in)
PIPE 322 (hcb_u1)	Pipe 322 (hcb_u1)
PIPE 332 (hcb_u2)	Pipe 332 (hcb_u2)
PIPE 342 (hcb_u3)	Pipe 342 (hcb_u3)
PIPE 352 (hcb_u4)	Pipe 352 (hcb_u4)
PIPE 362 (sl1)	Pipe 362 (sl1)
PIPE 372 (sl2)	Pipe 372 (sl2)
PIPE 382 (bl1_1)	Pipe 382 (bl1_1)
PIPE 392 (bl1_2)	Pipe 392 (bl1_2)

Table 3-1. Excerpt of conversion report….(continued)

PIPE 402 (bl2_1)	Pipe 402 (bl2_1)
PIPE 412 (bl2_2)	Pipe 412 (bl2_2)
PIPE 422 (bl3_1)	Pipe 422 (bl3_1)
PIPE 432 (bl3_2)	Pipe 432 (bl3_2)
PUMP 272 (pmp1)	Pump 272 (pmp1)
PUMP 312 (pmp2)	Pump 312 (pmp2)
SNGLJUN 103 (dskri_o)	Hydraulic [5] from Pipe 102 to Pipe 122
SNGLJUN 113 (dskrb_o)	Hydraulic [6] from Pipe 112 to Pipe 122
SNGLJUN 131 (core_i)	Hydraulic [8] from Pipe 132 to Pipe 122
SNGLJUN 133 (core_o)	Hydraulic [9] from Pipe 132 to Pipe 142
SNGLJUN 143 (core_u_o)	Hydraulic [10] from Pipe 142 to Pipe 152
SNGLJUN 153 (up_o)	Hydraulic [11] from Pipe 152 to Pipe 162

Table 3-2. Problems encountered during RELAP5 -> TRACE conversion and the corresponding corrective method.

Error	Revise
Generic Signal Variable (R5:errmax) 147 Error Error: Contains an invalid variable reference: R5:errmax	Delete Generic Signal Variable 147
Generic Signal Variable (R5:systms) 148 Error Error: Contains an invalid variable reference: R5:systms	Delete Generic Signal Variable 148
Junction Flow Area (Pipe 192: Edge 5) exceeds 1.1 * the flow area of the adjacent cells.	Set the NOFAT namelist variable to TRUE.
Large area change between Junction Flow Area and Adjacent cells detected at pipe 142, 152, 182, 192 and 342.	Specify Friction factor correlation option NFF = -1, the abrupt area flag.
material error	RELAP5 uses Cv, the volumetric heat capacity (J/m^3K), while TRACE uses Cp, the specific heat [J/(kg K)]. So the density needs to be used in order to convert RELAP5 material property to TRACE material property.
Conversion of RELAP5 valve with special choking discharge coefficient resulted in TRACE to valve with default choking option.	In namelist variables, set CHM12=0.8, CHM22=0.8
The constant heat transfer coefficient (HTC) boundary condition could not be converted correctly; it resulted in a normal convective boundary condition.	Set outer surface boundary condition option for heat structure 1325, IDBCON = 4; add table 203 for constant HTC, where (in table 203) also correct signal source SCBSVID is provided according to Figure 3-3; and add table 204 for sink temperature.
This kind of trip "0000508 time 0 ge timeof 504 **0.** n" cannot be converted correctly. If the time is not zero, as "0000508 time 0 ge timeof 504 **10.** n" then it would be ok.	Connect it with right trip signal.
Wrong conversion of control variable for "time after trip become true"	See Figure 3-3.

Table 3-2. Problems encountered during RELAP5….(continued)

Wrong conversion of core power (the scaling factor was lost, and the decay power table did not come into function due to wrong control variable conversion)	• Set reactivity scale factor RPWSCL to correct value. • Do as Figure 3-3.
Wrong conversion of pump speed control, control function 50 for pump1 and control function 100 for pump2 are connecting with wrong control variable, should be time after trip 604 become true.	Set correct control variable.
Control function 1188 "divided" was wrongly converted; the numerator and denominator were in wrong order.	Set it in the right order.
Wrong conversion of feed water boundary flow control (TDJ453), ICBVL is connecting with wrong control variable.	See Figure 3-3
Wrong conversion of steam relief flow control (valve 503), IVSV is connecting with wrong control variable.	See Figure 3-3
Wrong conversion of cooling water boundary flow control (TDJ483), ICBVL is connecting with wrong control variable.	See Figure 3-3
Wrong conversion of spray water boundary flow control (TDJ473), ICBVL is connecting with wrong control variable.	See Figure 3-3

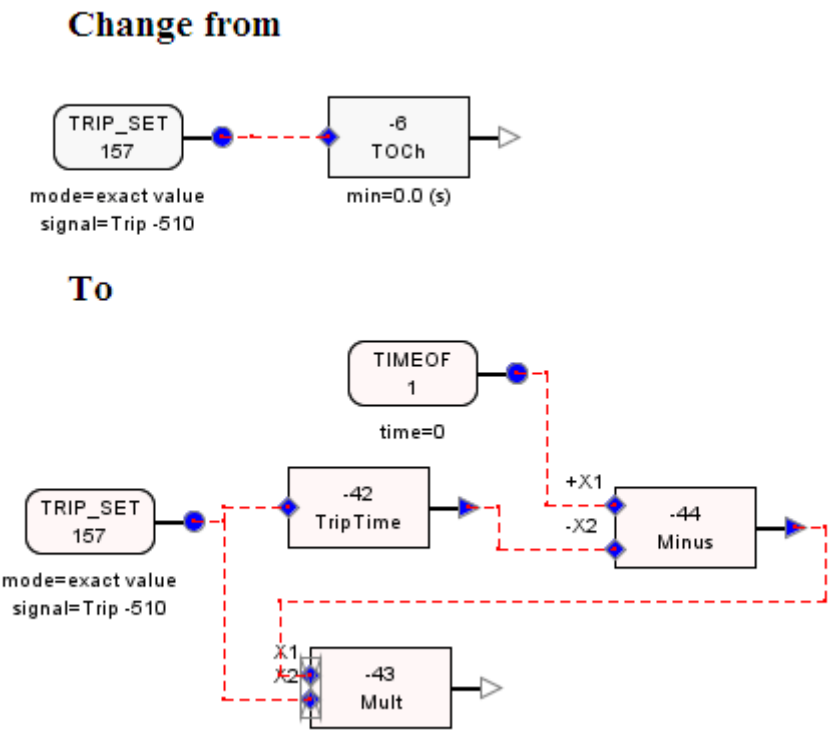

Figure 3-3. The method to get the correct control variable for time after a trip becomes true.

3.3 The RELAP5 Model

The FIX-II test facility model is mainly based on the detail geometric information from Table 2 in [1], and the modeling principle is to include all regions and to model the geometry in adequate high resolution.

The RELAP5 input data is generated by the help of a separately developed input data generation program. This provides a major advantage in generating for instance inputs models with different variation in nodalization. The system is divided into regions, each region is connected to the others by flow junction. By the help of the input generation program, each region will be divided automatically into different amount of cells depending on the node length selected by the user. The nodalization information for the different experiments is shown in Table 3-3. The RELAP5 heat structure input could also be generated by means of the input generation program.

Table 3-3. RELAP5 and TRACE nodalization information.

Experiment	Nodalization	Node length	Number of volumes	Number of junctions	Code
5052	regular	0.3 m	219	221	RELAP5
	fine	0.15 m	371	373	RELAP5 and TRACE
4011	fine	0.15 m	371	373	RELAP5 and TRACE
3051	fine	0.08 m	655	657	RELAP5 and TRACE

The region component diagram for the geometric modeling is shown in Figure 3-4. A list of all pipe regions is shown in Table 3-4 and the other components as pumps, tanks, etc. are listed in Figure 3-5 through Figure 3-8 illustrate different regions and their geometry of the modeled test facility.

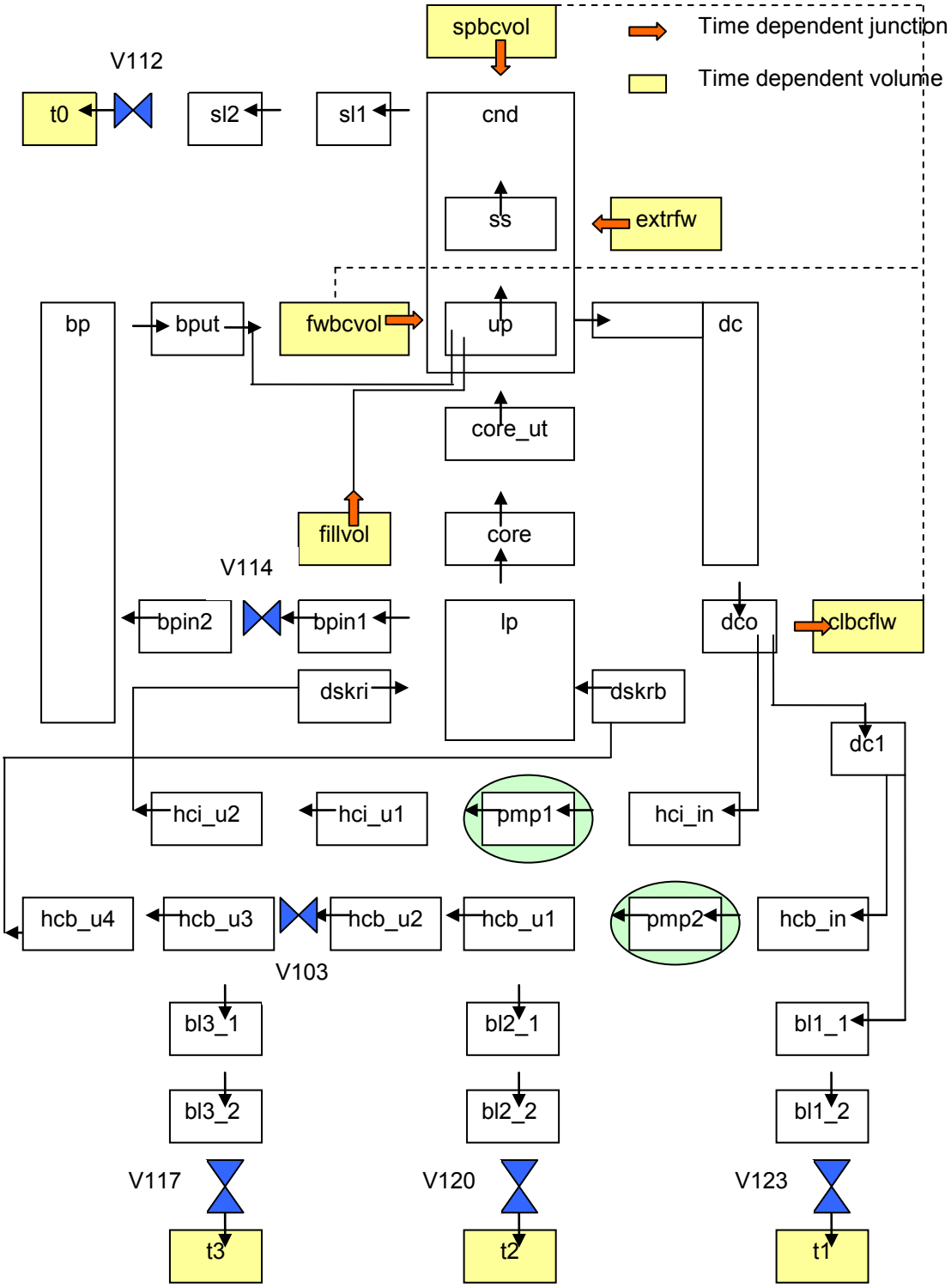

Figure 3-4. The RELAP5 component diagram for FIX-II experiments.

Table 3-4. Modeled RELAP5 pipe regions.

Region pipe name	Desciption	RELAP5 pipe no.	Reference figure
bl1_1	Break line to tank 1, part 1	382	Figure 3-8
bl1_2	Break line to tank 1, part 1	392	Figure 3-8
bl2_1	Break line to tank 2, part 2	402	Figure 3-8
bl2_2	Break line to tank 2, part 2	412	Figure 3-8
bl3_1	Break line to tank 3, part 3	422	Figure 3-8
bl3_2	Break line to tank 3, part 3	432	Figure 3-8
bp	Bypass	182	Figure 3-7
bpin1	Bypass inlet, part 1	192	Figure 3-7
bpin2	Bypass inlet, part 2	212	Figure 3-7
bput	Bypass outlet	222	Figure 3-7
cnd	Steam condenser	172	Figure 3-6
core	Core	132	Figure 3-5
core_ut	Core outlet	142	Figure 3-5
dc	Downcomer	232	Figure 3-7
dc1	Downcomer before break line	252	Figure 3-7
dco	The end of downcomer	242	Figure 3-7
dskrb	Inlet in lower plenum inside the baffle (from break line)	112	Figure 3-5
dskri	Inlet in lower plenum inside the baffle (from intact loop)	102	Figure 3-5
hcb_in	Main recirculation break line inlet	302	Figure 3-7
hcb_u1	Main recirculation break line outlet part 1	322	Figure 3-7
hcb_u2	Main recirculation break line outlet part 2	332	Figure 3-7
hcb_u3	Main recirculation break line outlet part 3	342	Figure 3-7
hcb_u4	Main recirculation break line outlet part 4	352	Figure 3-7
hci_in	Main recirculation intact loop inlet	262	Figure 3-7
hci_u1	Main recirculation intact loop outlet part 1	282	Figure 3-7
hci_u2	Main recirculation intact loop outlet part 2	292	Figure 3-7
lp	Lower plenum	122	Figure 3-5
pmp1	Recirculation pump in intact loop	272	Figure 3-7
pmp2	Recirculation pump in break line	312	Figure 3-7
sl1	Steam line part 1	362	Figure 3-8

Table 3-4. Modeled RELAP5 pipe regions….(continued)

sl2	Steam line part 2	372	Figure 3-8
ss	Steam separator	162	Figure 3-6
up	Upper plenum	152	Figure 3-6

Table 3-5. RELAP5 components other than pipe.

Components	Name	Description
pump 272	pmp1	Recirculation pump in break line
pump 312	pmp2	Recirculation pump in intact loop
tmdpvol 452	fwbcvol	Feed water boundary condition volume
tmdpvol 462	extrfw	Extra feed water using for regulating condenser liquid level
tmdpvol 472	spbcvol	Spray water boundary condition volume
tmdpvol 482	clbcvol	fluid drawn from downcomer for cooling
tmdpvol 492	fillvol	Volume between filler body and pressure vessel
tmdpvol 502	t0	Time dependent volume where main steam flows to
tmdpvol 512	t1	Tank 1
tmdpvol 522	t2	Tank 2
tmdpvol 532	t3	Tank 3
tmdpjun 453	fwbcflw	Time dependent junction connecting to tmdpvol 452
tmdpjun 463	fwbcregf	Time dependent junction connecting to tmdpvol 462
tmdpjun 473	spbcflw	Time dependent junction connecting to tmdpvol 472
tmdpjun 483	clbcflw	Time dependent junction connecting to tmdpvol 482
tmdpjun 493	zeroflw	Time dependent junction connecting to tmdpvol 492
valve 193	bpin1_o	Valve 114 locating at bypass inlet pipe
valve 333	hcb_u2_o	Valve 103 used to separate the break line in order to simulate double ended break
valve 503	slv112	Steam relief valve 112
valve 513	brkv123	Break valve 123 to tank 1
valve 523	brkv120	Break valve 120 to tank 2
valve 533	brkv117	Break valve 117 to tank 3

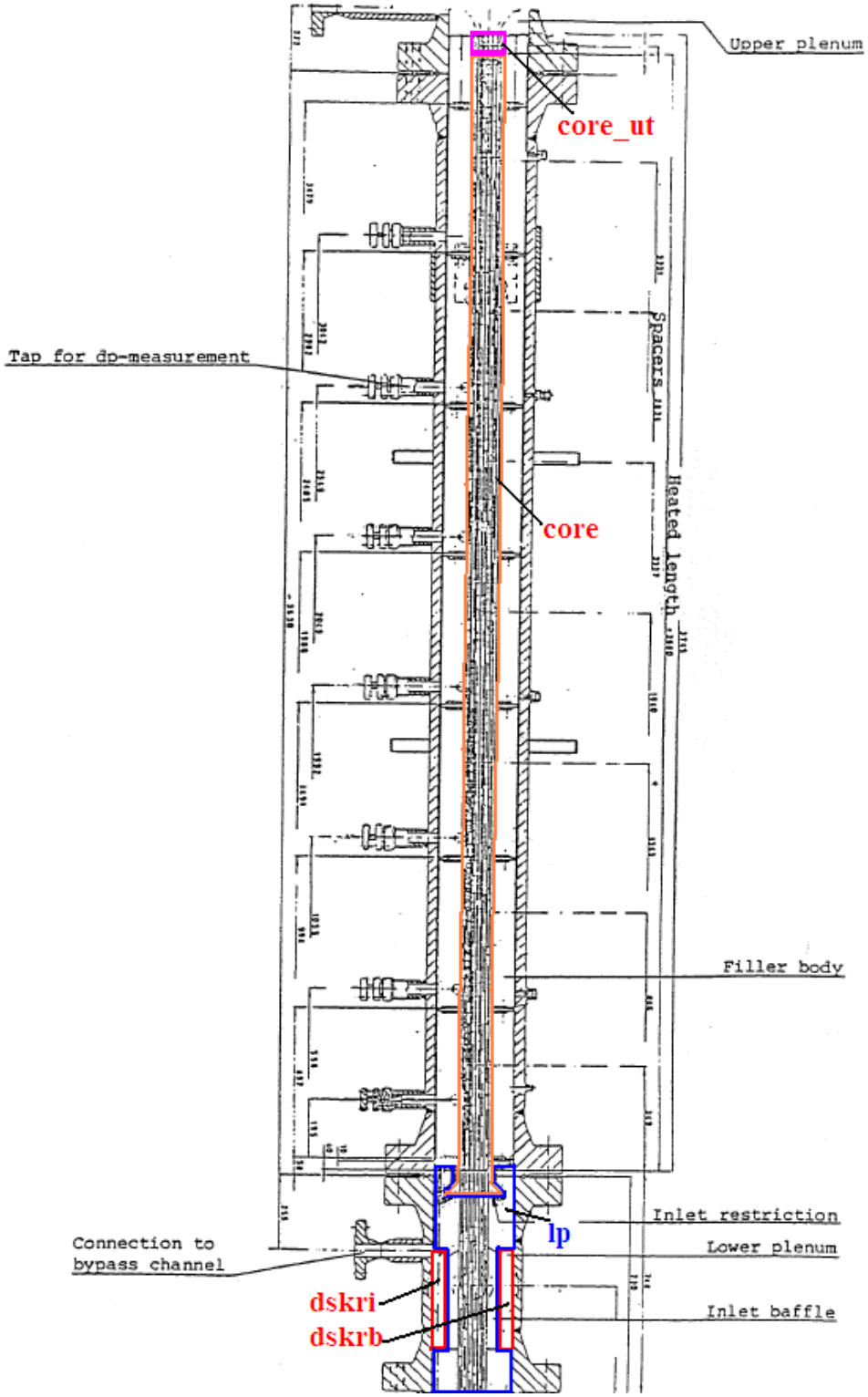

Figure 3-5. Layout of the lower plenum and core regions.

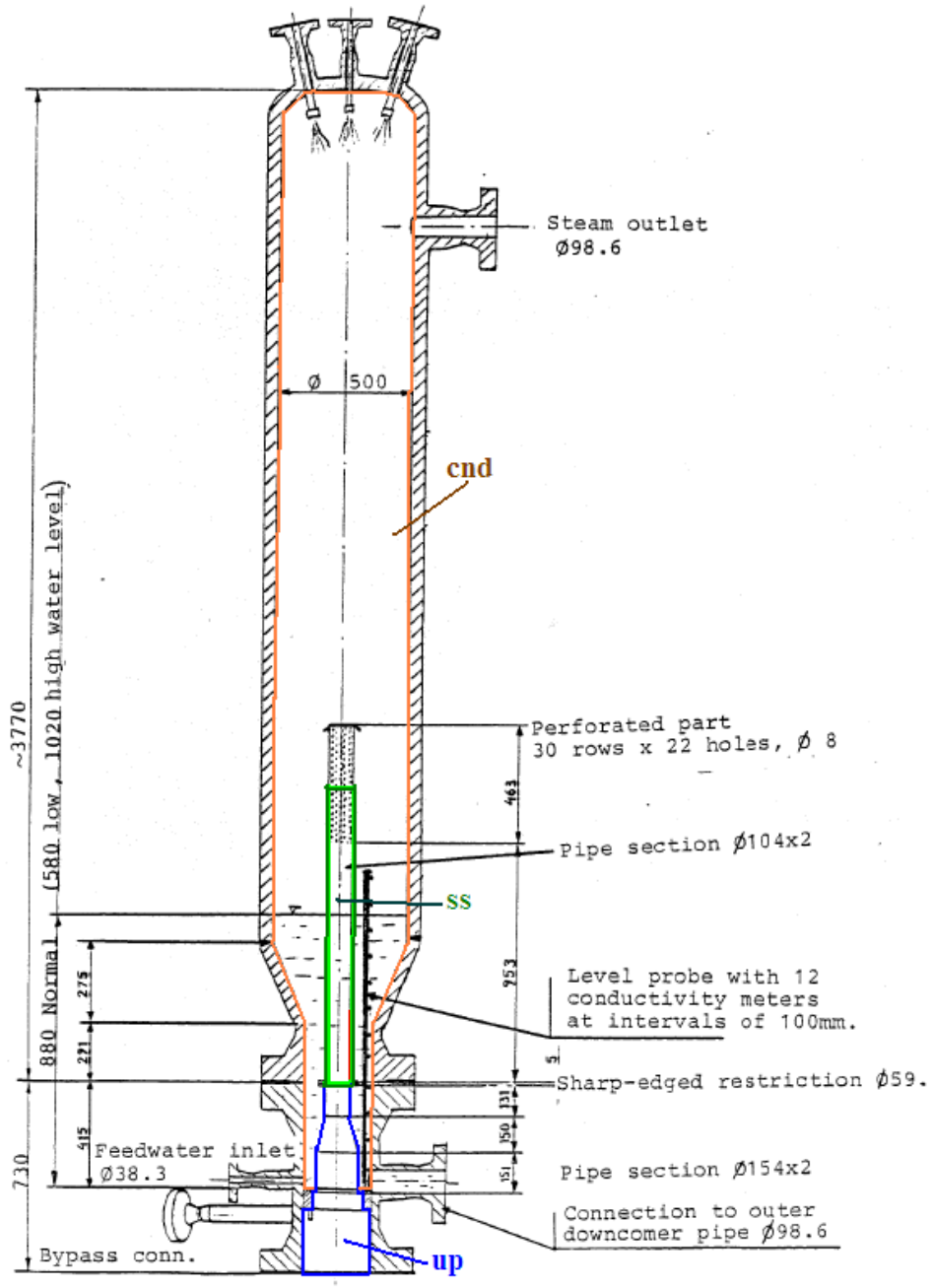

Figure 3-6. Layout of the upper plenum, steam separator and steam condenser regions.

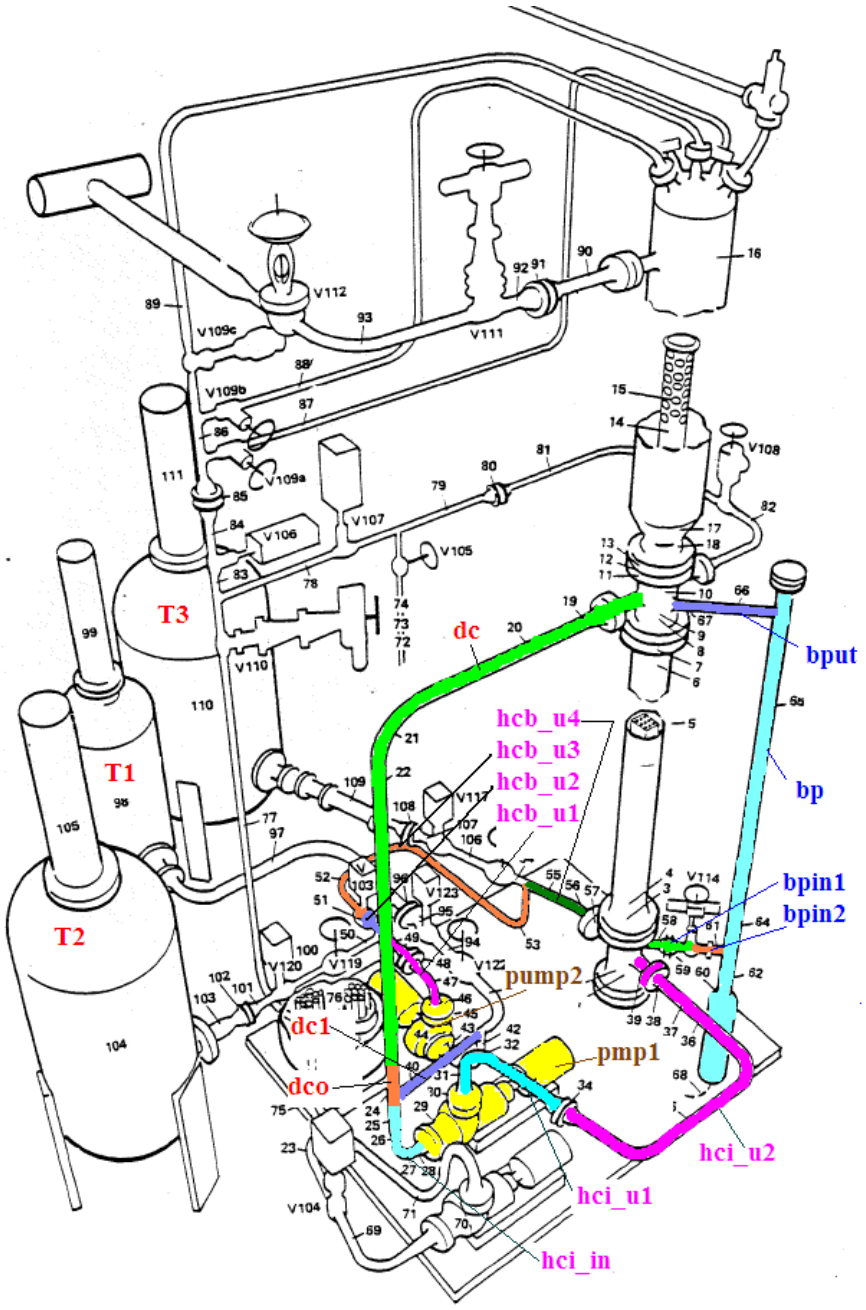

Figure 3-7. Layout of the downcomer, bypass and the main recirculation pipe lines.

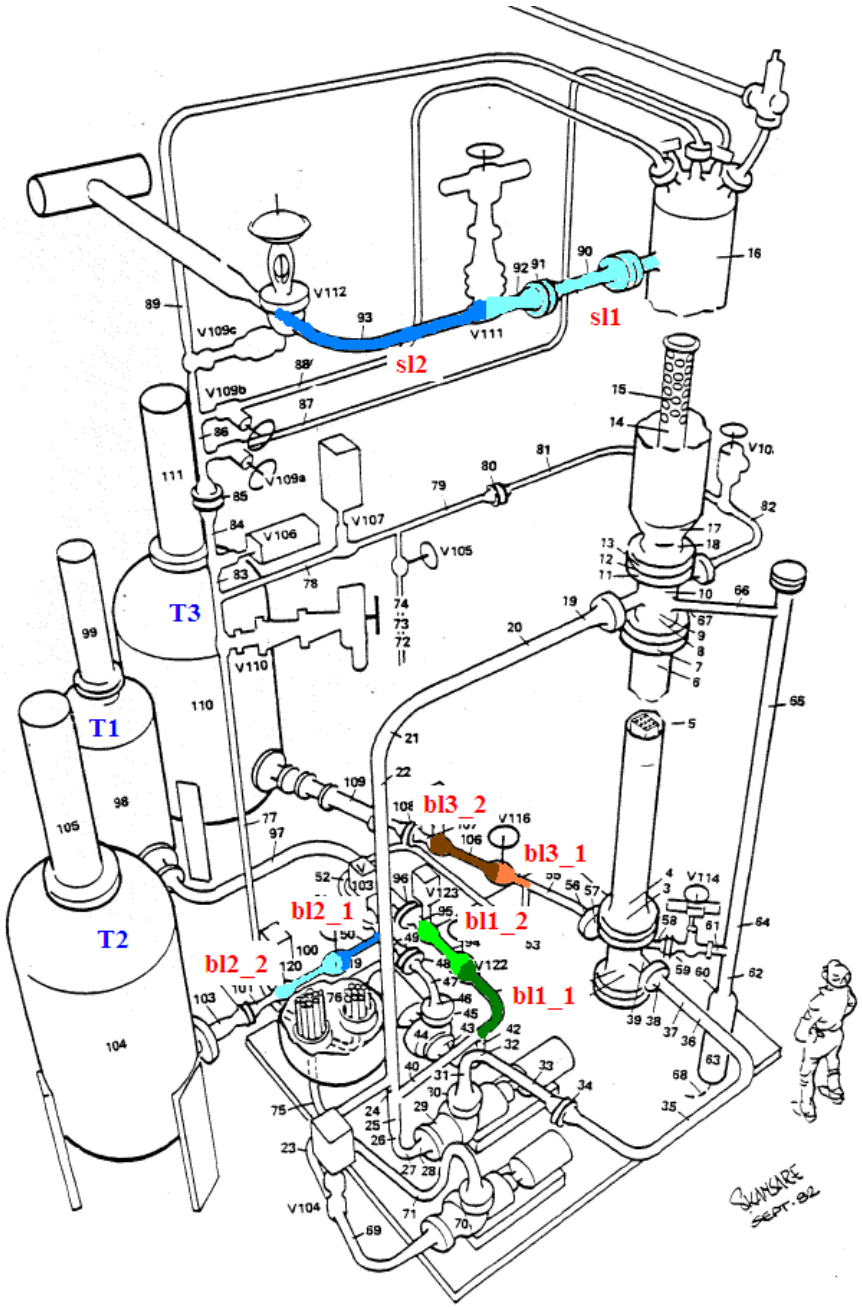

Figure 3-8. Layout of the steam relief line and the break lines.

Cross section geometrical data for the 36-rods bundle are provided in Figure 2-3. An axial power distribution comprising eight steps has been introduced by variations of the rod cladding wall thickness. In each rod there are five thermocouples for measurement of the cladding temperature. The power steps and the locations of the thermocouples are shown in Figure 3-9. By a combination of four different patterns of thermocouple locations, cladding temperatures can be measured at sixteen axial levels. The axial power distribution for the bypass is shown in Figure 3-10. The radial power distribution should be uniform but minor deviations exist due to variations in the electrical resistance of the fuel rods. However, the radial power distribution is not considered in the model, the same power is introduced in all the rods, and the core is modeled as one pipe in this RELAP5 model.

Only limited pump data was provided in [1] and [6] so the pump input data from a previous analysis [7] is adapted. The pump is modeled by homologous curves, with the data from GOBLIN calculations.

The condenser liquid level measurement is modeled according to the real measurement principle, i.e. the liquid level is calculated from the pressure difference measured between two axial locations in the condenser. The basic assumption of the condition is that it is saturated liquid in the lower part and saturated steam above it. The measured liquid level is a function of the measured pressure difference over the distance between the two measurement locations, the liquid and steam density in the condenser at the condenser pressure and the reference density of the fluid in the measurement pipe line.

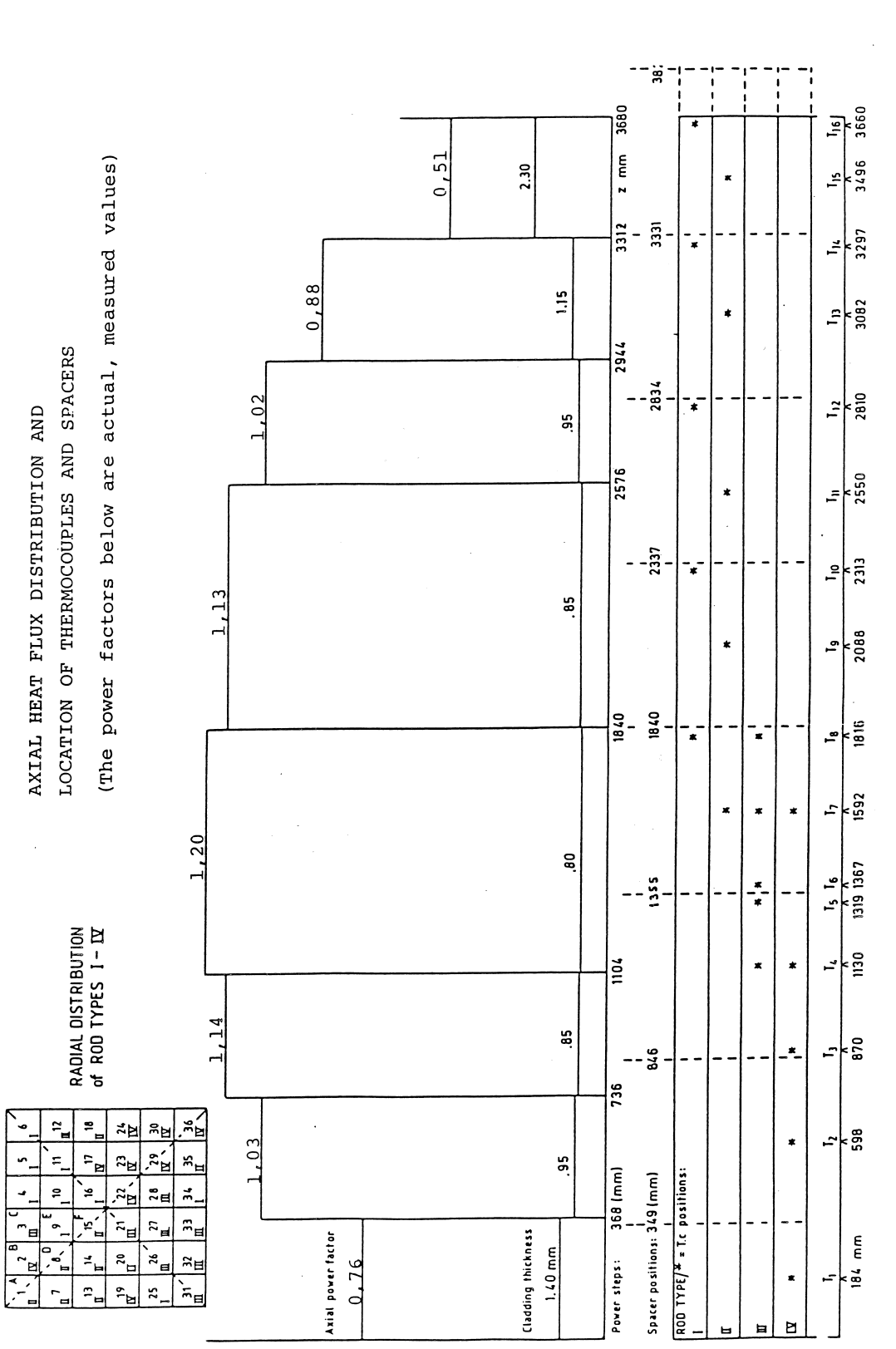

Figure 3-9. Core axial heat flux distribution.

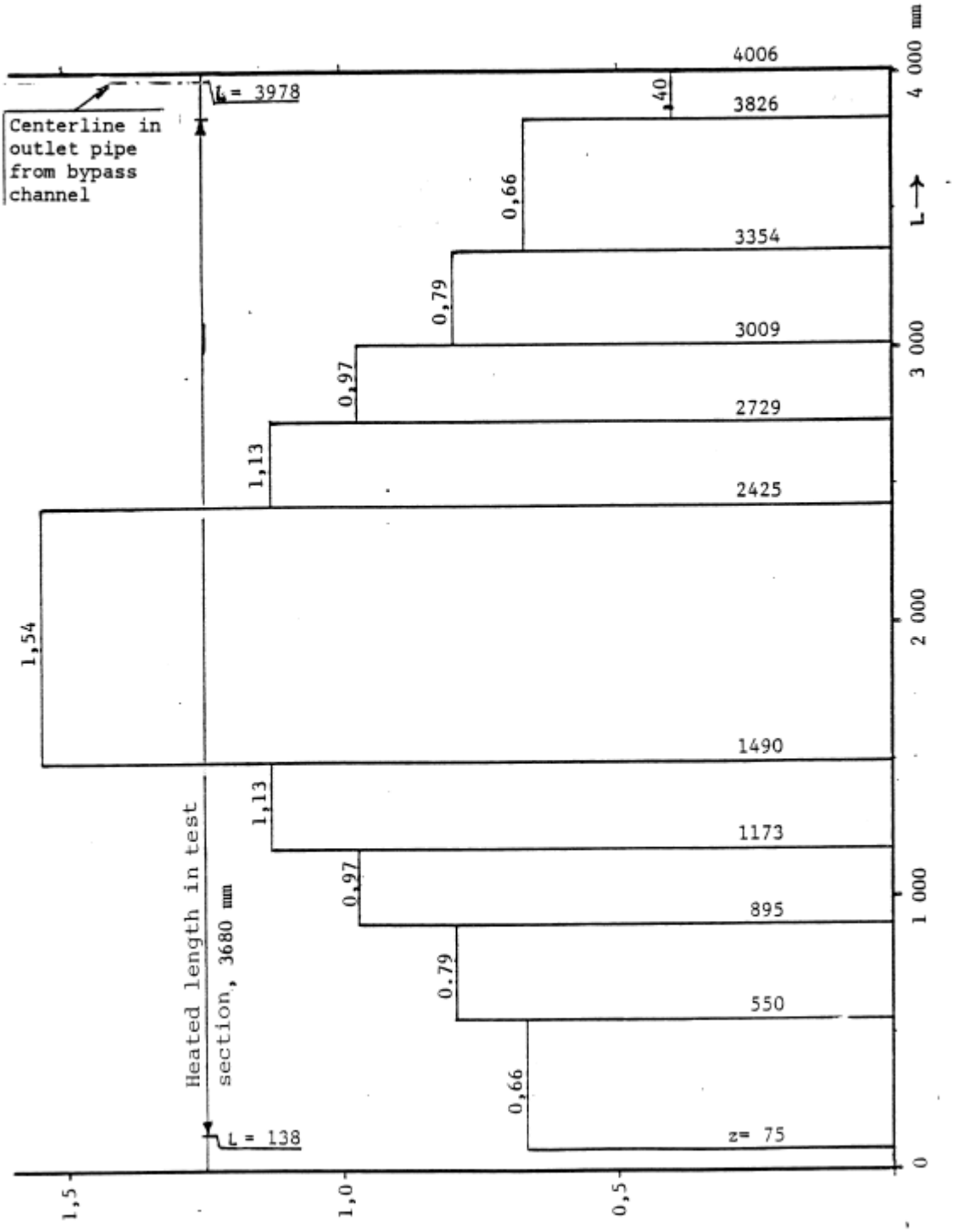

Figure 3-10. Bypass axial heat flux distribution.

To reproduce the fundamental measured steady state quantities, the input for the steady state calculations is modeled by some additional components and control systems:

- The steady state steam dome pressure is achieved by regulating the core heat loss transfer coefficient through the filler body.
- The speed of the main recirculation pumps P1 and P2 are controlled by the RELAP5 control system to reproduce the measured mass flows.
- To divert the correct mass flow into the bypass, the junction between the two bypass inlet pipes is modeled as a motor valve. By trip logic, the amount of valve opening is controlled to provide the measured bypass mass flow rate. When entering into the transient calculation, the valve setting is fixed.
- The steam condenser liquid level was controlled to obtain the measured value by connecting an auxiliary time dependent volume and time dependent junction to the condenser. The flow through the time dependent junction is controlled according to the offset liquid level.

The steady state input model is made as complete as possible in order to also cover the transient actions. The steady state controls were disconnected by a first trip and the additional trips followed to simulate the system actions when the transient starts. In the transient restart, the first trip is set at time zero with a new initiation of the time scale. Until the second trip, which is the one initiating the actual transient, the transient calculation is run at the initial steady state as to confirm the initial steady state stability.

4. ANALYSIS RESULTS

4.1 Experiment 5052

Experiment 5052 simulates a guillotine break in one of the four main recirculation lines. The total break area, equally divided between the two broken discharge pipe line sections, was 200 % of the scaled down pipe area of the reactor recirculation line. The initial heating power of the 36-rod bundle in the FIX-II loop was 3.356 MW, corresponding to 2500 MW of the real plant, which is about the power after PLEX. The detail experiment description can be found in [3].

Experiment 5052 is a C type break shown in Figure 2-2, the initial condition is shown in Table **4-1**. The list of sequence of events is shown in Table 4-2.

The following is a summary of the main experiment and analysis results: The large size of the break resulted in reversed core flow and in dryout conditions along the whole heated length of the rod bundle. The void fraction increased towards the lower part of the bundle, which resulted in the highest rod temperatures in that region (the phenomena are well predicted in the analyses). A peak clad temperature of 716 ^{o}C (about 650 ^{o}C in TRACE and 630 ^{o}C in RELAP5 analyses) was measured 12 s after the break at rod No 29, level 4, Figure A-12. However, the temperatures decreased again after around 10 s, in several cases due to rewetting (no rewetting could be predicted in the analyses). The maximum temperature at the end of the blowdown, at 27.4 s, was 620 ^{o}C (well predicted in the analyses shown in Figure A-12 to Figure A-14). The steam dome pressure had then decreased to 1.9 MPa (1.35 MPa in the RELAP5 analyses and 1.25 MPa in the TRACE analyses, the latter which predicted somehow faster depressurization).

Some main experimental and analysis results of pressure, differential pressure, mass flow rates and temperatures at different locations are shown in figures in Appendix A and discussed briefly in relation to the figures. The detail experiment transient description can be found in [8]. Measurement locations are shown in Figure 2-4.

In general, the results are quite similar between RELAP5 and TRACE analyses and they are in good agreement with the experimental results, although some differences were revealed:

- Almost the same pressure decrease rate in the system (Figure A-1, Figures A-7 and A-8).

- TRACE provided a faster depressurization rate and higher break flow rate at the very beginning of the transient, but later on, almost the same break flow rate (Figures A-2 and A-3), the same steam relief flow (Figure A-4) and pump flow rate (Figures A-5 and A-6) as for the RELAP5 analysis. Although the discharge flow rates are quite similar between RELAP5 and

TRACE analyses, the small difference is nevertheless one of the reasons resulting in the different rod temperatures as discussing below. This will also be discussed in detail related to experiment 3051 where the discharge flow rate revealed bigger differences between the TRACE and RELAP5 analyses.

- There are quite big differences in rod temperatures between the two analyses (Figures A-9 through Figure A-20) due to different void distribution (Figures A-21 and A-22) in the core both during the steady-state and the course of the transient, although the same power and total flow rate through the core were applied. Thus RELAP5 and TRACE analyses resulted in different distribution of the liquid and vapour mass flow rate, and this is most likely due to somewhat different correlations applied in the two codes for interfacial friction and interfacial area concentration. A more thorough examination of the causes to the found differences is however beyond the scope of the current effort, and has to be left to the future.

Table 4-1. Initial condition for experiment 5052.

Break configuration (Figure 2-2)	C
Break restriction nozzles I.D.	21.6 + 21.6 mm
Steam relief valve area, V112	0.56 cm2
Pressure in the steam dome	6.9 MPa
Power to the 36-rod bundle	3.356 MW
Power to the bypass heaters	56.6 kW
Mass flow rate through pump 1	4.4 kg/s
Mass flow rate through pump 2	1.68 kg/s
Mass flow rate in the bypass	0.57 kg/s
Mass flow rate in the 36-rod bundle	5.51 kg/s
Mass flow rate in the spray line	5.1 kg/s
Mass flow rate in the feed water line	2.3 kg/s
Temperature of water at the bundle inlet (TE2)	268.7 ^{o}C
Temperature of feed and spray water	181.3 ^{o}C
Water level in the spray condenser	6.223 m
Rotation speed of pump 1	24.78 revs/s
Rotation speed of pump 2	32.51 revs/s

Table 4-2. Events list for experiment 5052.

Event	Time (s)
Break valve V120 starts to open	0
Start of coast down of pump 1	0
Break valve V117 starts to open	0.2
Valve V103 in the broken RCL starts to close	0.3
Start of power decay in the bundle	0.4
The SRV starts to open	0.7
Start of power decay in the bypass heaters	1.2
The SRV is fully open	1.2-27.5
The spray flow is closed	2.1
The feed water flow is closed	2.2
Valve V104 to the evaporation cooler is closed	2.3
Tripping of the bundle power	27.4
The break valves are closed	27.8
Termination of data acquisition	37.7

4.2 Experiment 4011

Experiment 4011 simulates a guillotine break in one of the four main recirculation lines. A simplified loop configuration was applied, with only one recirculation line in operation, the other recirculation lines being shut off. The simulated break was located at extensions from the lowermost part of the downcomer and from the lower plenum, with break areas of 55 and 100 percent of the scaled down area of one recirculation line, respectively. The initial heating power of the 36-rod bundle was 2.324 MW, corresponding to 1800 MW for the real plant, which represents the current full power. The detail experiment description can be found in [4].

Experiment 4011 is a B type break shown in Figure 2-2, the initial condition is shown in Table 4-3. The list of sequence of events is shown in Table 4-4.

The following is a summary of the main experiment and analysis results: The large size of the break resulted in a reversed flow in the bundle throughout the blowdown phase. The dryout conditions therefore became more serious in the lower part (the phenomena are well predicted in the analyses). A maximum rod temperature of 520 ^{o}C (460 ^{o}C in TRACE analyses, 478 ^{o}C in RELAP5 analyses) was measured at 12 s after the break at rod No 21, level 4, Figure B11. However, the temperatures decreased again after about 12 to 15 s, also at not rewetted rod positions, for which the final maximum temperature, 451 ^{o}C was obtained at the end of the blowdown. The steam dome pressure was then at 1.55 MPa (1.2 MPa in the RELAP5 analyses and 0.85 MPa in the TRACE analyses, the latter which predicted somehow faster depressurization).

Some main experimental and analysis results of pressure, differential pressure, mass flow rates and temperatures at different locations are presented in figures in Appendix B and discussed briefly in relation to the figures. The detail experiment transient description can be found in [8]. Measurement locations are shown in Figure 2-4.

In general, the results are quite similar between RELAP5 and TRACE analyses and they are in good agreement with the experimental results, although some differences were revealed. The analysis here is very close to the analysis of the previous experiment 5052:

- Almost the same depressurization rate in the system (Figure B-1, Figures B-6 and B-7).

- TRACE provided a faster depressurization rate and higher break flow rate at the very beginning of the transient, but later on, almost the same break flow rate (Figures B-2 and B-3), a somewhat less steam relief flow (Figure B-4) and pump flow rate (Figure B-5) as for the RELAP5 analysis. Although the discharge flow rates are quite similar between RELAP5 and TRACE analyses, the small difference is nevertheless one of the reasons resulting in the different rod temperatures as discussing below. This will also be discussed in detail related to experiment 3051 where the discharge

flow rate revealed bigger differences between the TRACE and RELAP5 analyses.

- There are quite big differences in rod temperatures between the two analyses (Figure B-8 through Figure B-15) due to different void distribution (Figures B-16 and B-17) in the core both during the steady-state and the course of the transient, although the same power and total flow rate through the core were applied. Thus RELAP5 and TRACE analyses resulted in different distribution of the liquid and vapour mass flow rate, and this is most likely due to somewhat different correlations applied in the two codes for interfacial friction and interfacial area concentration. A more thorough examination of the causes to the found differences is however beyond the scope of the current effort, and has to be left to the future.

Table 4-3. Initial condition for experiment 4011.

Break configuration (Figure 2-2)	B
Break restriction nozzles I.D.	16.0 + 21.6 mm
Steam relief valve area, V112	0.56 cm2
Pressure in the steam dome	6.79 MPa
Power to the 36-rod bundle	2.324 MW
Power to the bypass heaters	54.8 kW
Mass flow rate through pump 1	6.05 kg/s
Mass flow rate in the bypass	0.43 kg/s
Mass flow rate in the 36-rod bundle	5.62 kg/s
Mass flow rate in the spray line	3.18 kg/s
Mass flow rate in the feed water line	1.9 kg/s
Temperature of water at the bundle inlet (TE2)	266.6 ^{o}C
Temperature of feed and spray water	180.5 ^{o}C
Water level in the spray condenser	6.31 m
Rotation speed of pump 1	26.9 revs/s

Table 4-4. Events list for experiment 4011.

Event	Time (s)
Start of coast down of pump 1	-0.1
Break valve V123 starts to open	0.0
Start of power decay in the bundle	0.0
Break valve V117 starts to open	0.1
The SRV starts to open	0.3
The SRV is fully open	0.7-32.6
Start of power decay in the bypass heaters	0.8
The spray flow is closed	1.8
The feed water flow is closed	1.9
Valve V104 to the evaporation cooler is closed	1.9
The break valves are closed	32.6
Termination of data acquisition	43.0

4.3 Experiment 3051

Experiment 3051 simulates a split break case, and had the smallest break area of all FIX-II tests, the break area was 10 % of the scaled down pipe area of the reactor recirculation line. The initial heating power of the 36-rod bundle in the FIX-II loop was 2.38 MW, corresponding to 1800 MW of the real plant, which represents the current full power. The detail experiment description can be found in [5].

Experiment 3051 is an A type break shown in Figure 2-2, the initial condition is shown in Table 4-5. The list of sequence of events is shown in Table 4-6.

The following is a description of the main experiment transient: The small break area plus the low average channel power did not lead to any initial dryout in the 36-rod bundle and no associated bundle heat up indicating no core uncovery. In test 3051 a comparatively large fraction of energy, was lost through the steam relief and contributed to the depressurization, although the second valve opening was delayed to 39.6 s after the break. The steam dome pressure was then decreased to 2.2 MPa in the experiment.

Some main experimental results along with RELAP5 and TRACE analysis results of pressure, differential pressure, mass flow rates and temperatures at different locations are shown and discussed in figures in Appendix C. The detail experiment transient description can be found in [8]. The measurement locations are shown in Figure 2-4.

In general, the results are quite similar between RELAP5 and TRACE analyses and they are in good agreement with the experimental results, although some differences were revealed:

- Almost the same pressure decrease rate in the system (Figure C-1, Figures C-6 and C-7).

- As for the other two experiments, TRACE provided faster depressurization rate and higher break flow rate at the very beginning of the transient, but later on, quite similar break flow rate (Figure C-2) as for the RELAP5 analysis, and both analyses revealed almost the same steam relief flow (Figure C-3) and pump flow rate (Figures C-4 and C-5).

- Although the flow rate through the break appears to be quite similar between RELAP5 and TRACE analysis results (Figure C-2), the discharged mass differs quite much as shown in Figure C-19, and Figure C-18. This is one of the reasons for providing the different rod temperatures as discussing below.

- Figure C-18 also shows that it is somewhat different mass inventory in the system even during the steady state. Since the same liquid level in the condenser, the same system pressure, and the same core inlet liquid

temperature prevailed, it is reasonable to assume that different two-phase distribution in the core and the bypass is a major cause for the differences, and this is also proved by the void distribution curve from Figures C-16 and C-17.

- For the rods temperatures, the RELAP5 shows very good agreement with the experimental data (Figure C-8 to Figure C-15), whereas TRACE provided slightly higher temperature already at steady state and predicted even a dryout along the whole rod length in the core during the last period of the transient. The reason to the different rods temperature results of the TRACE and RELAP5 analyses is most probably due to the following: First, due to quite different void distribution (Figure C-16, 17) in the core both during the steady-state and during the course of the transient, although the same power and total flow rate through the core were applied. This meant that RELAP5 and TRACE analyses resulted in different distribution of the liquid and vapour mass flow rate due to most likely somewhat different correlations applied in these two codes for interfacial friction and interfacial area concentration. Second, different discharge flow rate correlations which resulted in different mass inventory remaining in the system.

Table 4-5. Initial condition for experiment 3051.

Break configuration (Figure 2-2)	A
Break restriction nozzles I.D.	6.82 mm
Steam relief valve area, V112	0.94 cm2
Pressure in the steam dome	6.99 MPa
Power to the 36-rod bundle	2.38 MW
Power to the bypass heaters	61.1 kW
Mass flow rate through pump 1	4.85 kg/s
Mass flow rate through pump 2	1.59 kg/s
Mass flow rate in the bypass	0.69 kg/s
Mass flow rate in the 36-rod bundle	5.75 kg/s
Mass flow rate in the spray line	3.08 kg/s
Mass flow rate in the feed water line	1.95 kg/s
Temperature of water at the bundle inlet (TE2)	266 ^{o}C
Temperature of feed and spray water	180 ^{o}C
Water level in the spray condenser	6.349 m
Rotation speed of pump 1	24.63 revs/s
Rotation speed of pump 2	31.64 revs/s

Table 4-6. Events list for experiment 3051.

Event	Time (s)
Break valve V120 starts to open	0
Start of coast down of pump 1	0
Start of power decay in the bundle and the bypass	0.0
The SRV starts to open	0.5
The SRV is fully open	1.1
The SRV starts to close	1.5
Break valve V117 starts to open	0.2
Valve V103 in the broken RCL starts to close	0.3
The spray flow is closed	2.0
The feed water flow is closed	2.1
Valve V104 to the evaporation cooler is closed	2.2
The SRV is closed	2.8
The SRV starts to open	39.6
The SRV is fully open	40.3-137.2
The break valves are closed	137.0
Termination of data acquisition	146

5. CONCLUSIONS AND EVALUATIONS

The TRACE Version 5.0 Patch 2 is validated against some FIX-II experiments, where the input is obtained by converting the legacy RELAP5 FIX-II model by means of SNAP. The SNAP model editor should ideally be capable to convert any RELAP5 input model into TRACE input. This functionality of SNAP however does not work to a full extent and consequently some user effort was needed to complete the model into a “runable” status. After the manual corrections the TRACE analyses could nevertheless be run with the same boundary condition as in RELAP5: the same core and bypass power, the same boundary flow rate, the same pump characteristics, the same trip time to activate the break flow, the decay power, the pump coast down, etc.

Three FIX-II transients (5052, 4011 and 3051) were analyzed. The performed TRACE analyses revealed in general quite good comparisons with RELAP5 results and corresponding measured parameters, however, not quite as good as the RELAP5 results when it comes to the system depressurization rate and the rod PCT and dryout predictions. It was specifically noted that:

- The various differential pressures around the test facility loops were well simulated indicating an overall favorable simulation of the liquid inventory distribution. Also the loop pressure decrease as a result of the flow expelled through the break was acceptably calculated although the rate of the decrease was somewhat exaggerated especially in the TRACE analyses. This exaggeration could have been made less pronounced by more careful tuning of the break conditions, i.e. basically tuning of the discharge coefficients associated with the used break flow model but also adjustments of the loss coefficients at and close to the break location.

- For the large break LOCA tests 5052 and 4011, the TRACE analyses could predict almost as well as the RELAP5 analyses on the dryout and the flow reversal in the test section bundle, with about 50 ^{o}C lower PCT in comparison to measurements from the tests 5052 (716 ^{o}C) and 4011 (520 ^{o}C).

- For the small break LOCA test 3051, where forced steam blow down occurred, the RELAP5 model well predicted the transient sequences in which no dryout occurred in the test section bundle due to the small loss of mass through the break; while the TRACE predicted a dryout in the later period of the transient due to larger loss of mass through the break and higher void distribution in the core.

It is likely that the critical flow and the heat transfer are modeled somewhat differently in TRACE and RELAP5, resulting in different PCT and dryout behavior of the core rods.

6. REFERENCES

1. Nilsson, L. et. al. (1983). “FIX-II – LOCA blowdown and pump trip heat transfer experiments, summary report of phase 2: description of experimental equipment. Parts 1, 2 and 3. Studsvik AB, Sweden (Technical Note NR-83/238).

2. TRACE V5.0 USER’S MANUAL.

3. Nilsson, L. et. al. (1983). FIX-II – LOCA blowdown and pump trip heat transfer experiments, experimental results from LOCA test No. 5052. Studsvik AB, Sweden (Technical Note NR-83/323).

4. Nilsson, L. et. al. (1983). FIX-II – LOCA blowdown and pump trip heat transfer experiments, experimental results from LOCA test No. 4011. Studsvik AB, Sweden (Technical Note NR-83/321).

5. Nilsson, L. et. al. (1984). FIX-II – LOCA blowdown and pump trip heat transfer experiments, experimental results from LOCA test No. 3051. Studsvik AB, Sweden (Technical Note NR-84/486).

6. Nilsson, L. et. al. (1984). FIX-II – LOCA blowdown and pump trip heat transfer experiments, final report for phase 3: Results of running-in and pilot experiments. Studsvik AB, Sweden (Technical Note NR-84/363).

7. Eriksson, J. (1986). Assessment of RELAP5/MOD2, CYCLE 36.04 against FIX-II guillotine break experiment No.5061. Studsvik AB, Sweden (Technical Note NP-86/109).

8. Sheng, C. (2010). Validation of RELAP5/MOD3.3 against FIX-II LOCA experiments No. 5052, 4011, 3051. Studsvik Nuclear AB, Sweden (N-09/215).

APPENDIX A RESULT PLOTS OF FIX-II EXPERIMENT 5052

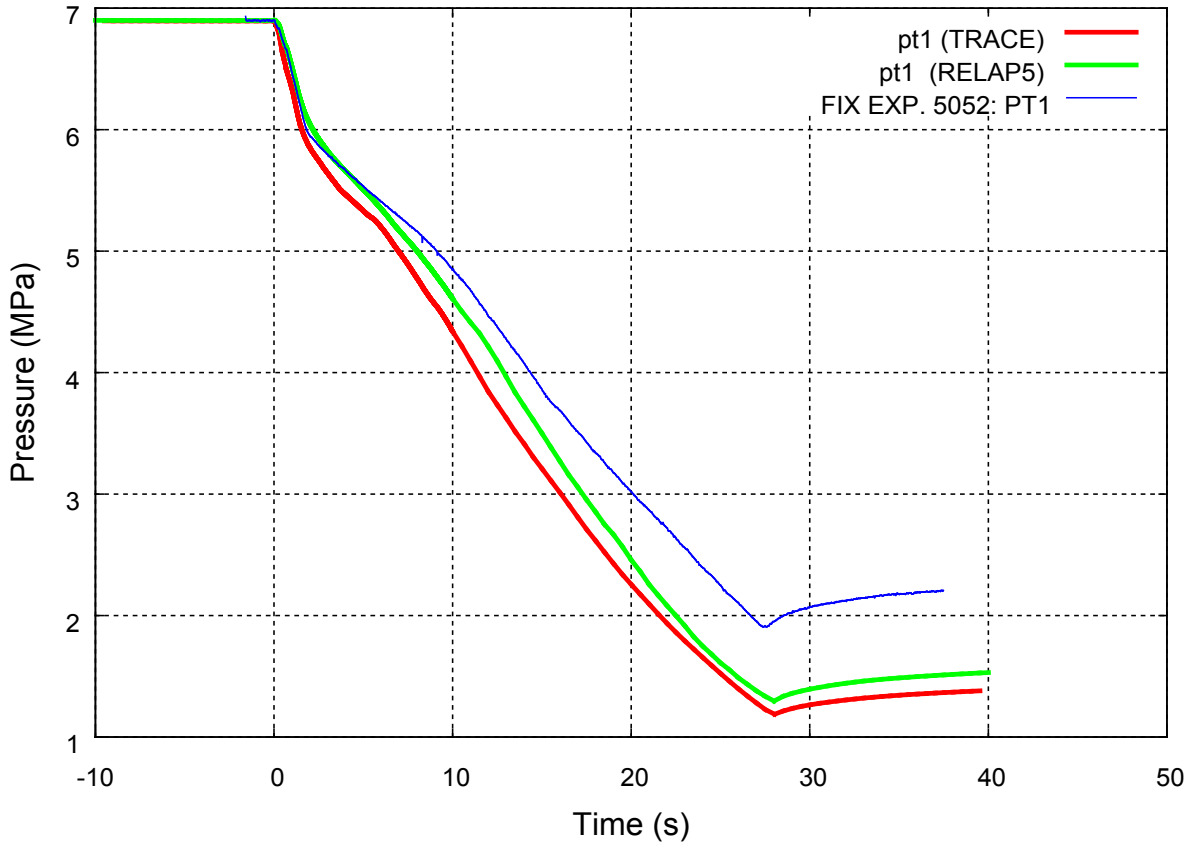

Figure A-1 Pressure in the steam dome.

The steam dome pressure dropped rapidly. The pressure decrease became less pronounced after the closure of the spray and feed water flows at 2.2 s. The pressure drops a little faster in the analysis compared to the experimental result.

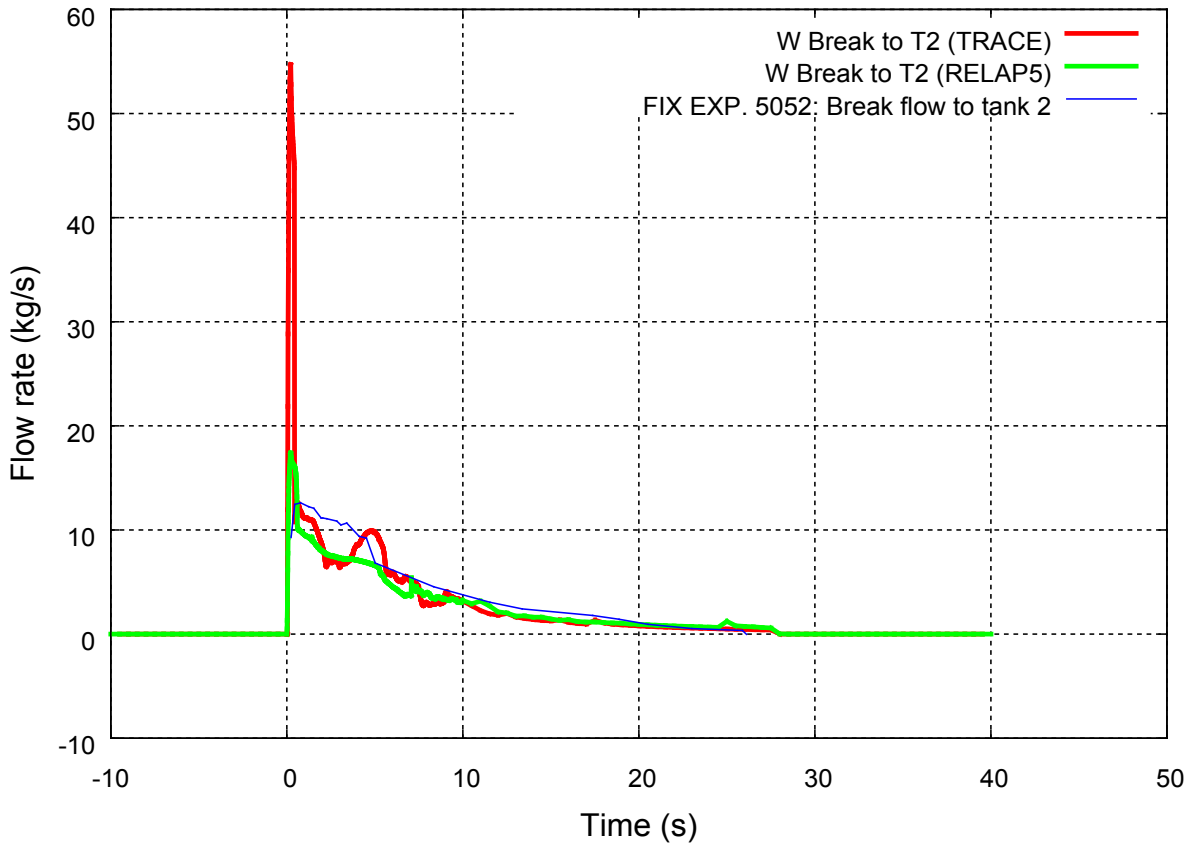

Figure A-2 Break mass flow rate into tank T2.

The break valve V120 (restriction nozzle I.D. 21.6 mm) starts to open at 0 s. A maximum mass flow rate of about 12.5 kg/s was obtained in the experiment. However, the initial break mass flow rate based on DPT 42 was very uncertain, since tank T2 had a too low initial water level, below the expansion pipe. The discharge flows through the breaks reached their maxima within 1 s after the break incident.

Both the TRACE and the RELAP5 analysis results are based on the critical flow model with both the subcooled and the two-phase discharge coefficient equal to 0.8. The used discharge coefficients reveal acceptable calculated flow rates compared to measured flow rates.

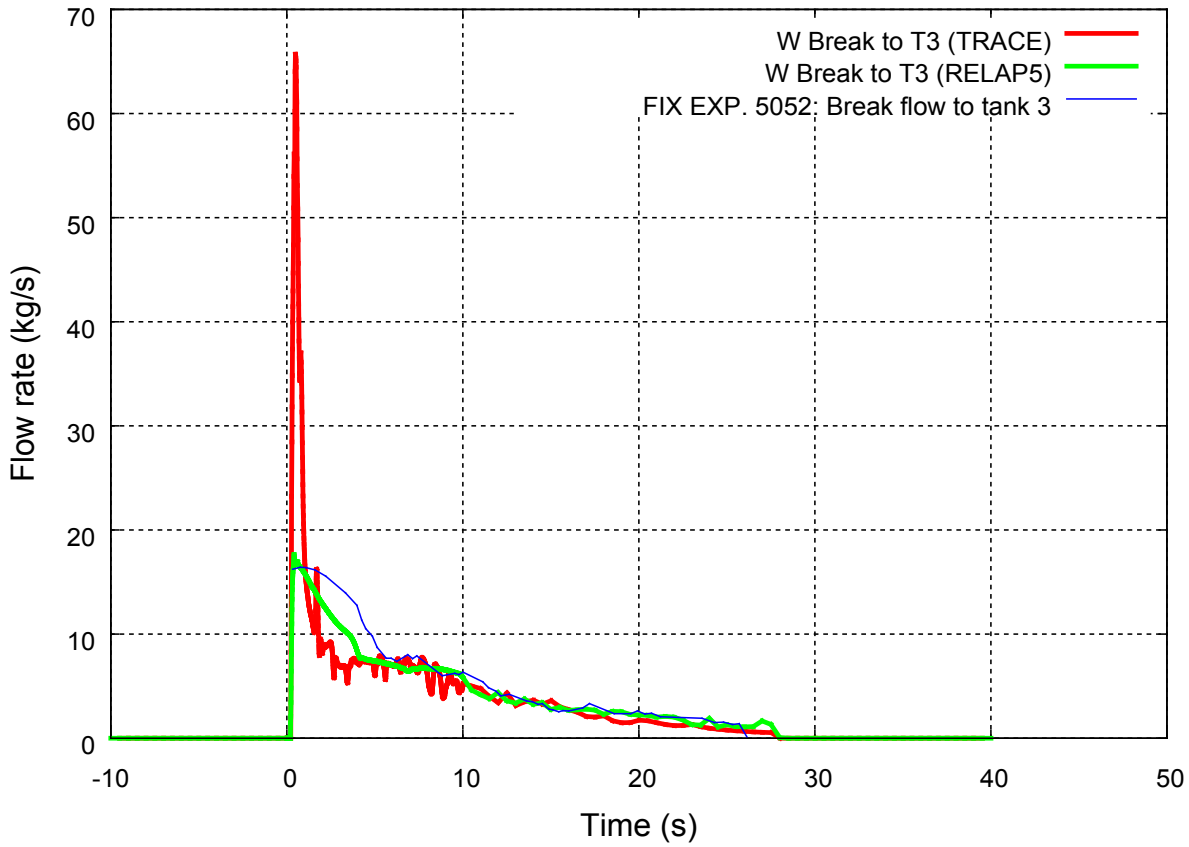

Figure A-3 Break mass flow rate into tank T3.

The break valve V117 (restriction nozzle I.D. 21.6 mm) starts to open at 0.2 s. A maximum mass flow rate of about 16.5 kg/s was obtained in the experiment. The discharge flows through the breaks reached their maxima within 1 s after the break incident.

Both the TRACE and the RELAP5 analysis results are based on the critical flow model with both the subcooled and the two-phase discharge coefficient equal to 0.8. The used discharge coefficients reveal acceptable calculated flow rates compared to measured flow rates.

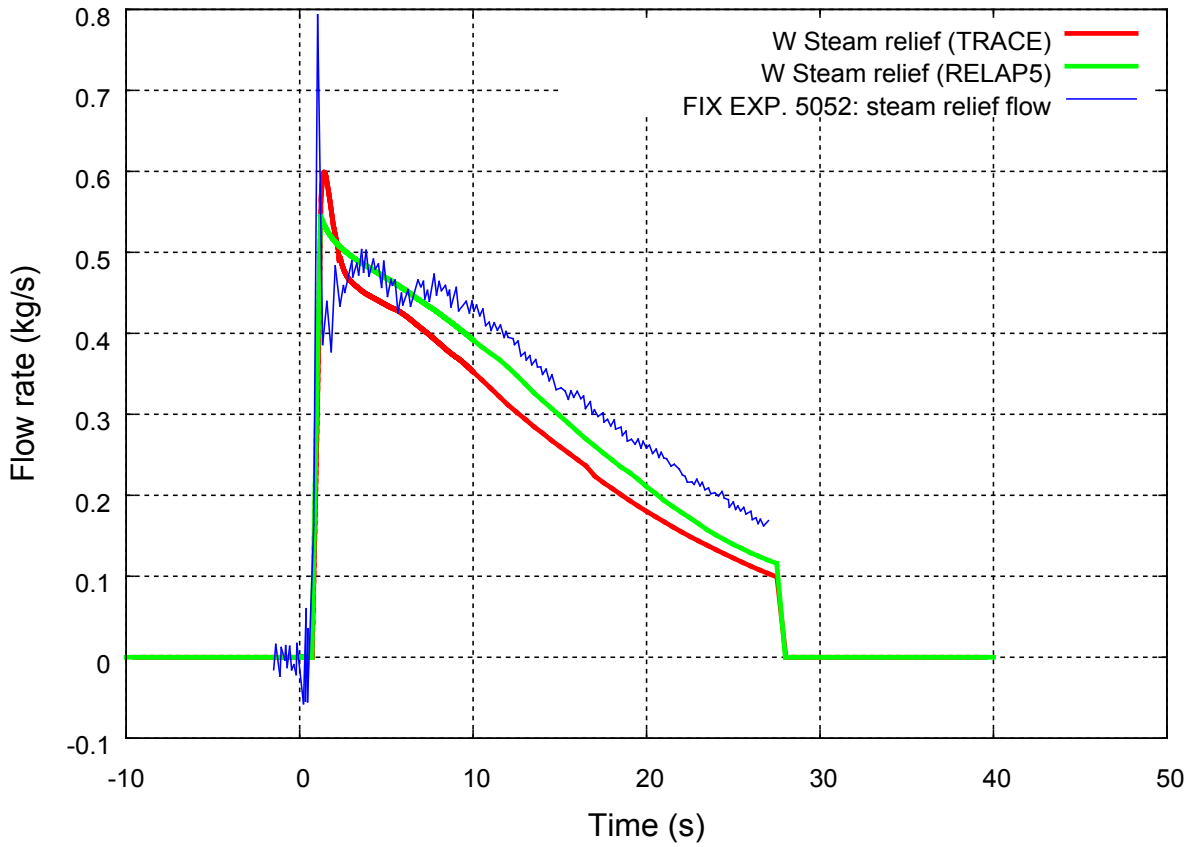

Figure A-4 Mass flow rate of steam through orifice meter K6 in the steam relief valve.

The steam relief valve (flow area 0.56 cm^2) starts to open at 0.7 s, was fully open at 1.2 s and remained so for the rest of the test. A maximum mass flow rate of 0.48 kg/s was obtained in the experiment. The analyses mass flow rate is a little bit less than measurement after about 4 s in the later period of experiment, and is caused by the steam dome being depressurized a little bit faster in the analyses compared to the experiment in that period (see Figure A-1).

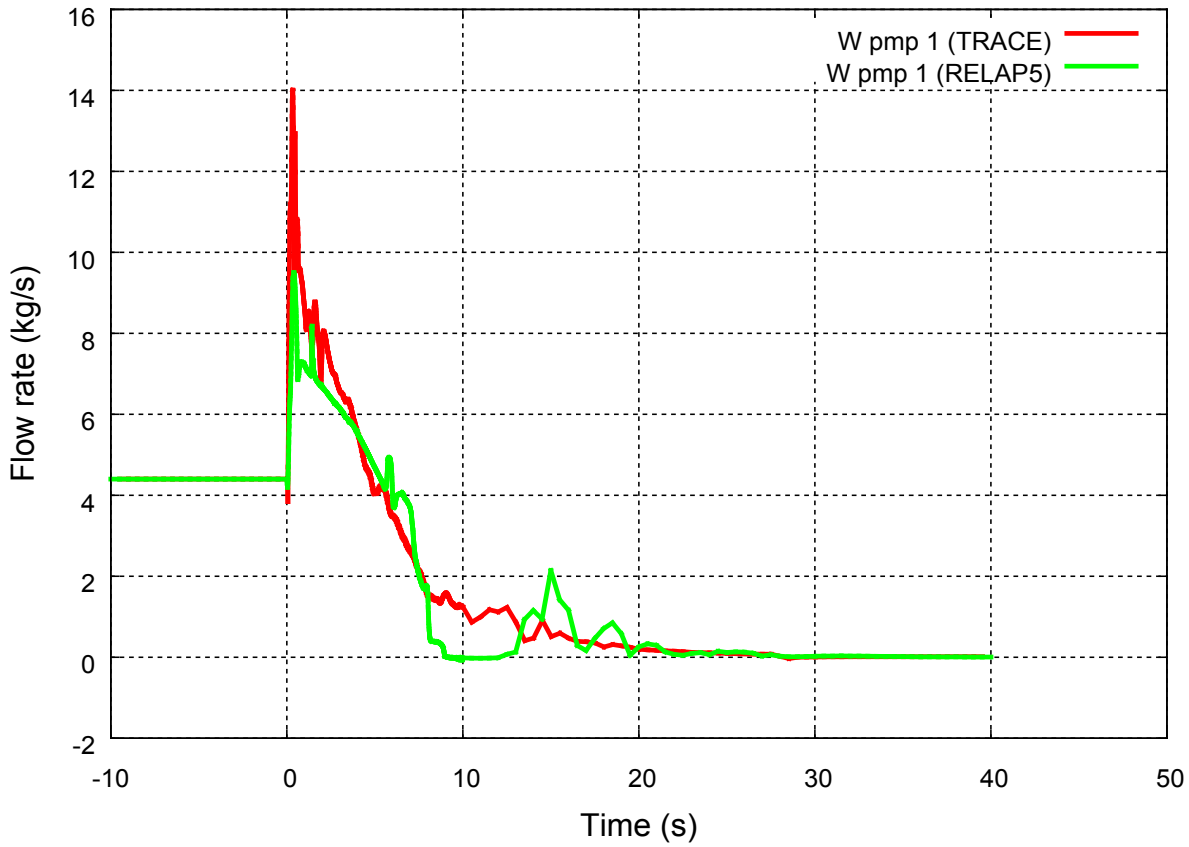

Figure A-5 Mass flow rate through pump 1 in the intact loop.

4.4 kg/s in steady state. The speed of the main recirculation pump P1 is controlled by the control system to reproduce the measured mass flows.

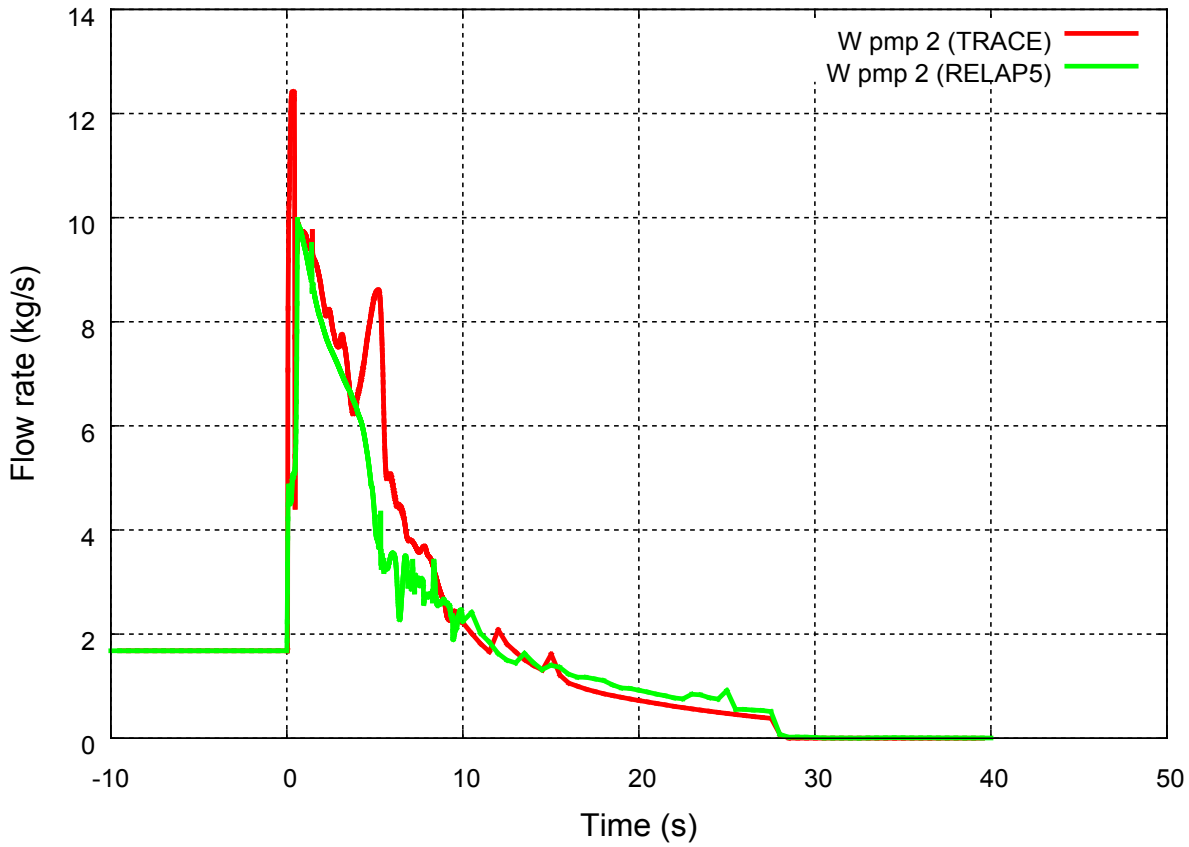

Figure A-6 Mass flow rate through pump 2 in the break pipe line.

1.68 kg/s in steady state. The speed of the main recirculation pump P2 is controlled by the control system to reproduce the measured mass flows.

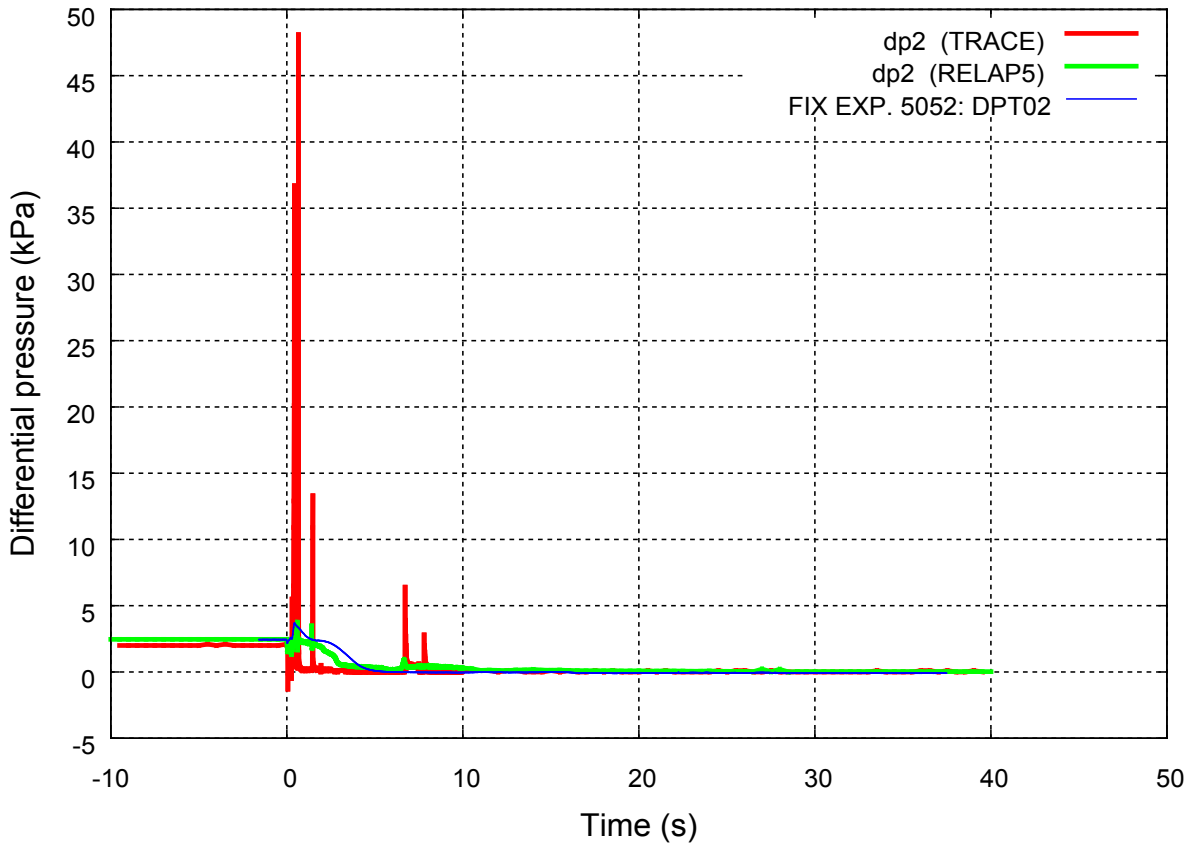

Figure A-7 Differential pressure in the lower plenum.

In the lower plenum, the flow from the intact recirculation line entered from one side, mixed with the downwards directed two-phase flow from the bundle, and passed out on the opposite side into the broken recirculation line. The fluid in the LP was quickly heated by the bundle flow to saturation temperature, which was reached after only 1.8 s, flashing took consequently place, which depleted the LP of most of its water after 5 s.

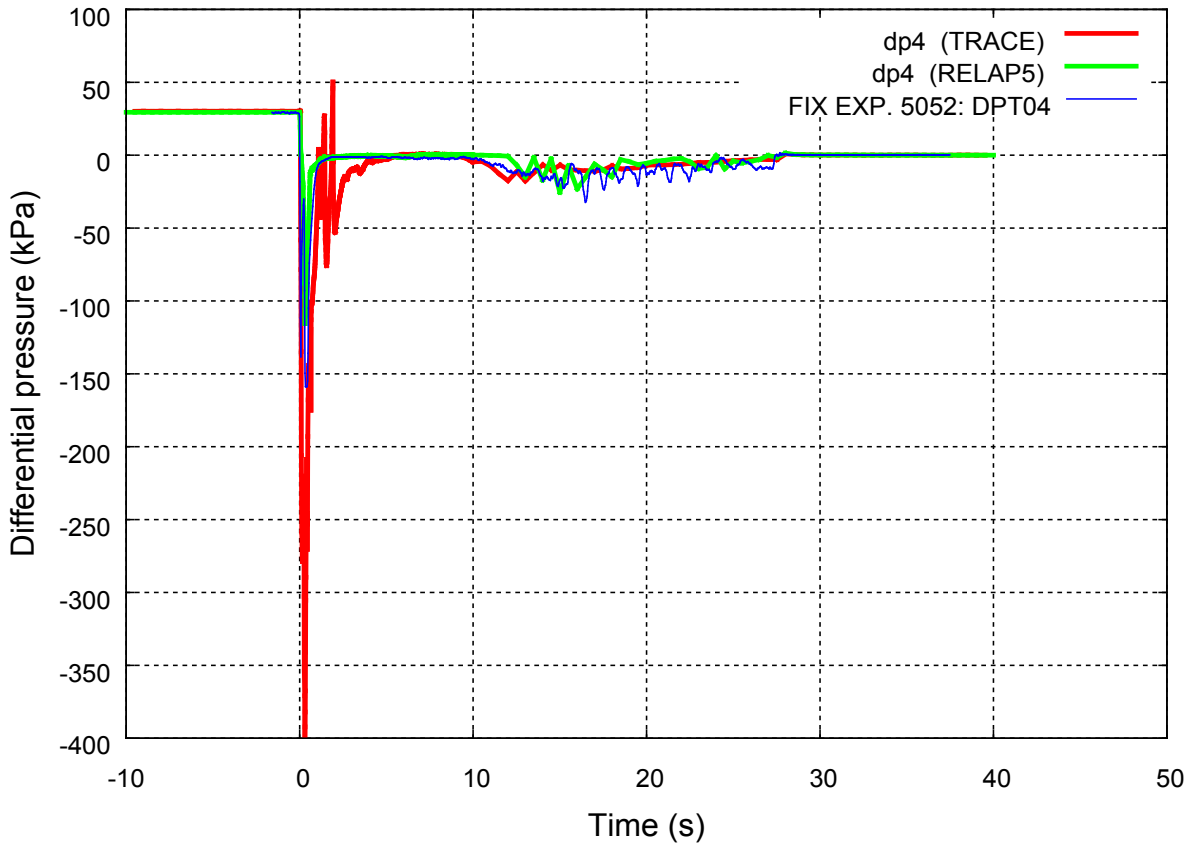

Figure A-8 Differential pressure over the bundle inlet restriction.

The core inlet flow reversed immediately after opening of the break valve 120 and the negative flow direction was then maintained throughout the blowdown period.

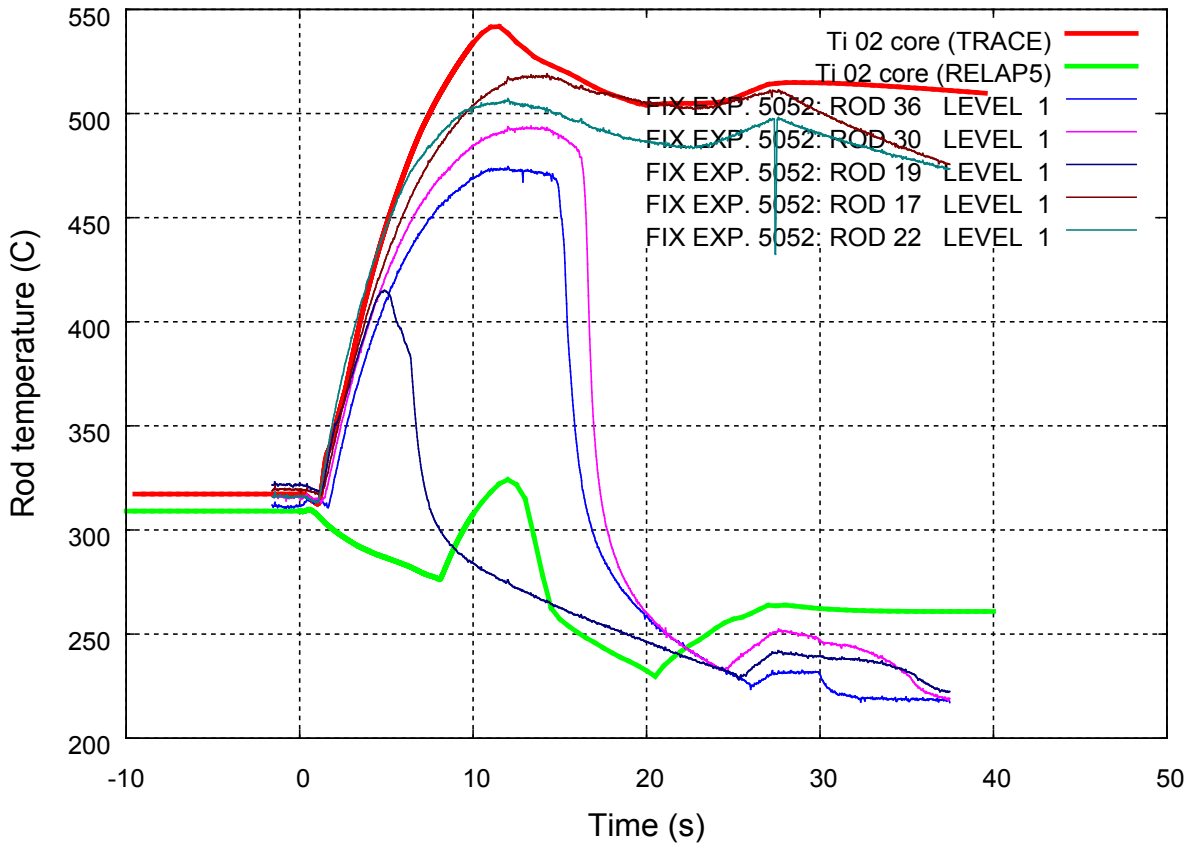

Figure A-9 Rod temperature at cell 2 level.

The heated rod is divided into 25 cells, cell 1 is at the bottom level and cell 25 is at the top of the core.

The TRACE analysis reveals good prediction of dryout onset and the maximum rod temperature at this level, and no rewetting was predicted.

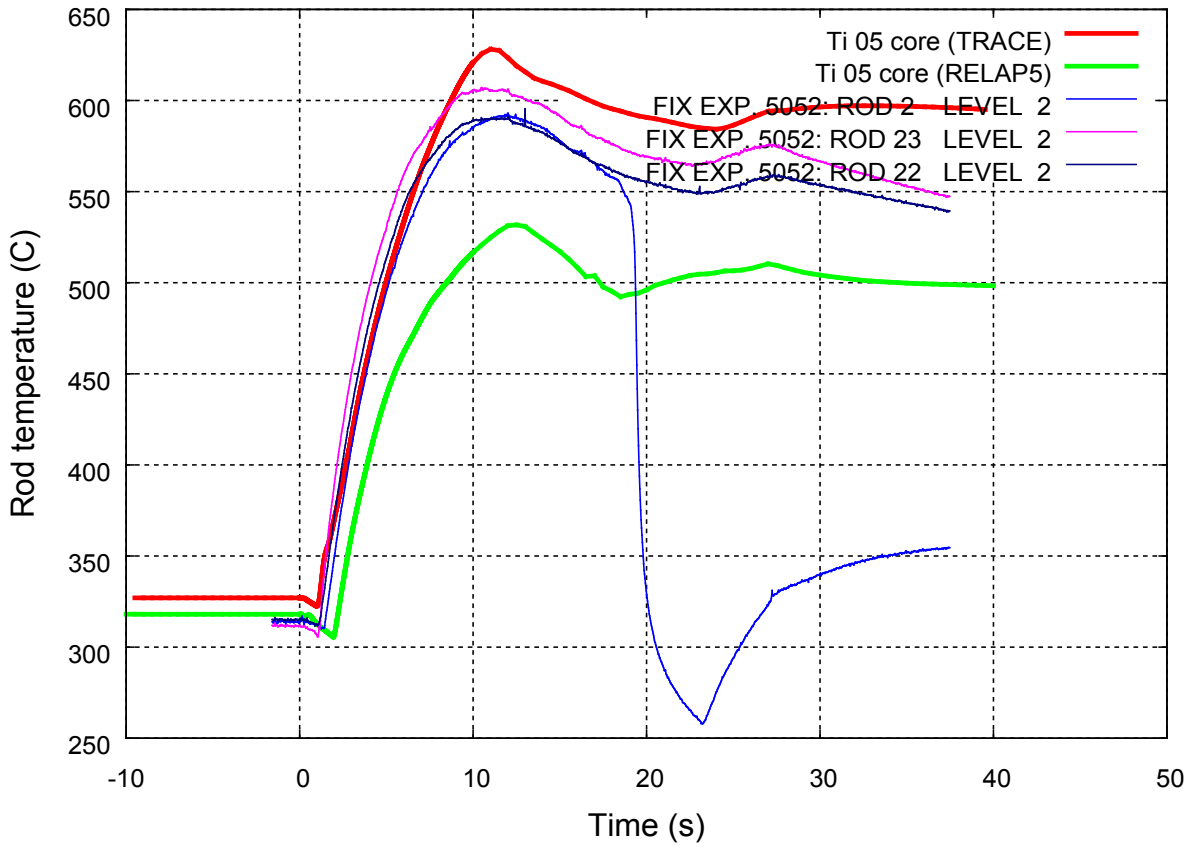

Figure A-10 Rod temperature at cell 5 level

The heated rod is divided into 25 cells, cell 1 is at the bottom level and cell 25 is at the top of the core.

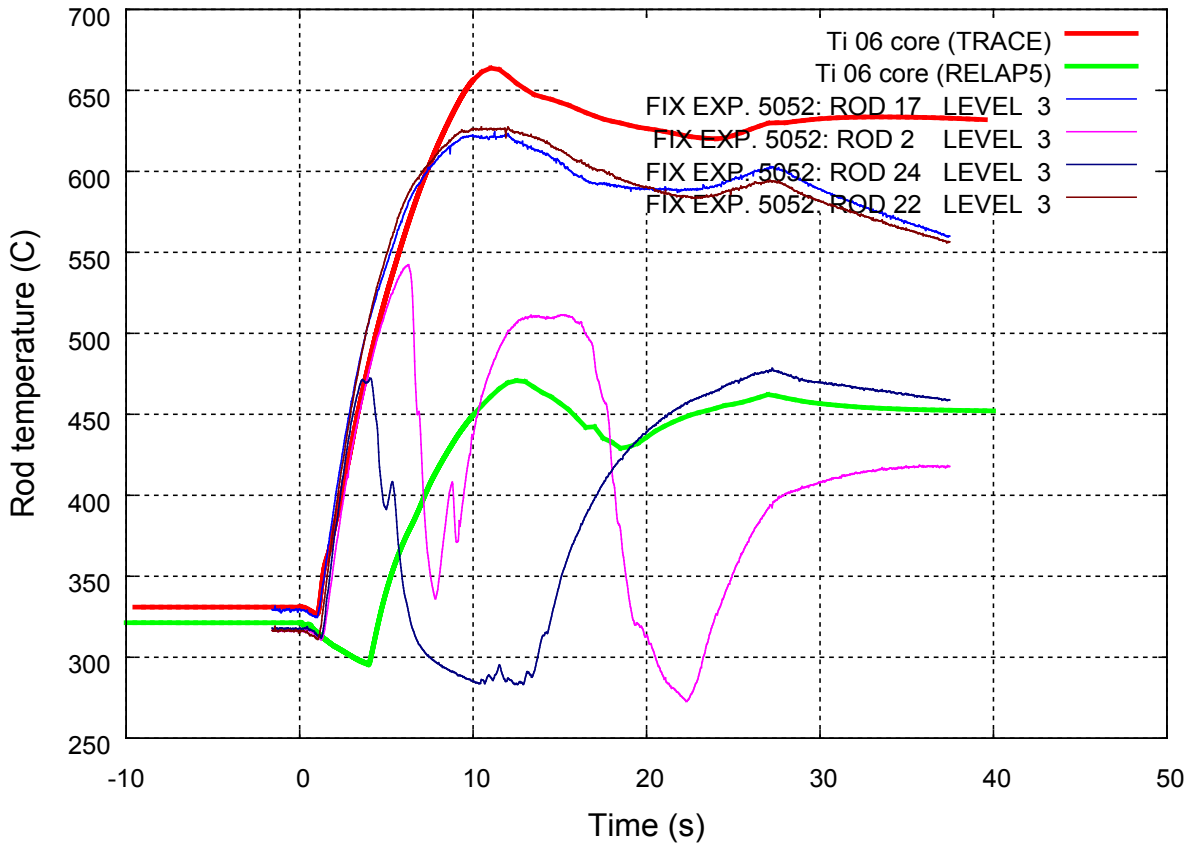

Figure A-11 Rod temperature at cell 6 level.

The heated rod is divided into 25 cells, cell 1 is at the bottom level and cell 25 is at the top of the core.

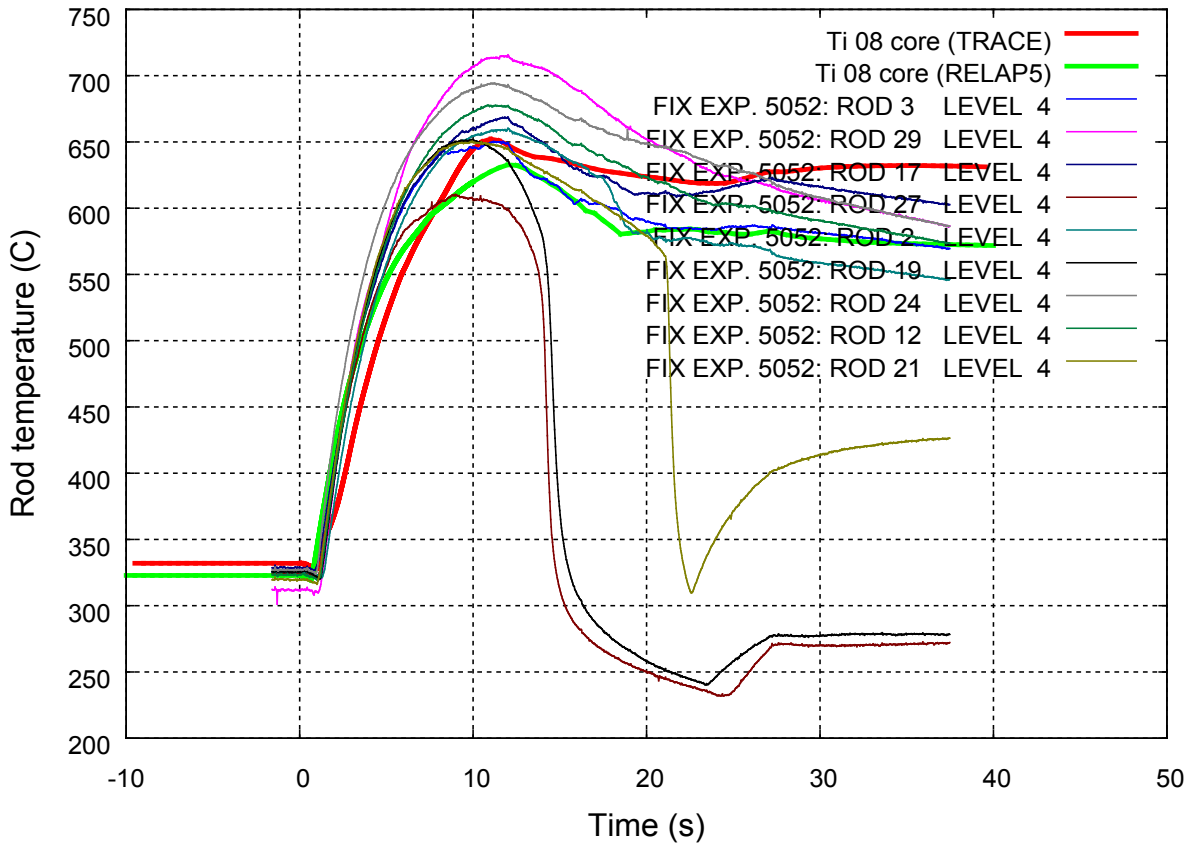

Figure A-12 Rod temperature at cell 8 level.

The heated rod is divided into 25 cells, cell 1 is at the bottom level and cell 25 is at the top of the core.

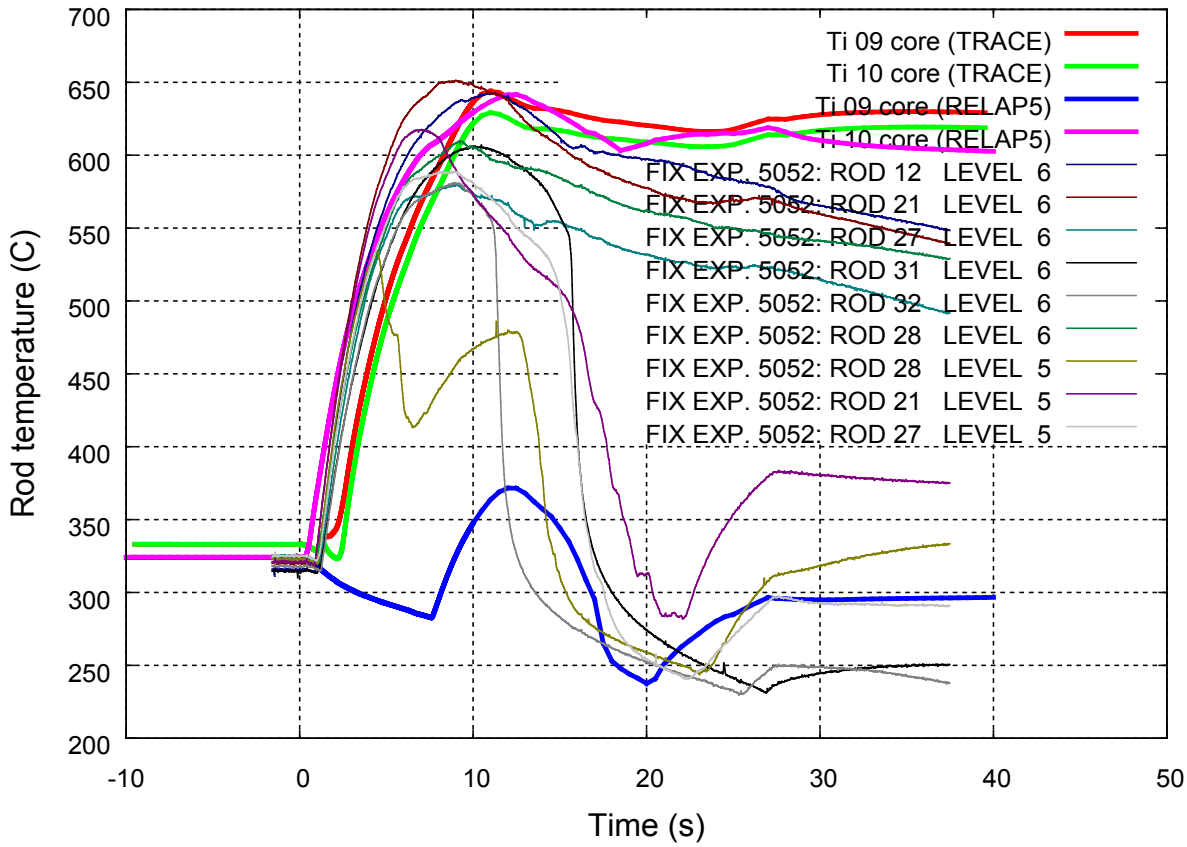

Figure A-13 Rod temperature at cell 9, 10 levels.

The heated rod is divided into 25 cells, cell 1 is at the bottom level and cell 25 is at the top of the core.

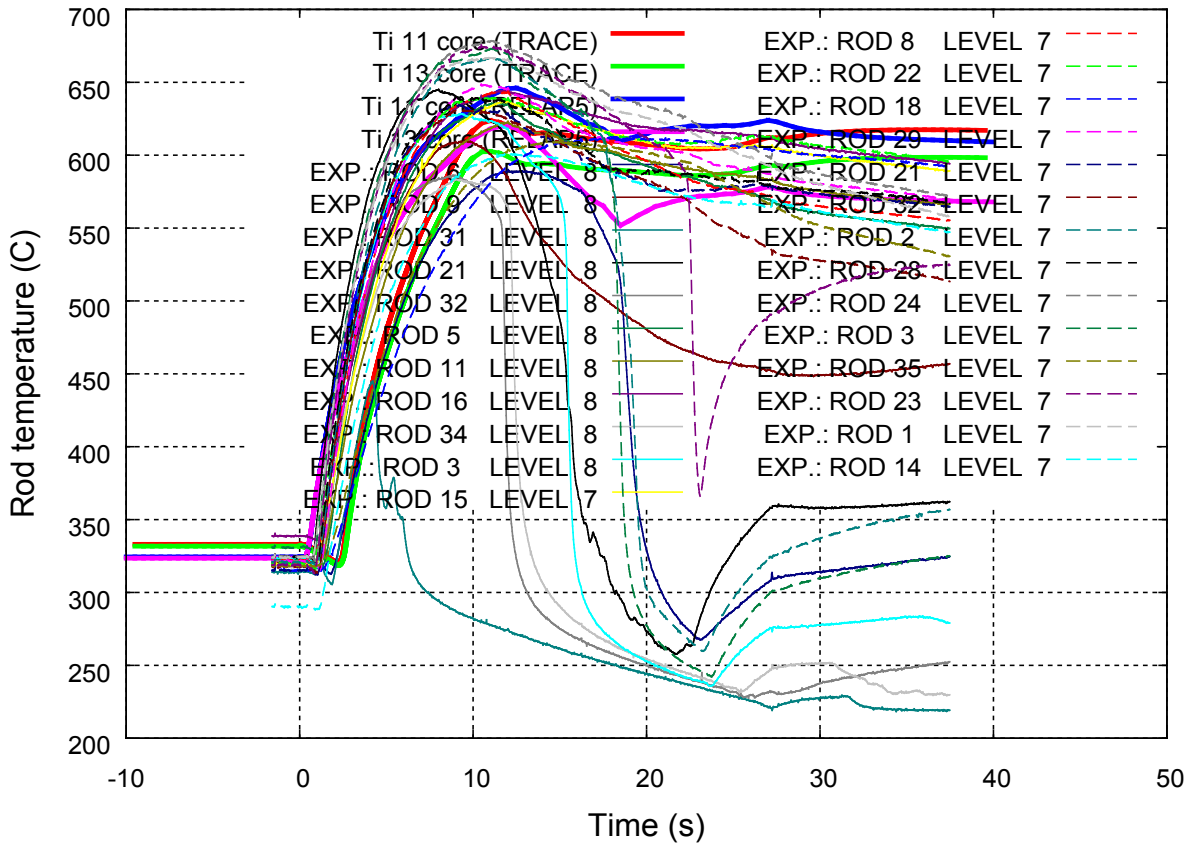

Figure A-14 Rod temperature at cell 11, 13 levels.

The heated rod is divided into 25 cells, cell 1 is at the bottom level and cell 25 is at the top of the core.

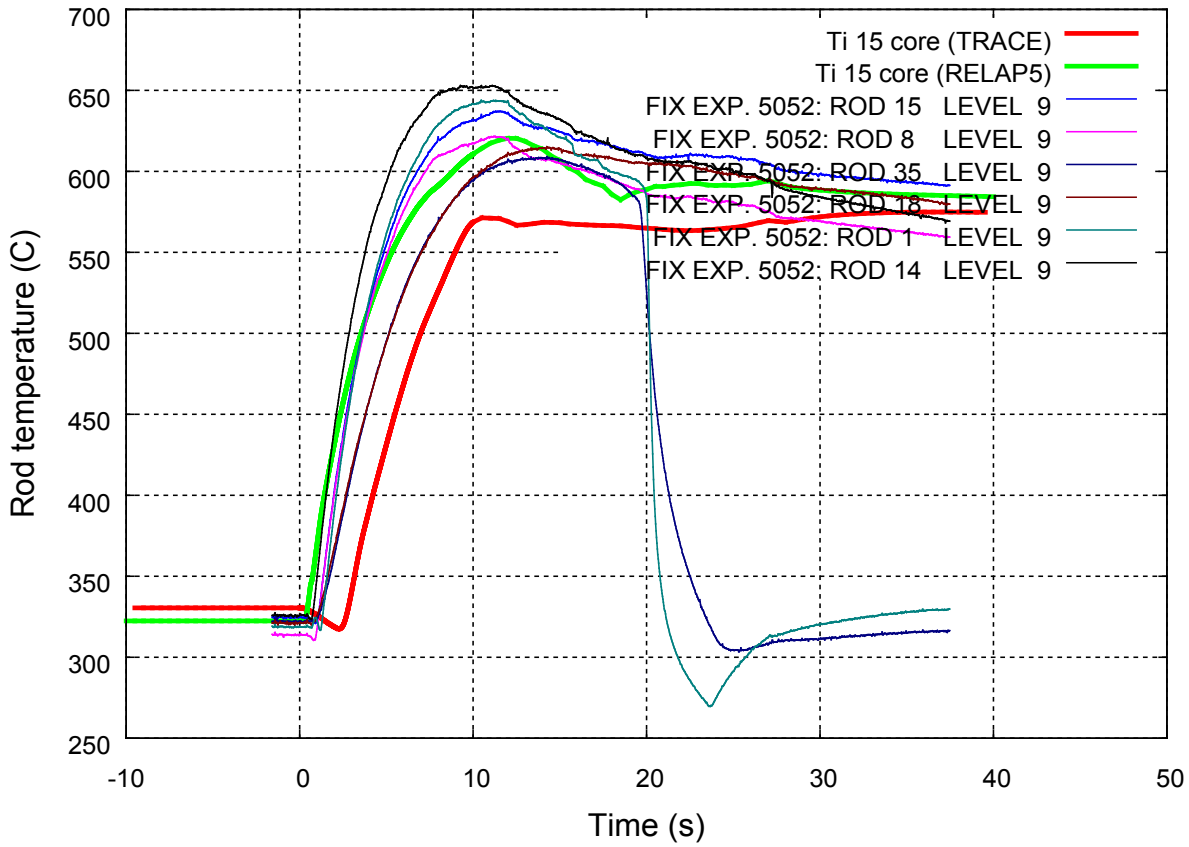

Figure A-15 Rod temperature at cell 15 level.

The heated rod is divided into 25 cells, cell 1 is at the bottom level and cell 25 is at the top of the core.

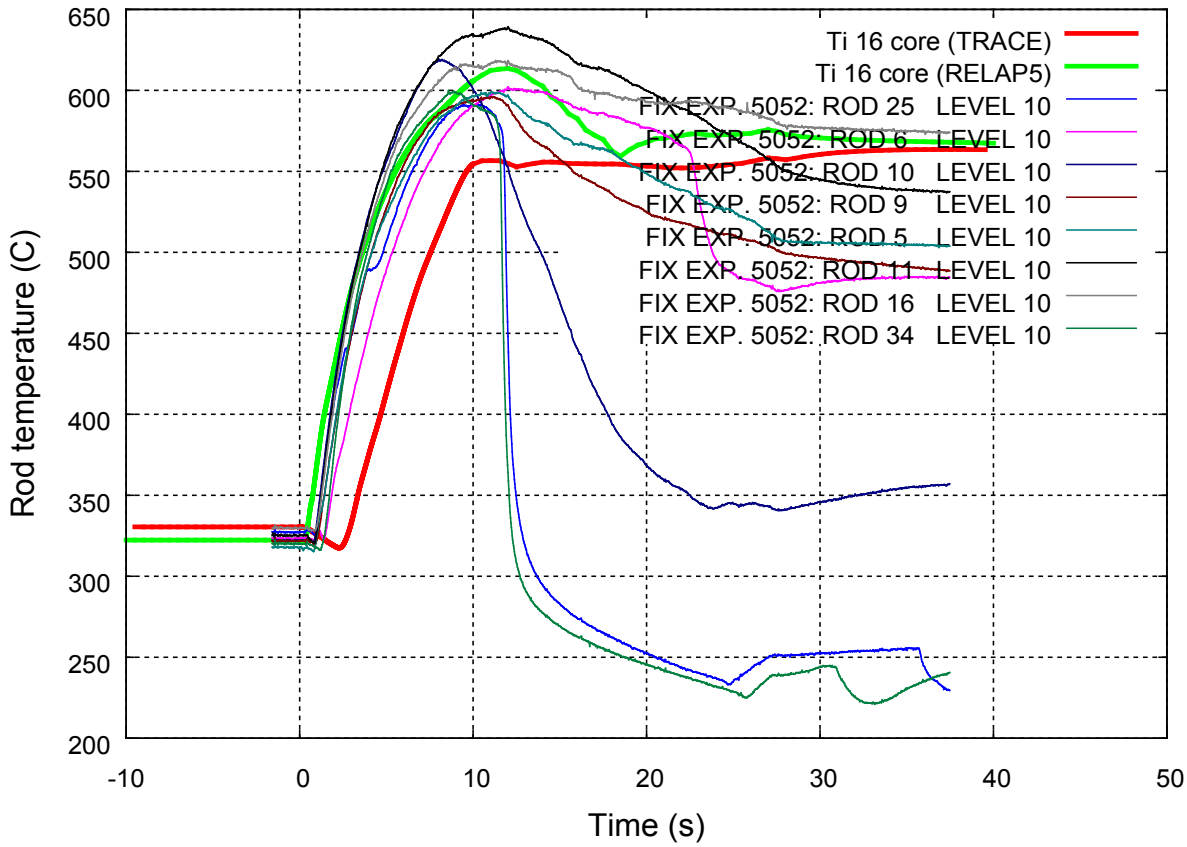

Figure A-16 Rod temperature at cell 16 level.

The heated rod is divided into 25 cells, cell 1 is at the bottom level and cell 25 is at the top of the core.

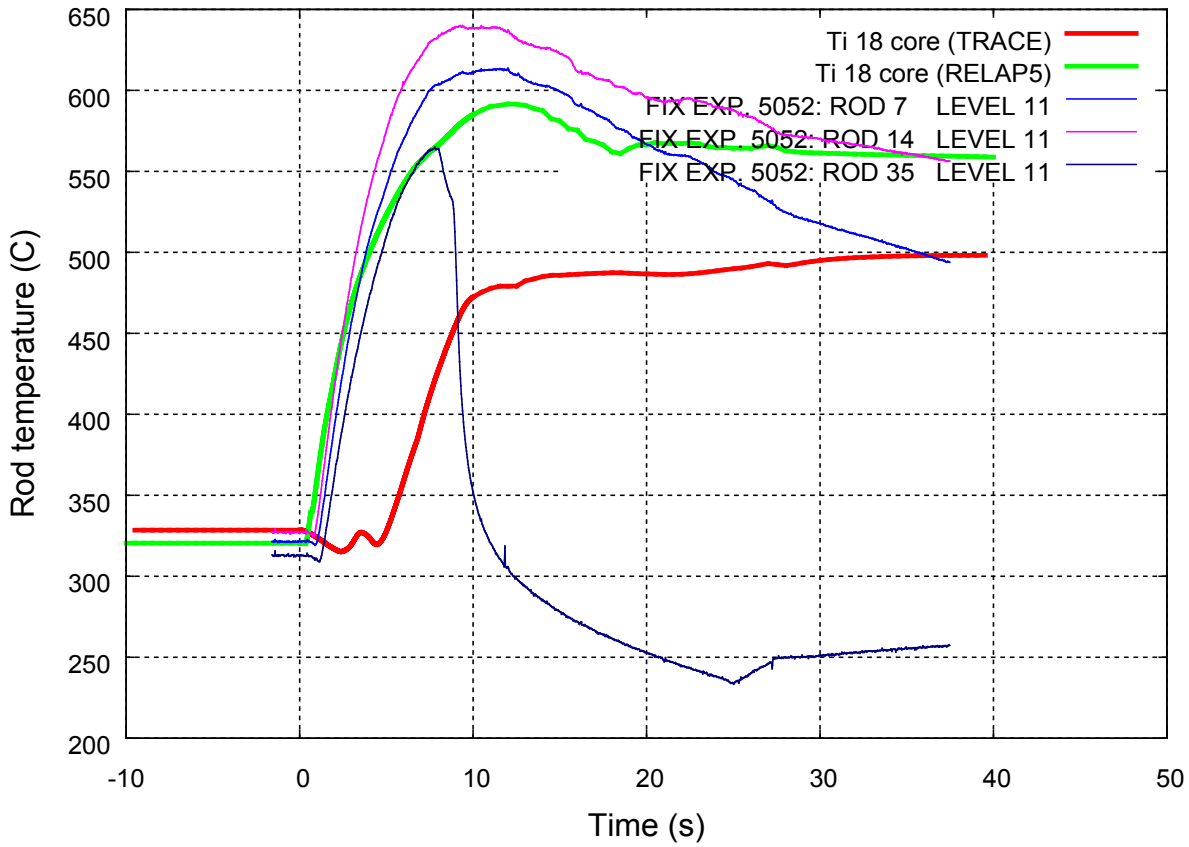

Figure A-17 Rod temperature at cell 18 level.

The heated rod is divided into 25 cells, cell 1 is at the bottom level and cell 25 is at the top of the core.

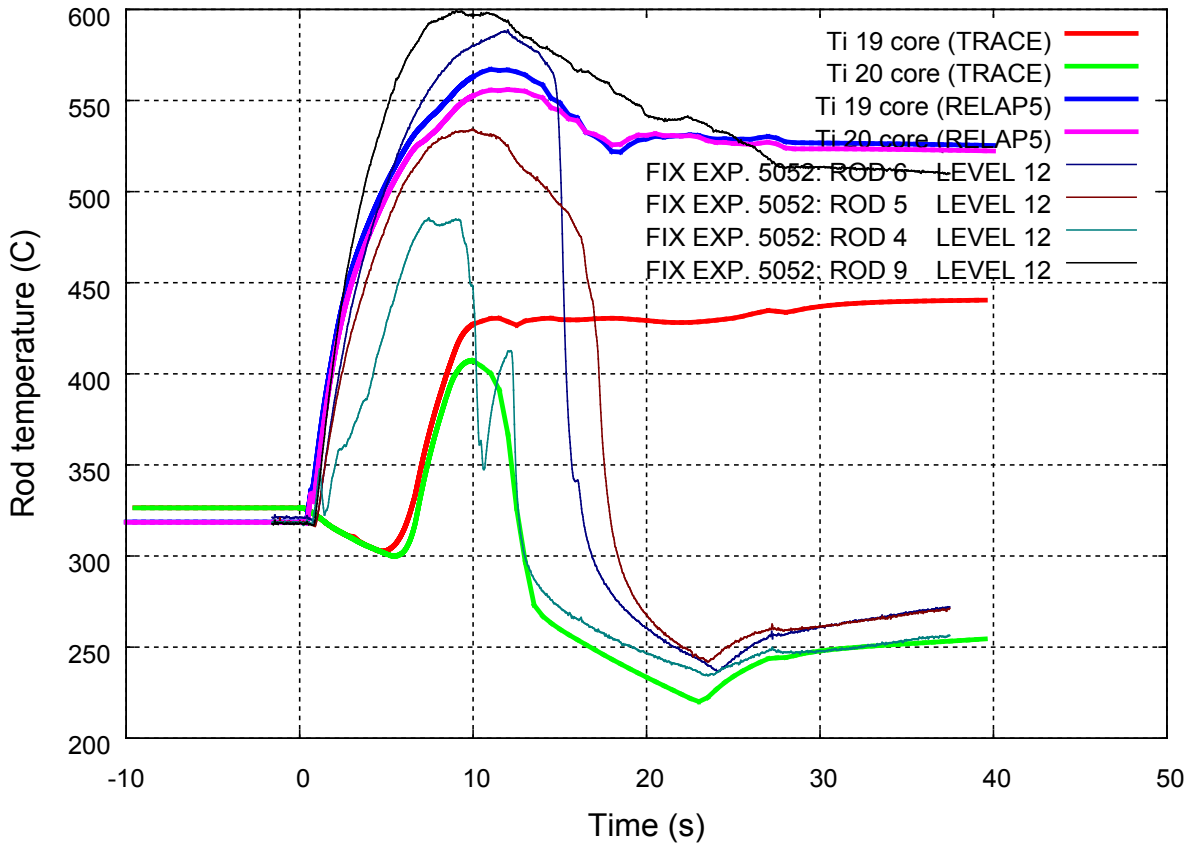

Figure A-18 Rod temperature at cell 19, 20 levels.

The heated rod is divided into 25 cells, cell 1 is at the bottom level and cell 25 is at the top of the core.

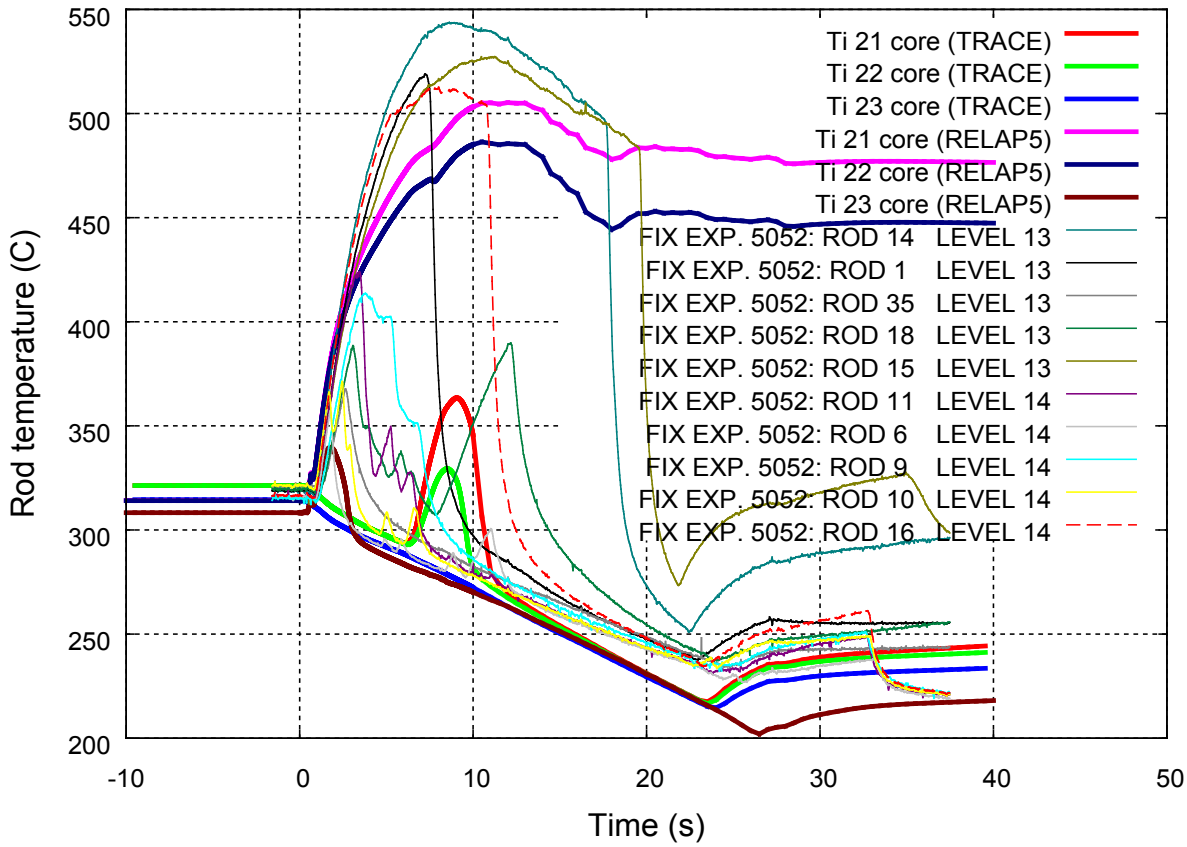

Figure A-19 Rod temperature at cell 21, 22, 23 levels.

The heated rod is divided into 25 cells, cell 1 is at the bottom level and cell 25 is at the top of the core.

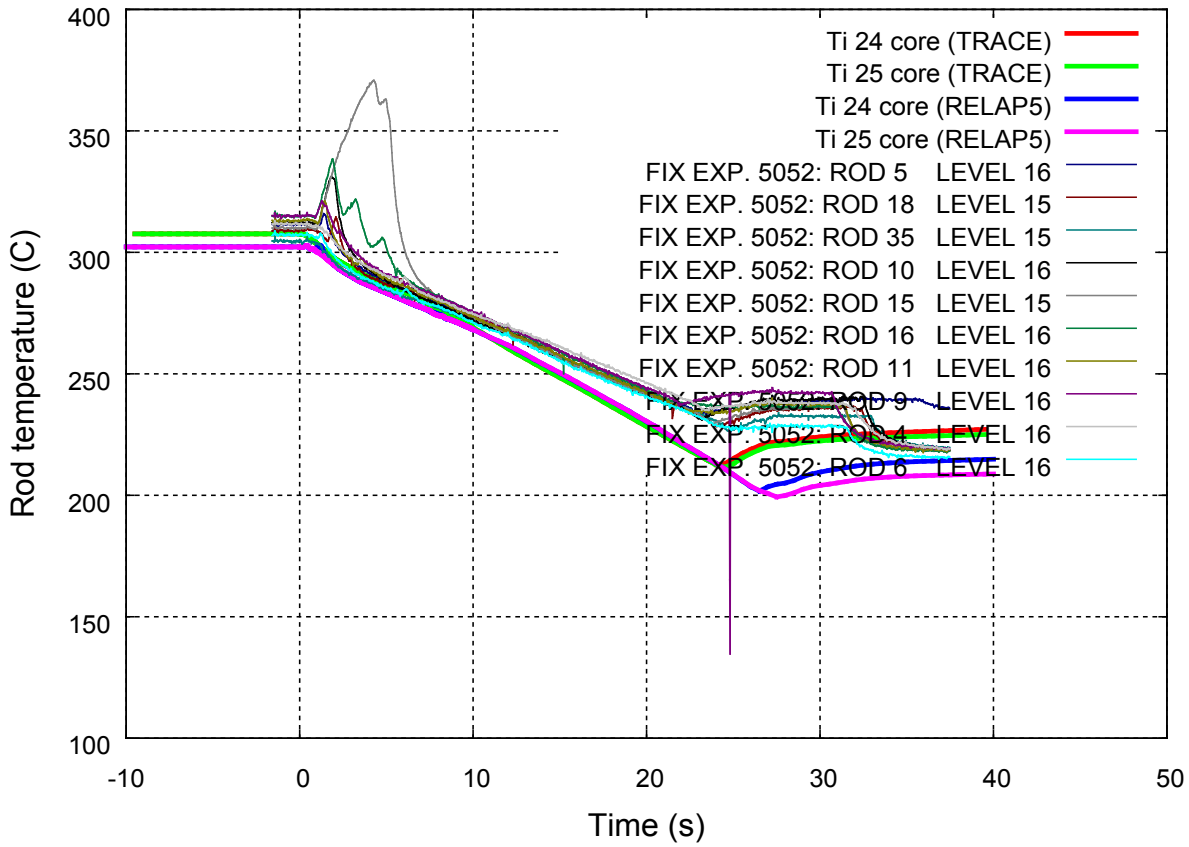

Figure A-20 Rod temperature at cell 24 level.

The heated rod is divided into 25 cells, cell 1 is at the bottom level and cell 25 is at the top of the core.

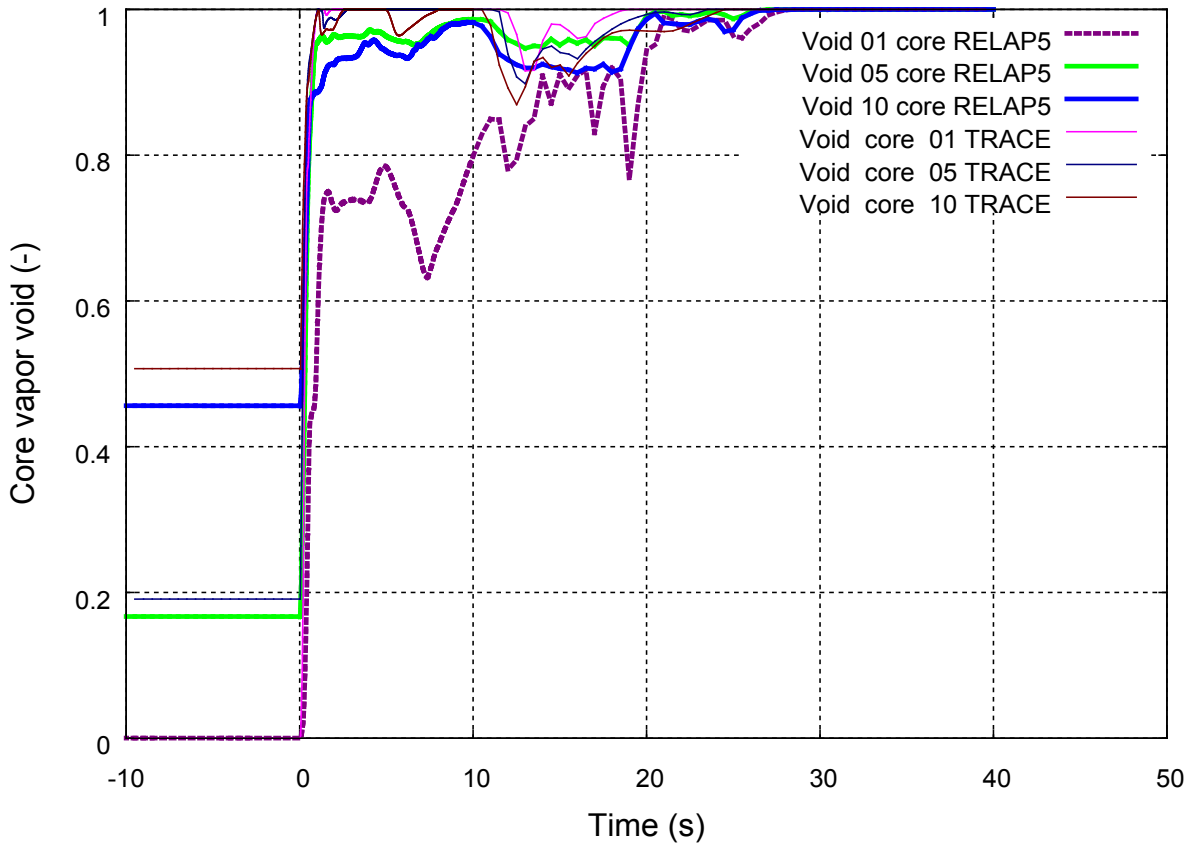

Figure A-21 Void distribution along the core at nodes 1, 5, 10

The core is divided into 26 nodes, node 1 is at the bottom level and node 26 is at the top of the core.

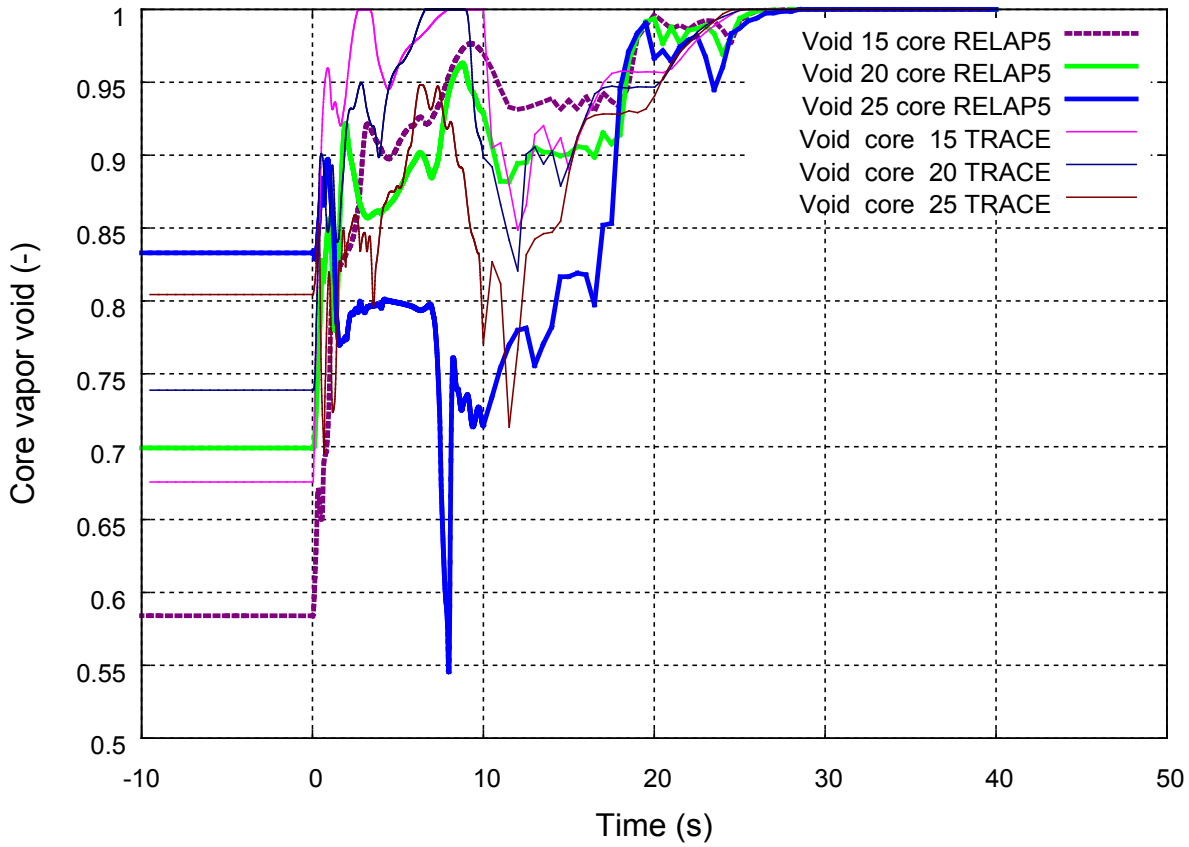

Figure A-22 Void distribution along the core at nodes 15, 20, 25.

The core is divided into 26 nodes, node 1 is at the bottom level and node 26 is at the top of the core.

APPENDIX B RESULT PLOTS OF FIX-II EXPERIMENT 4011

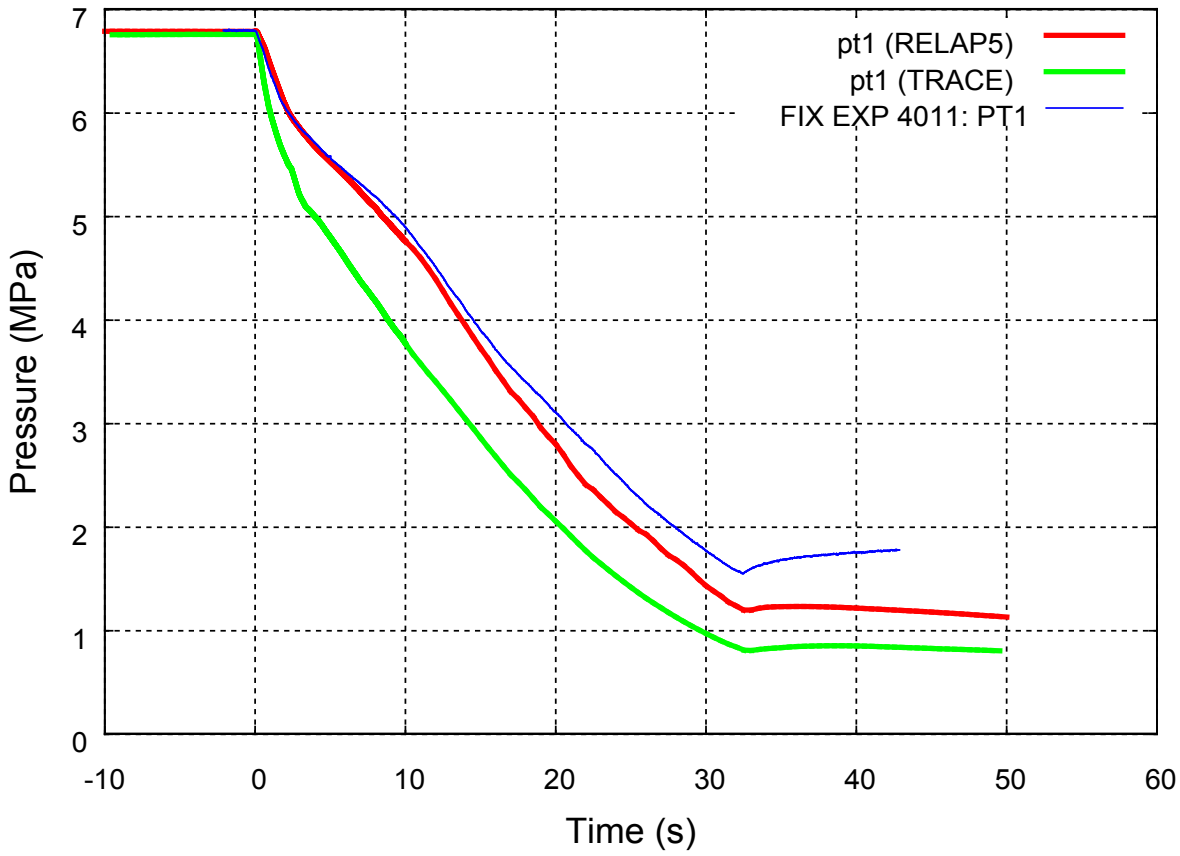

Figure B-1 Pressure in the steam dome.

The steam dome pressure dropped rapidly. The pressure decrease became less pronounced after the closure of the spray and feed water flows at about 2 s. The pressure drops a little faster in the analysis compared to the experimental result.

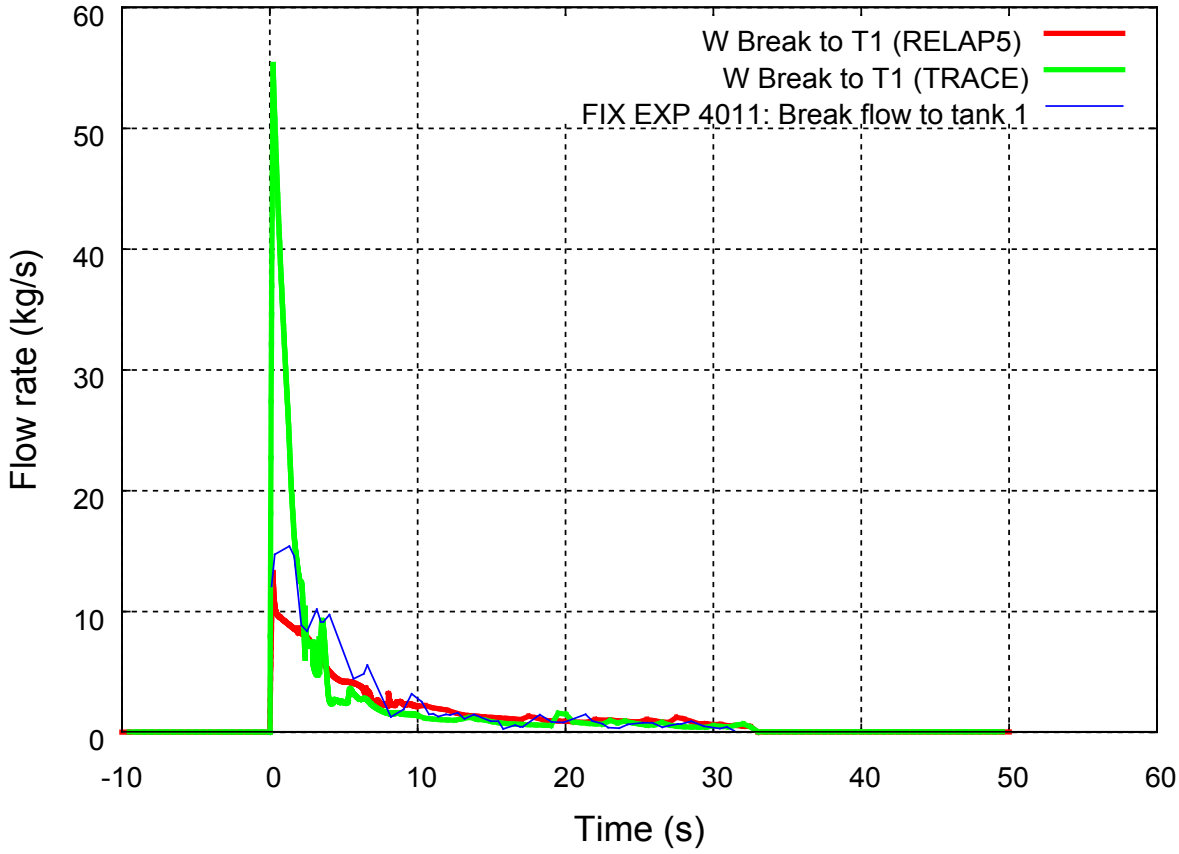

Figure B-2 Break mass flow rate into tank T1.

The break valve V123 (restriction nozzle I.D. 16 mm) starts to open at 0 s. A maximum mass flow rate was obtained immediately after the valve opened. However, the break mass flow rate measurement was uncertain as is mentioned in [4].

The analysis results are based on the critical flow model with both the subcooled and the two-phase discharge coefficient equal to 0.8. The used discharge coefficients reveal acceptable calculated flow rates compared to measured flow rates.

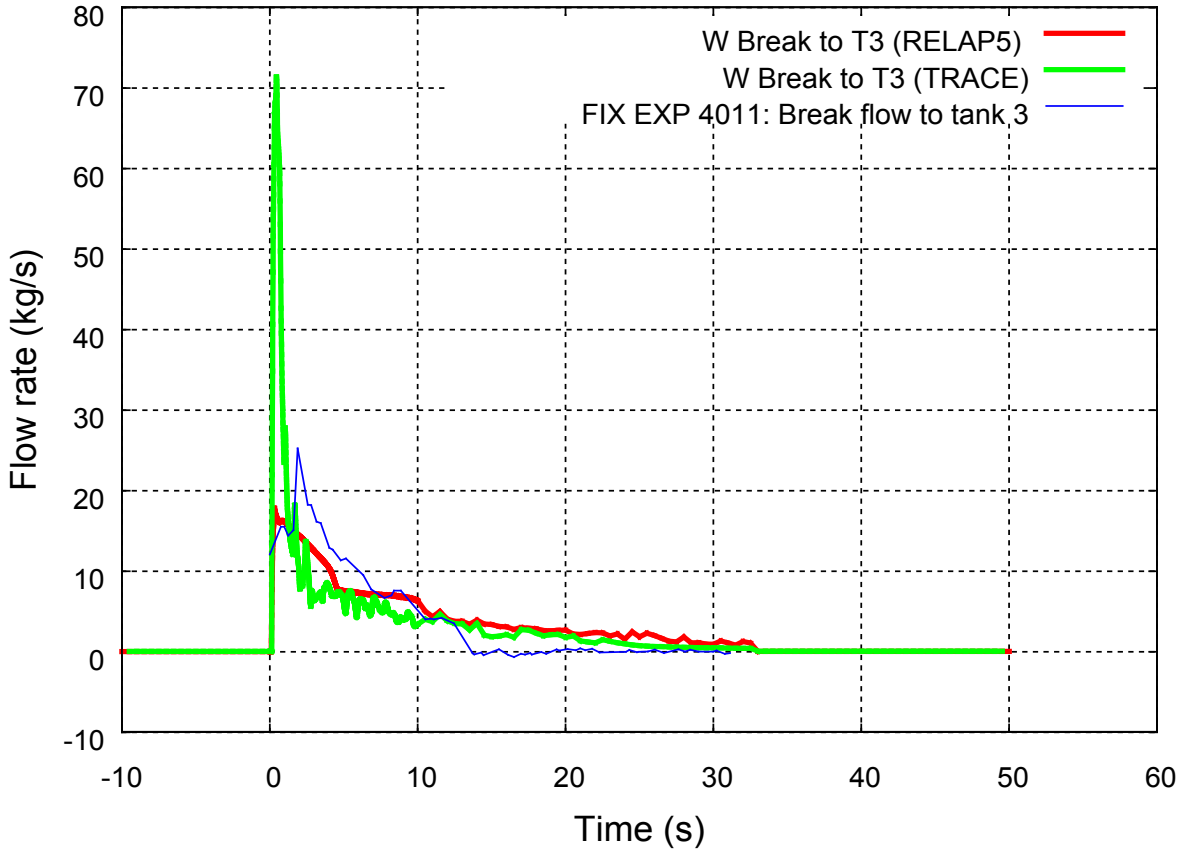

Figure B-3 Break mass flow rate into tank T3.

The break valve V117 (restriction nozzle I.D. 21.6 mm) starts to open at 0.1 s. A maximum mass flow rate was obtained immediately after the valve opened. However, the break mass flow rate measurement was uncertain as is mentioned in Ref. 4.

The analysis results are based on the critical flow model with both the subcooled and the two-phase discharge coefficient equal to 0.8. The used discharge coefficients reveal acceptable calculated flow rates compared to measured flow rates.

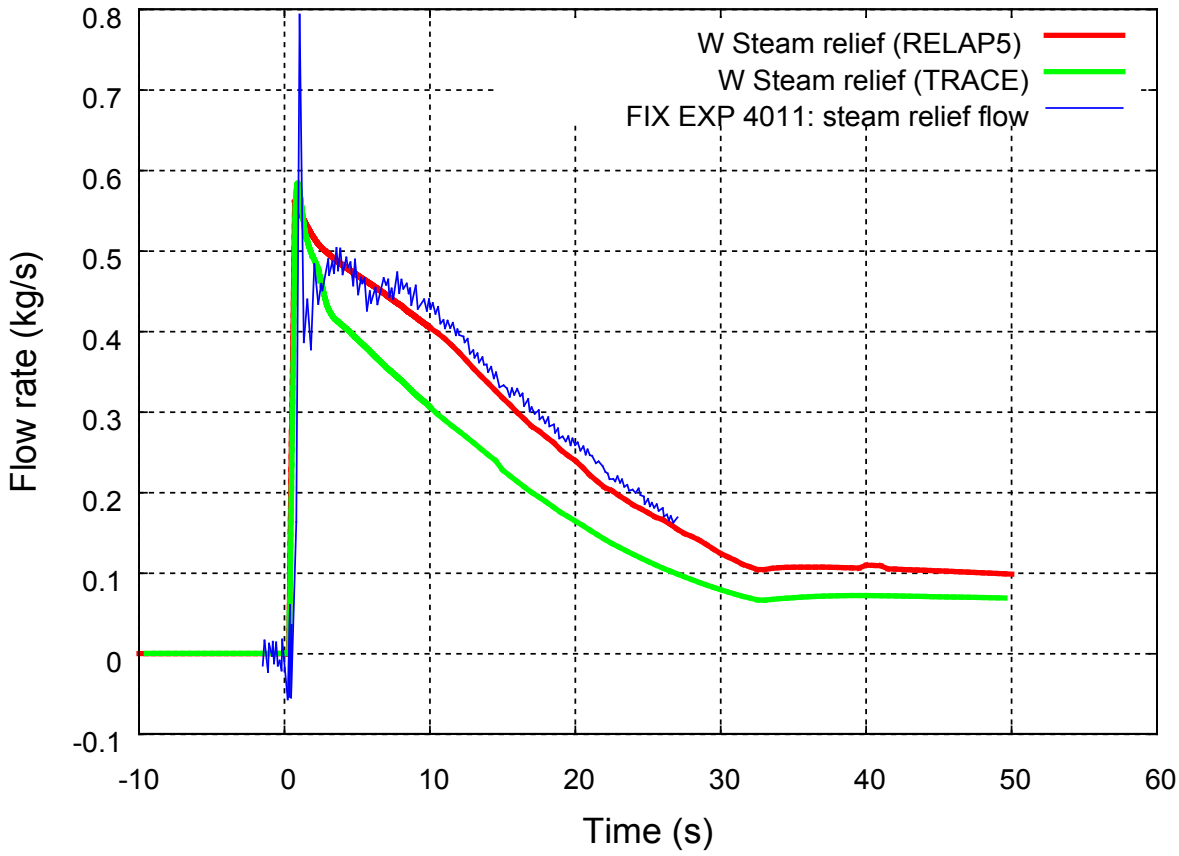

Figure B-4 Mass flow rate of steam through orifice meter K6 in the steam relief valve.

The steam relief valve (flow area 0.56 cm^2) starts to open at 0.3 s, was fully open at 0.7 s and remained so for the rest of the test. A maximum mass flow rate of 0.47 kg/s was obtained in the experiment.

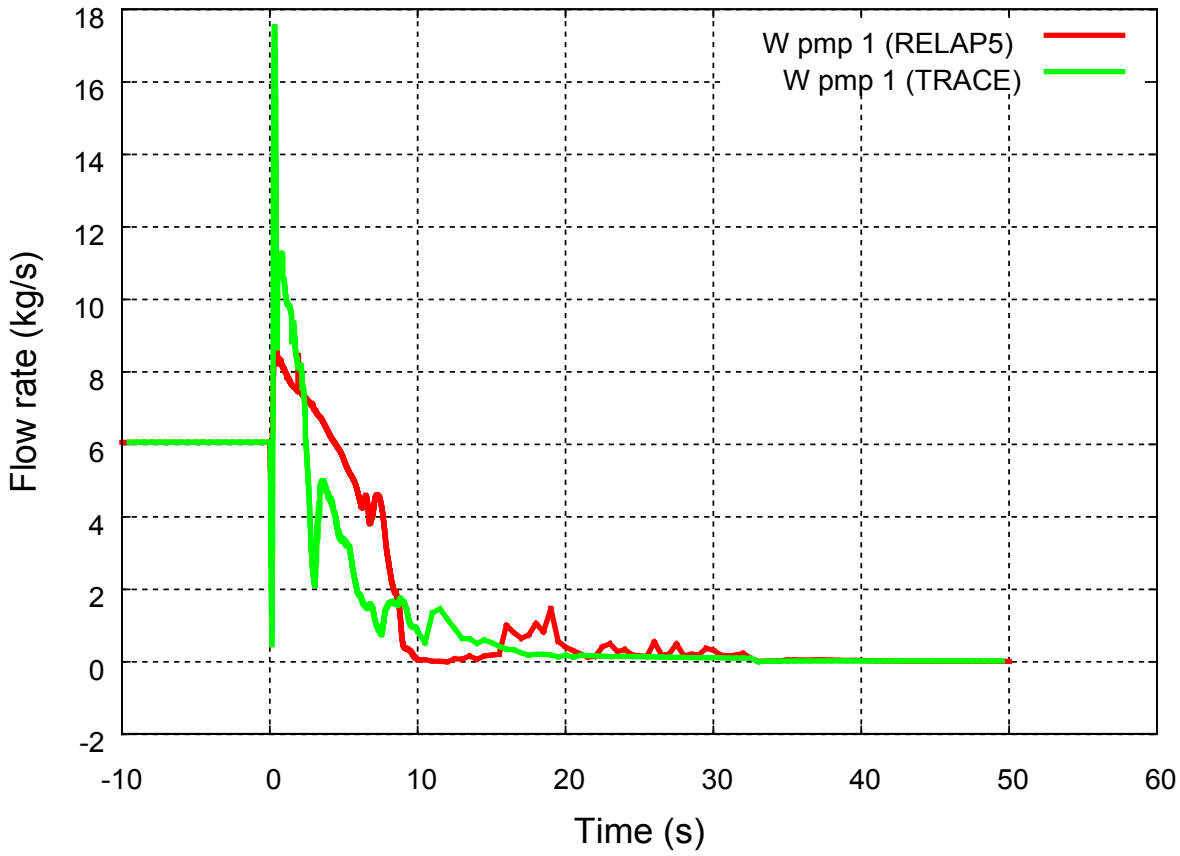

Figure B-5 Mass flow rate through pump 1 in the intact loop.

6.05 kg/s in steady state. The speed of the main recirculation pump P1 is controlled by the control system to reproduce the measured mass flows.

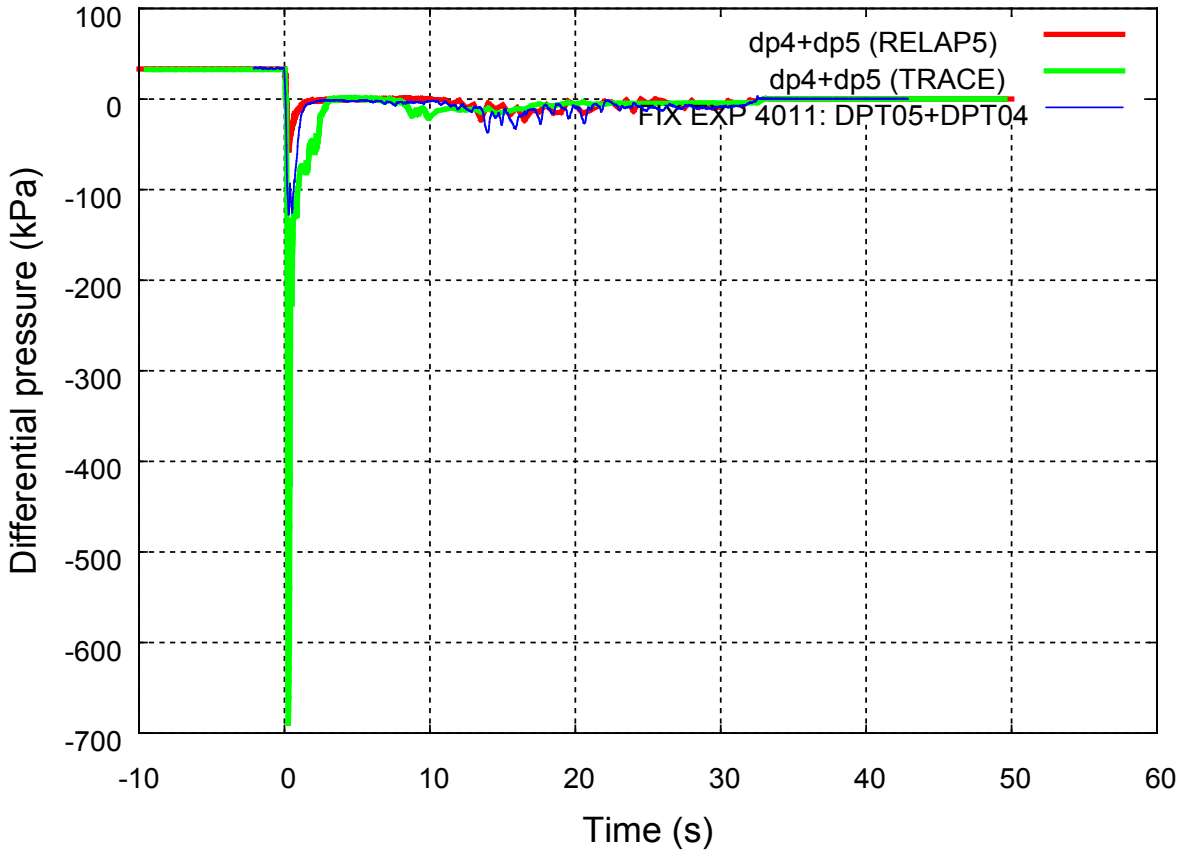

Figure B-6 Differential pressure over the bundle inlet restriction.

The depressurization through the breaks made the inlet flow to the bundle be reversed immediately. The negative flow direction was then maintained throughout the blowdown period.

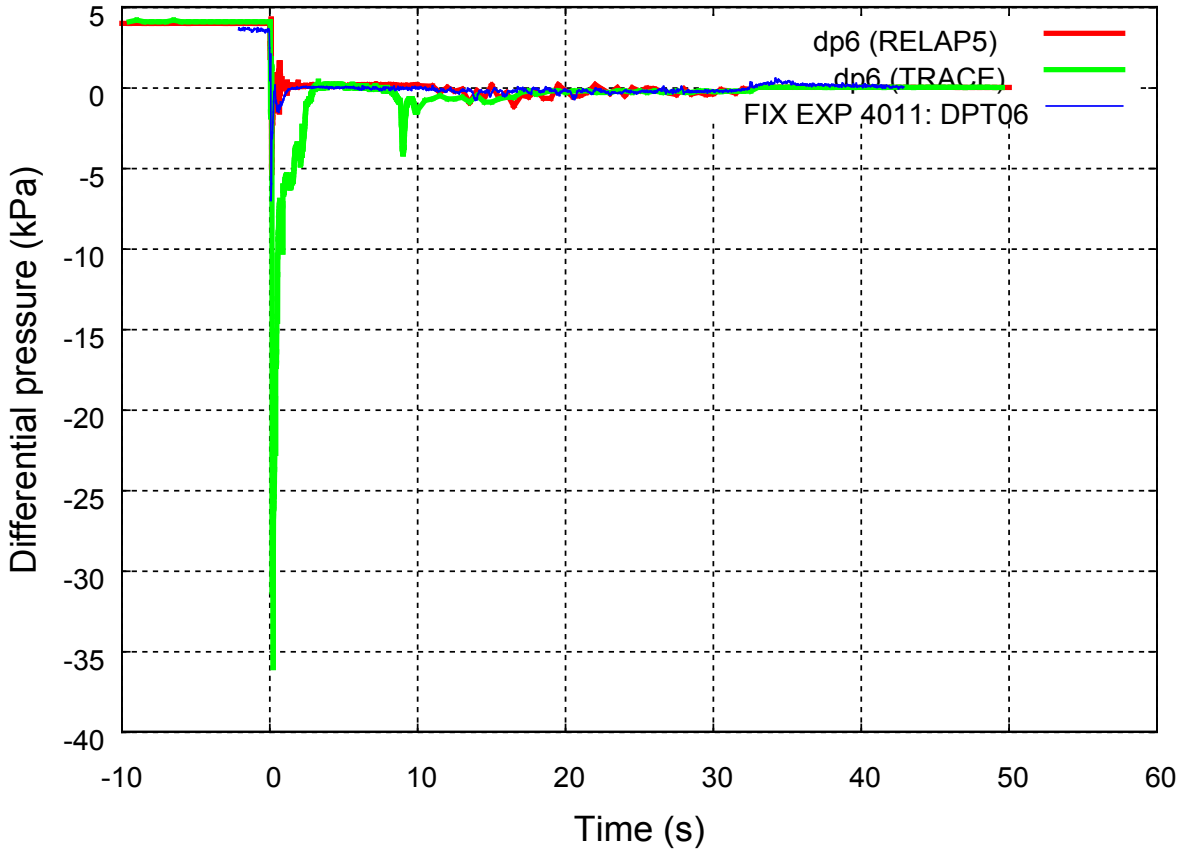

Figure B-7 Differential pressure over subdivisions in the lower part of the bundle.

The core flow reversed immediately after opening of the break valve 123, and decreased quickly to almost to 0.

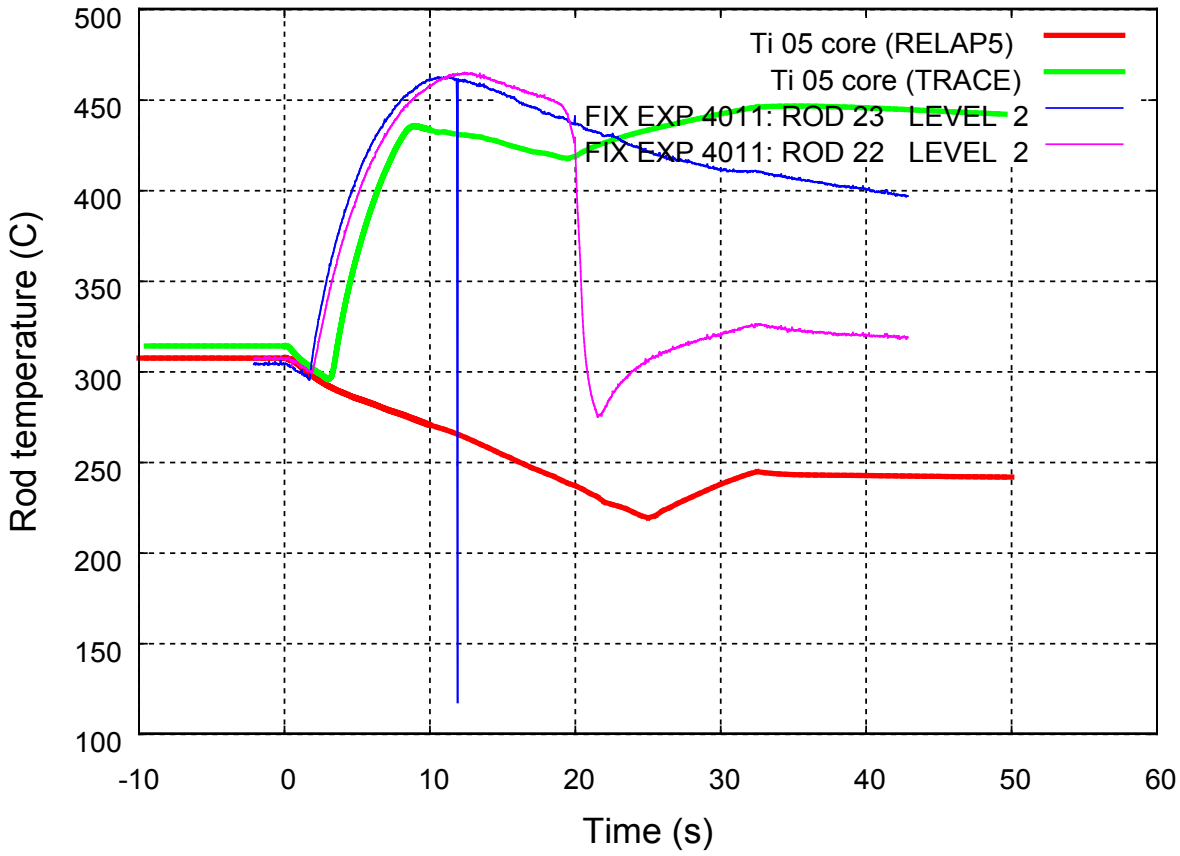

Figure B-8 Rod temperature at cell 5 level.

The heated rod is divided into 25 cells, cell 1 is at the bottom level and cell 25 is at the top of the core.

The rod temperatures increased to a maximum, then decreased again either slowly with decaying power (for example Rod 23, level 2 in Figure B-8), or rapidly due to rewetting (for example Rod 22, level 2 in Figure B-8). The highest temperature, 520 ^{o}C was obtained on rod No 21, at level 4 after 12 s (Figure B-9). Large variations in the course of the rod temperatures were observed for thermocouple positions at the same level but at different rods.

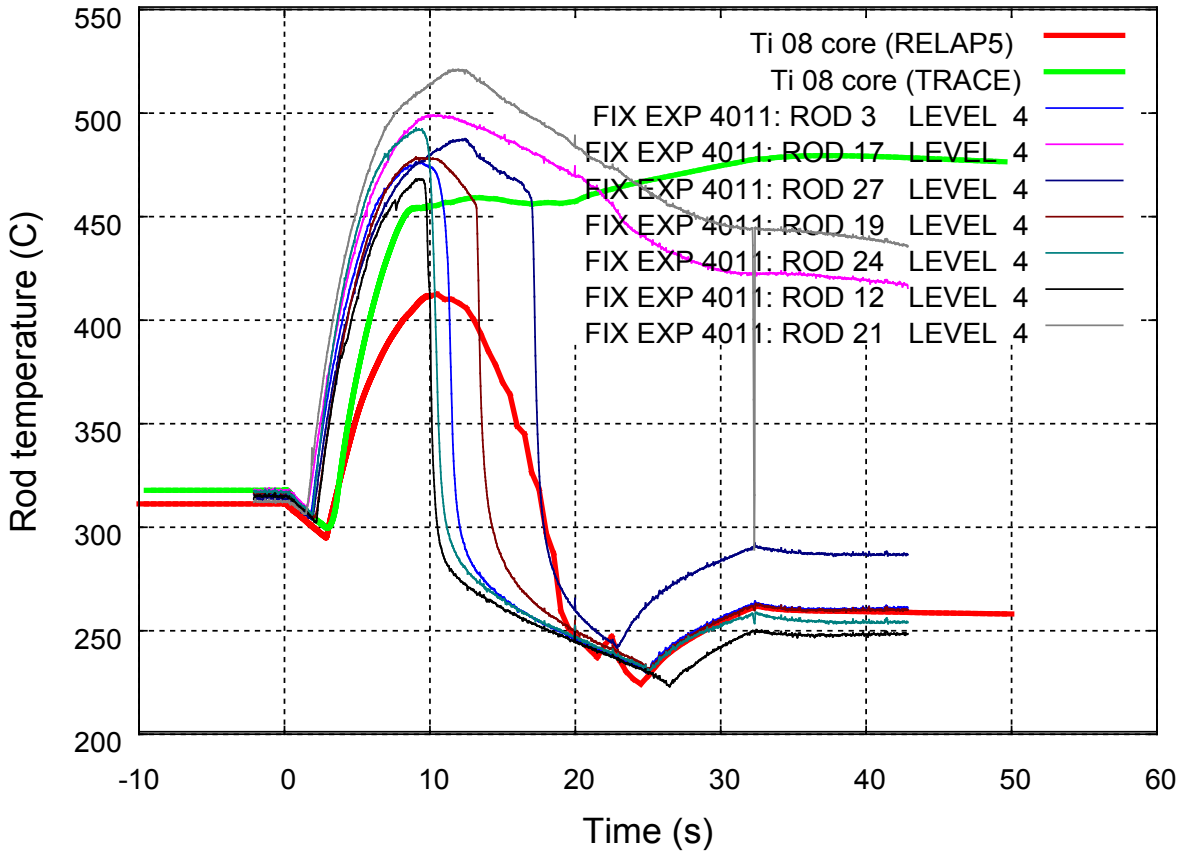

Figure B-9 Rod temperature at cell 8 level.

The heated rod is divided into 25 cells, cell 1 is at the bottom level and cell 25 is at the top of the core.

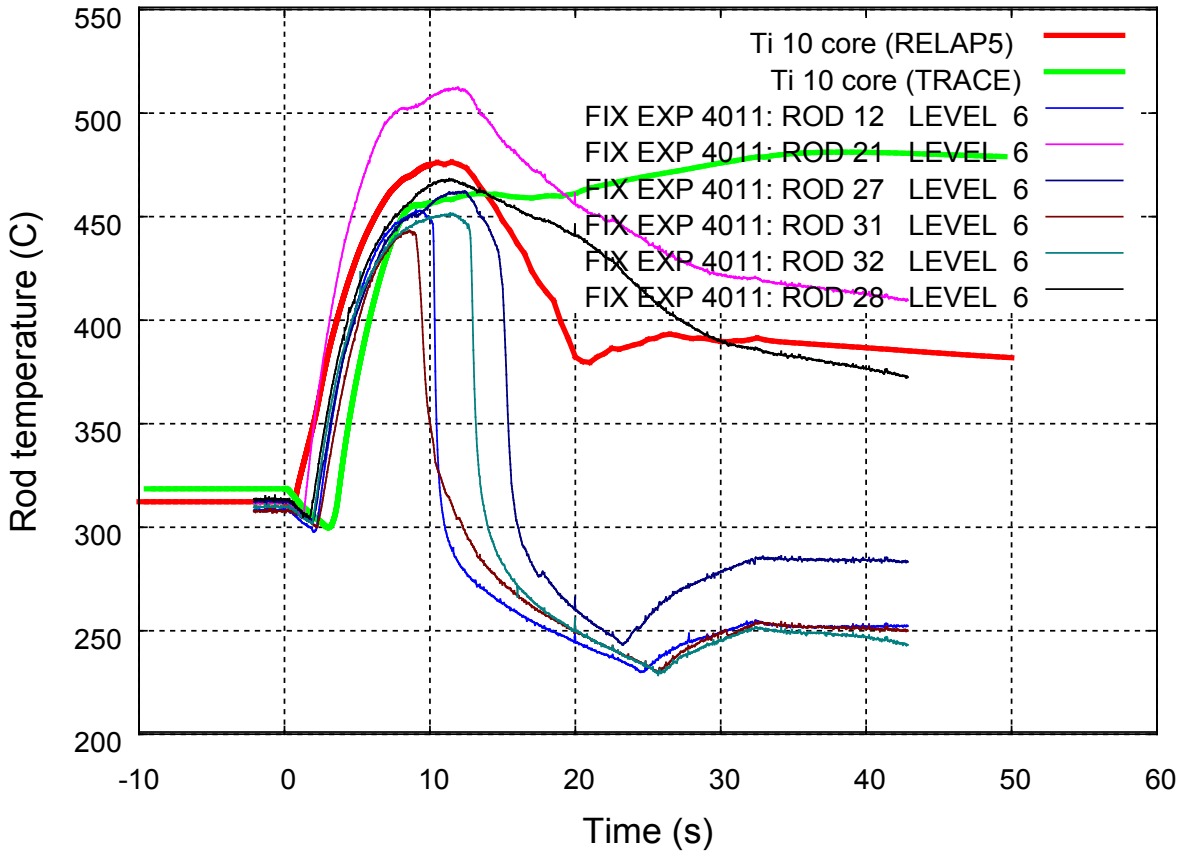

Figure B-10 Rod temperature at cell 10 level.

The heated rod is divided into 25 cells, cell 1 is at the bottom level and cell 25 is at the top of the core.

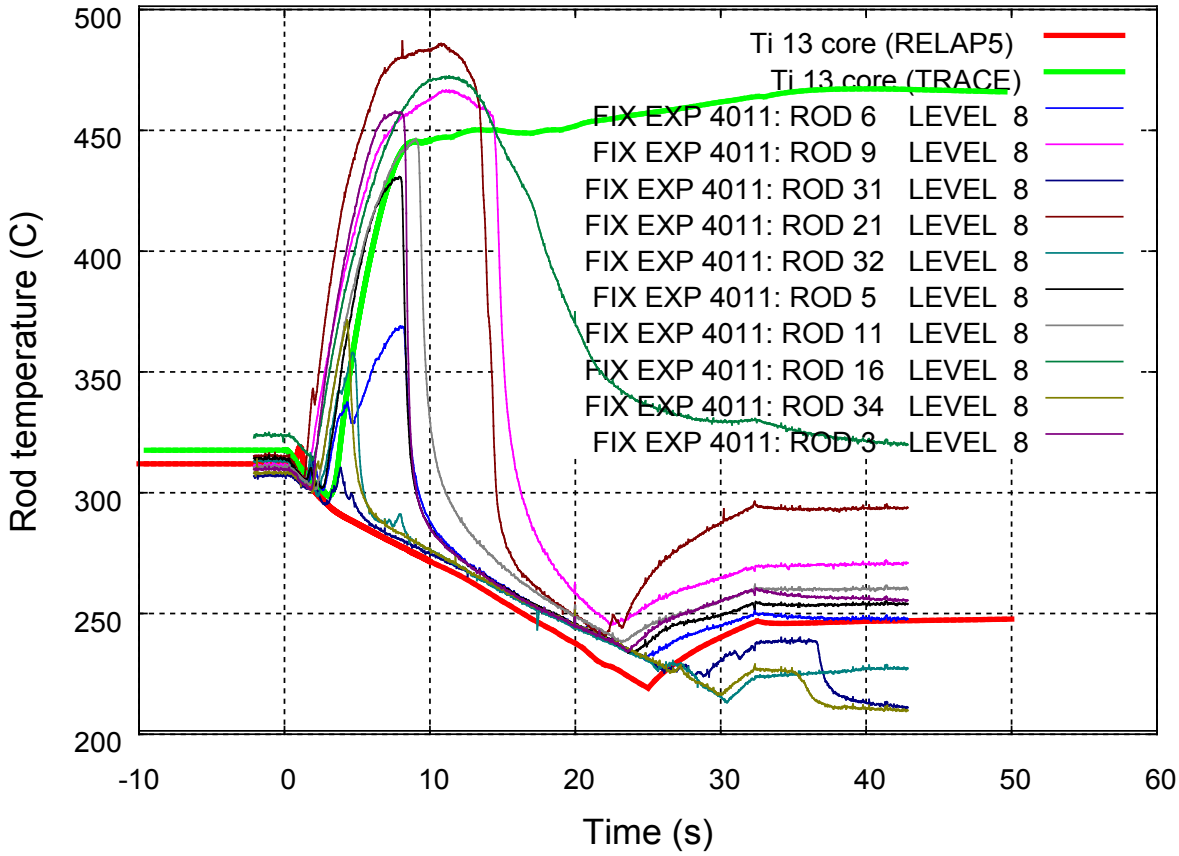

Figure B-11 Rod temperature at cell 13 level.

The heated rod is divided into 25 cells, cell 1 is at the bottom level and cell 25 is at the top of the core.

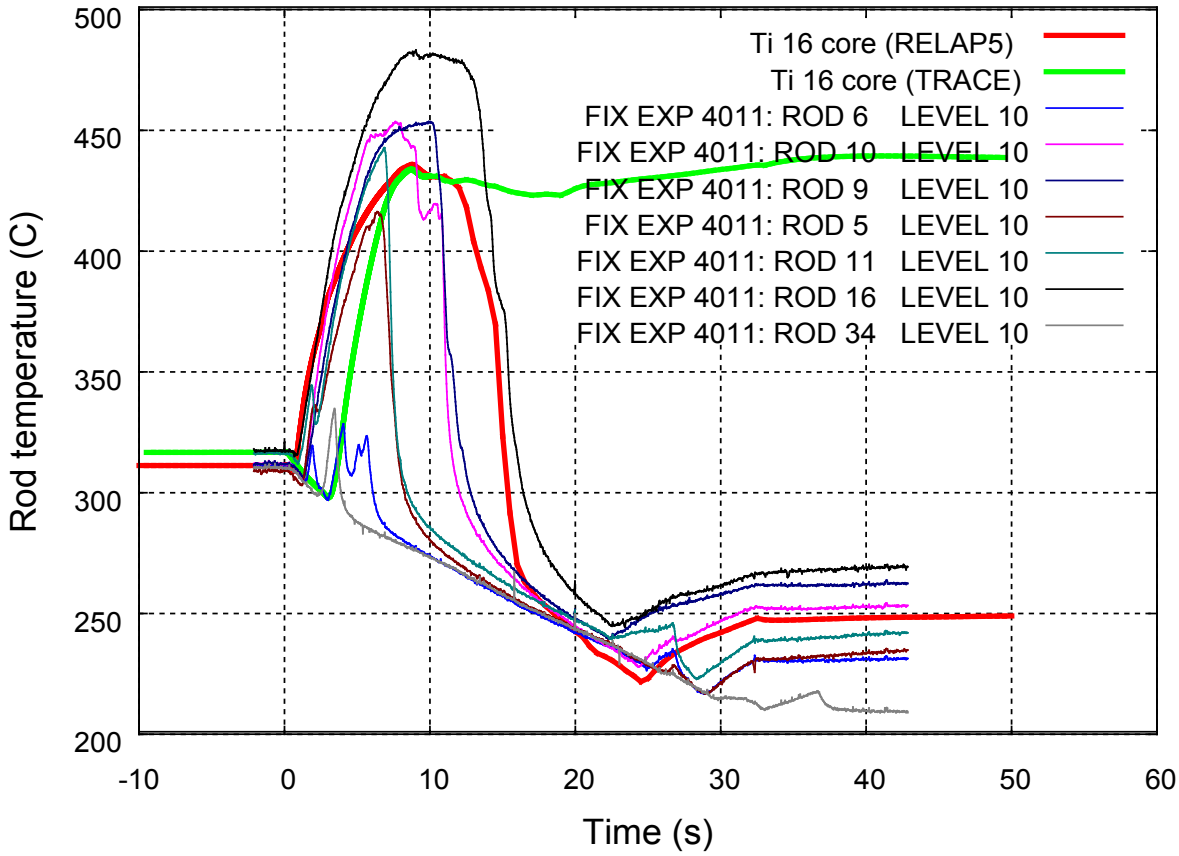

Figure B-12 Rod temperature at cell 16 level.

The heated rod is divided into 25 cells, cell 1 is at the bottom level and cell 25 is at the top of the core.

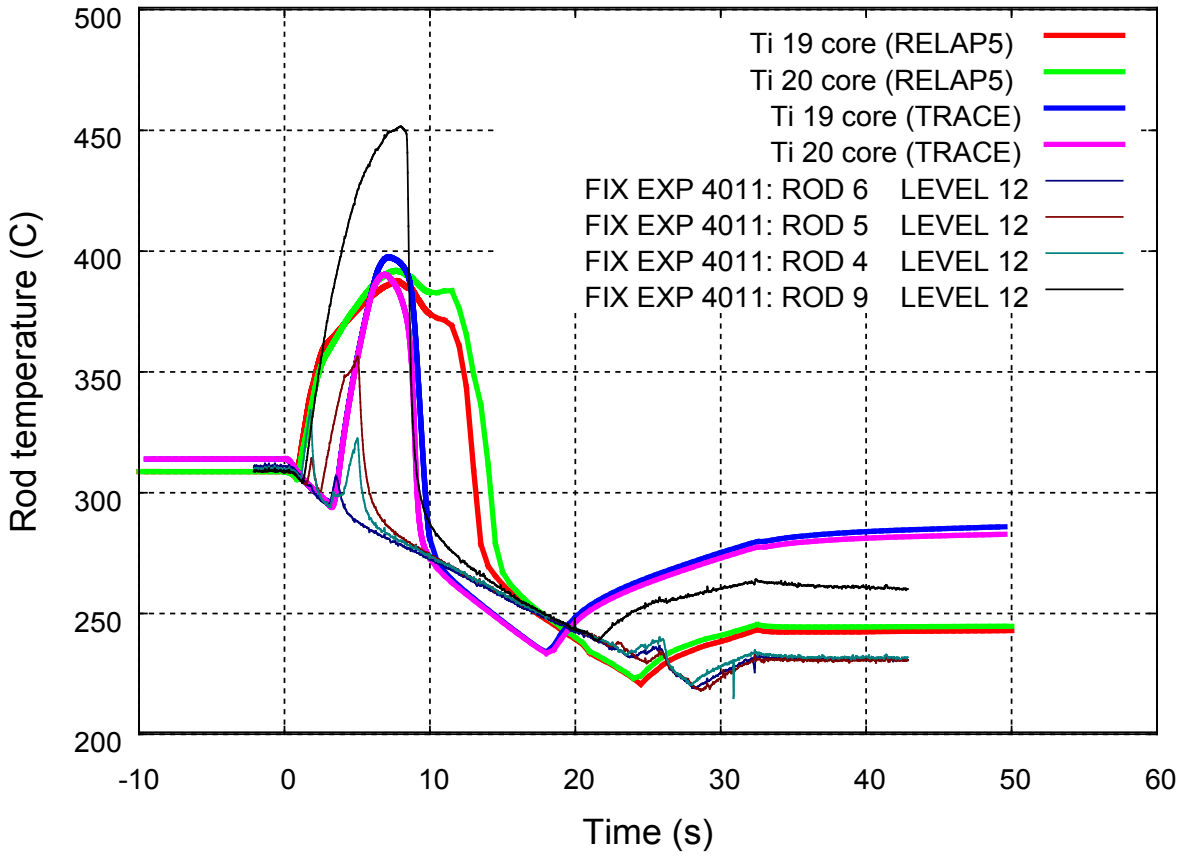

Figure B-13 Rod temperature at cell 19, 20 levels.

The heated rod is divided into 25 cells, cell 1 is at the bottom level and cell 25 is at the top of the core.

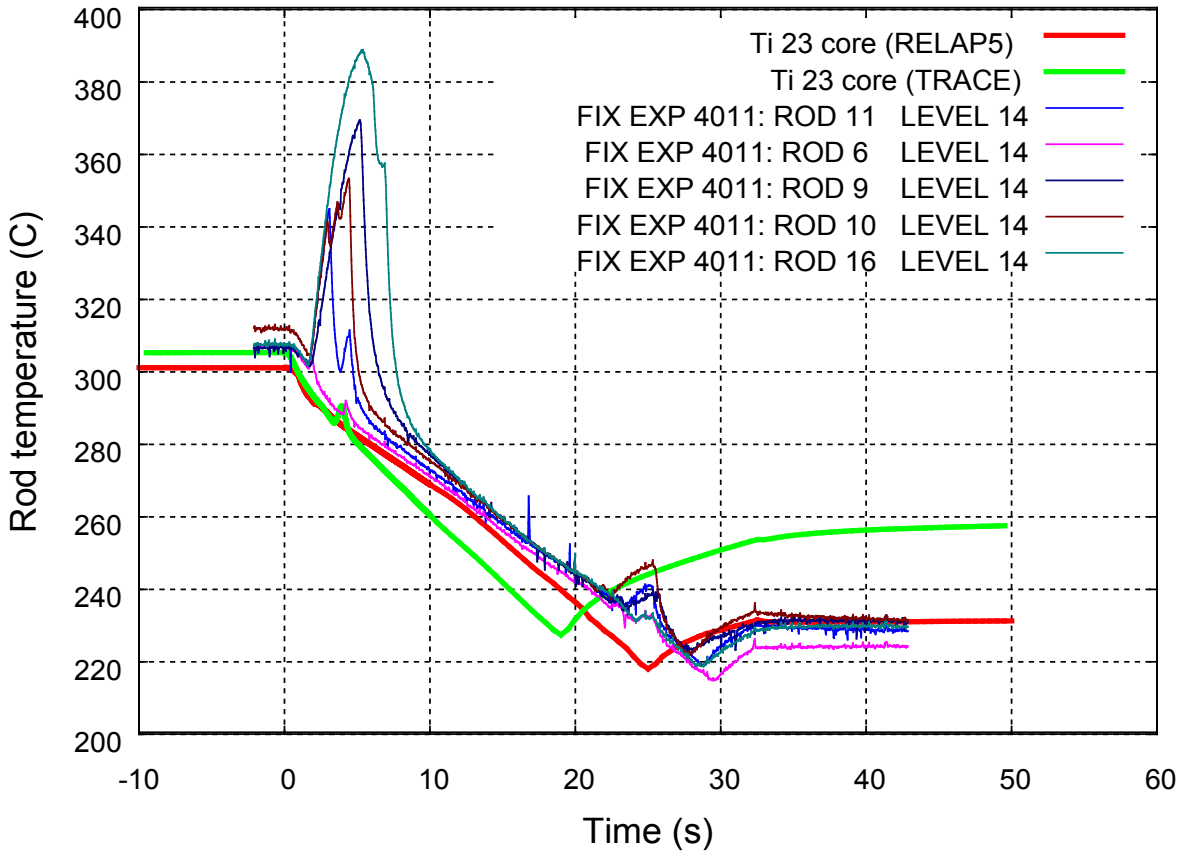

Figure B-14 Rod temperature at cell 23 level.

The heated rod is divided into 25 cells, cell 1 is at the bottom level and cell 25 is at the top of the core.

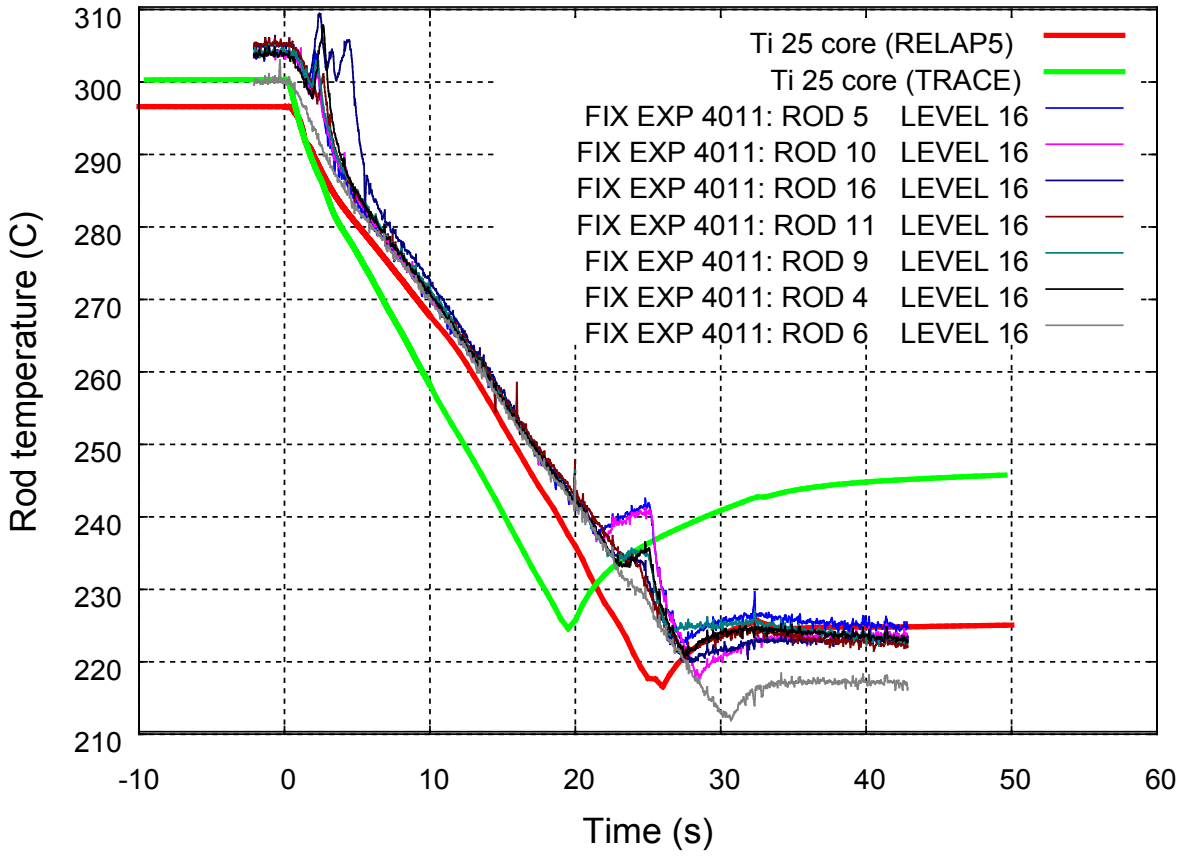

Figure B-15 Rod temperature at cell 25 level.

The heated rod is divided into 25 cells, cell 1 is at the bottom level and cell 25 is at the top of the core.

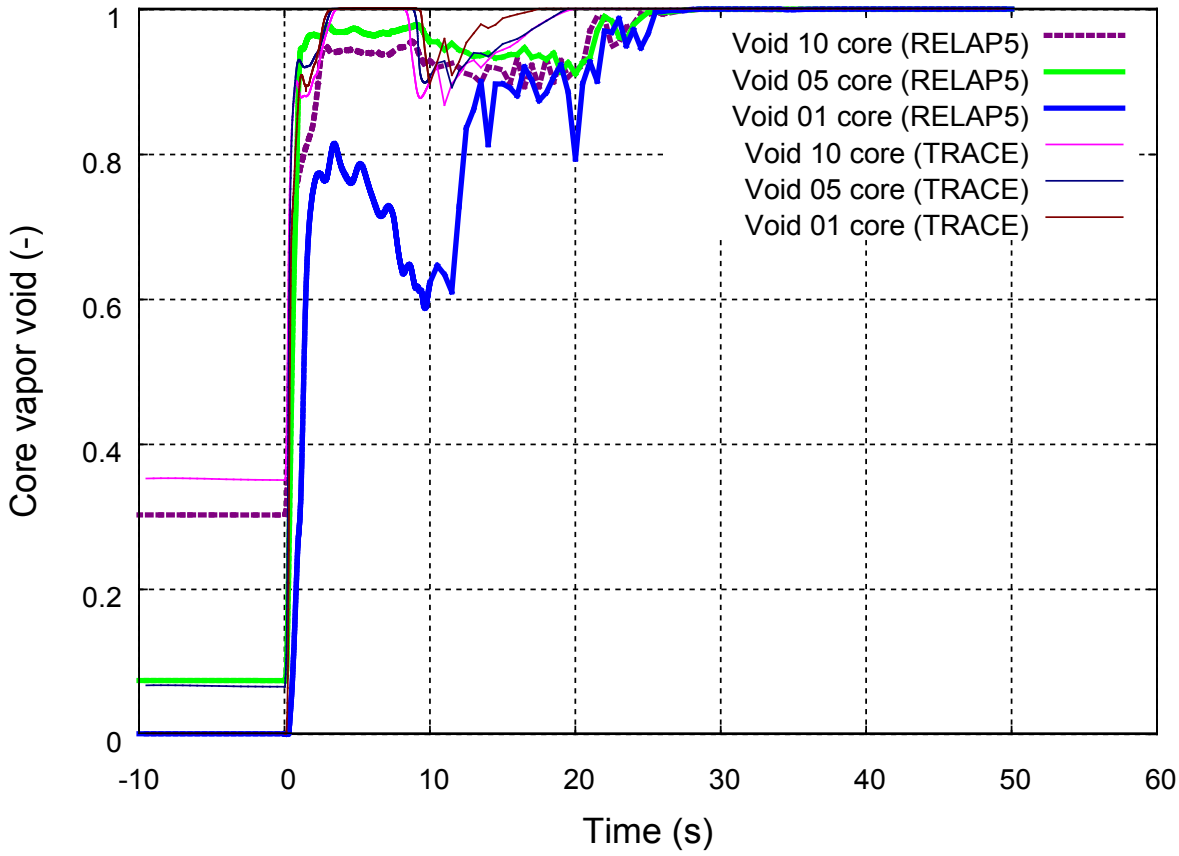

Figure B-16 Void distribution along the core at nodes 01, 10, 15.

The core is divided into 26 nodes, node 1 is at the bottom level and node 26 is at the top of the core.

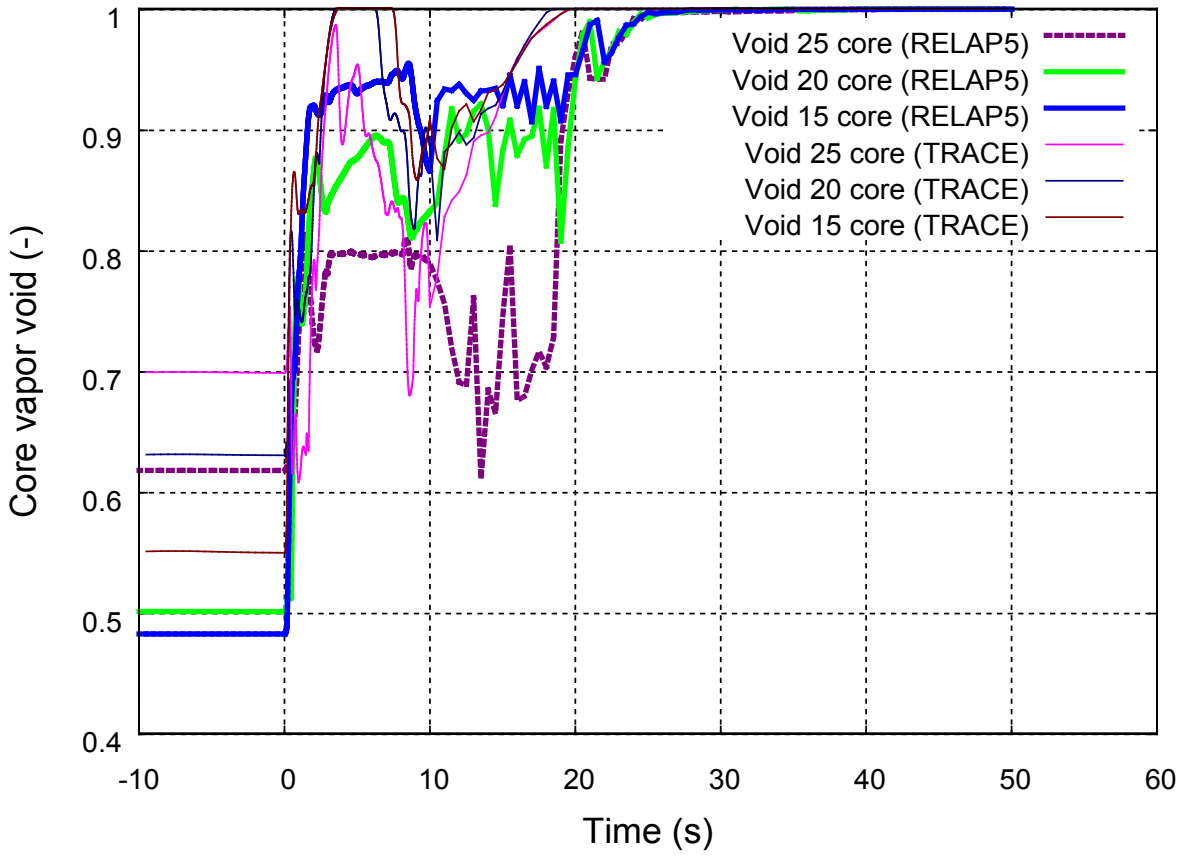

Figure B-17 Void distribution along the core at nodes 15, 20, 25.

The core is divided into 26 nodes, node 1 is at the bottom level and node 26 is at the top of the core.

APPENDIX C RESULT PLOTS OF FIX-II EXPERIMENT 3051

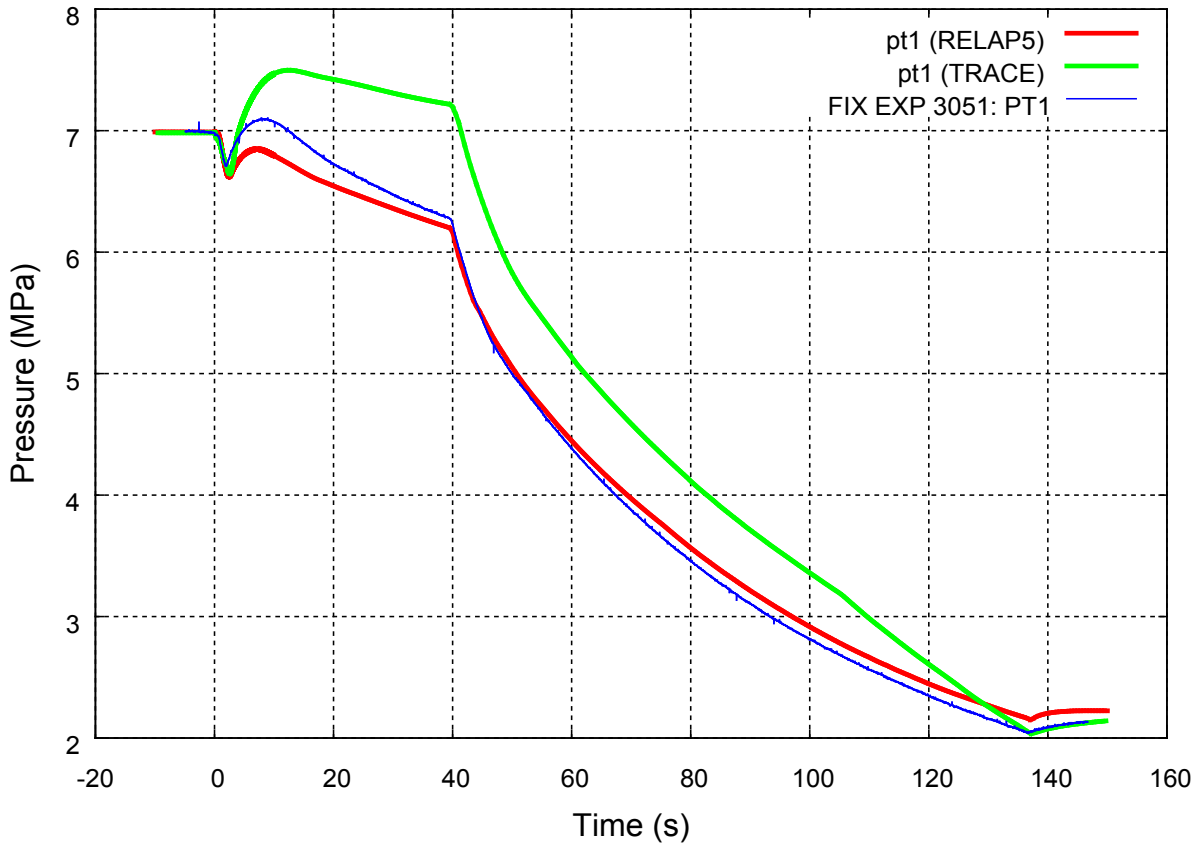

Figure C-1 Pressure in the steam dome.

The steam dome pressure dropped from 6.99 MPa to 6.7 MPa at 1.9 s. As the initial opening of the steam relief valve was closed almost simultaneously with the closing of the spray and feed water flows, the pressure increased again to a maximum of 7.1 MPa at 8.9 s in the experiment. The pressure decrease, caused by the relatively small bottom break, was then rather slow, until the steam relief valve opened a second time at 39.6 s, at which time the depressurization rate suddenly increased. The steam relief continued until the test was terminated.

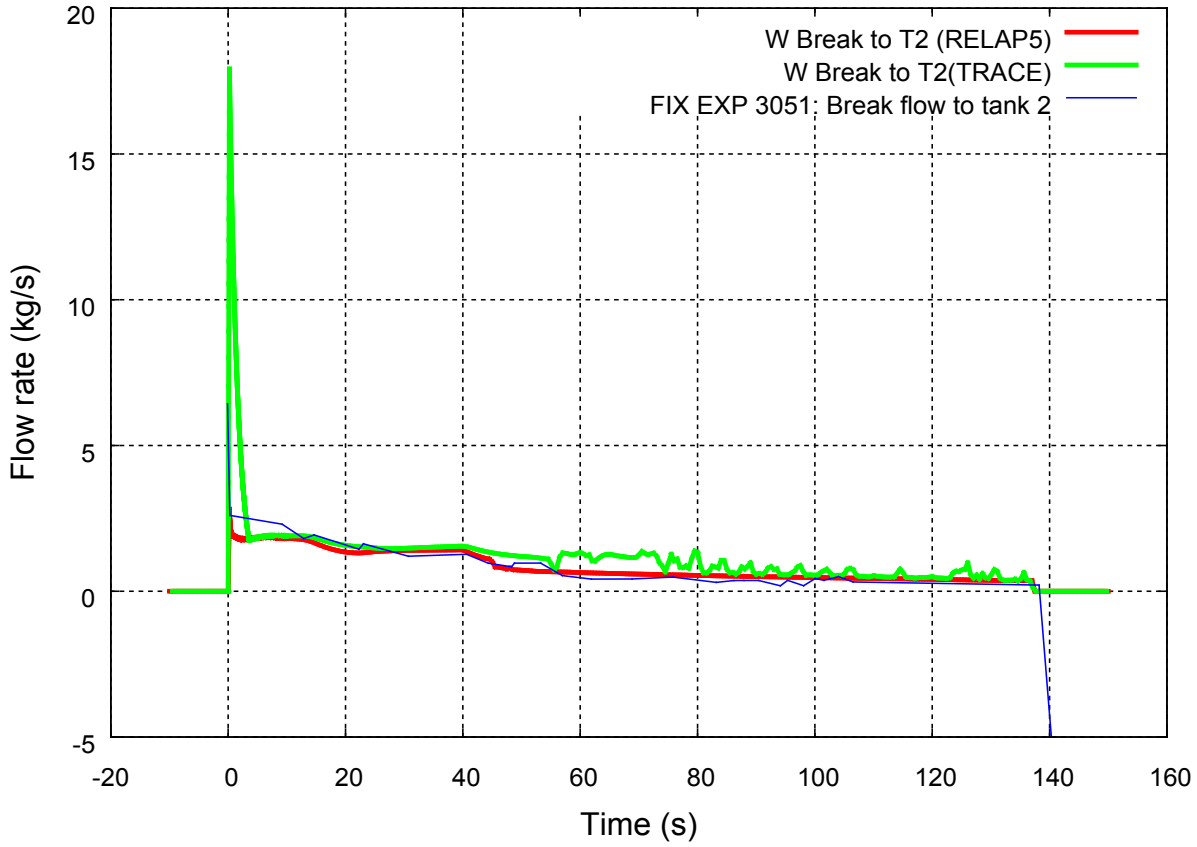

Figure C-2 Break mass flow rate into tank T2.

The break valve V120 (restriction nozzle I.D. 6.82 mm) started to open at 0 s. A maximum mass flow rate was obtained immediately after the valve opened.
Both the TRACE and RELAP5 analysis results are based on the critical flow model with both the subcooled and the two-phase discharge coefficient equal to 0.8. The used discharge coefficients reveal acceptable calculated flow rates compared to measured flow rates.

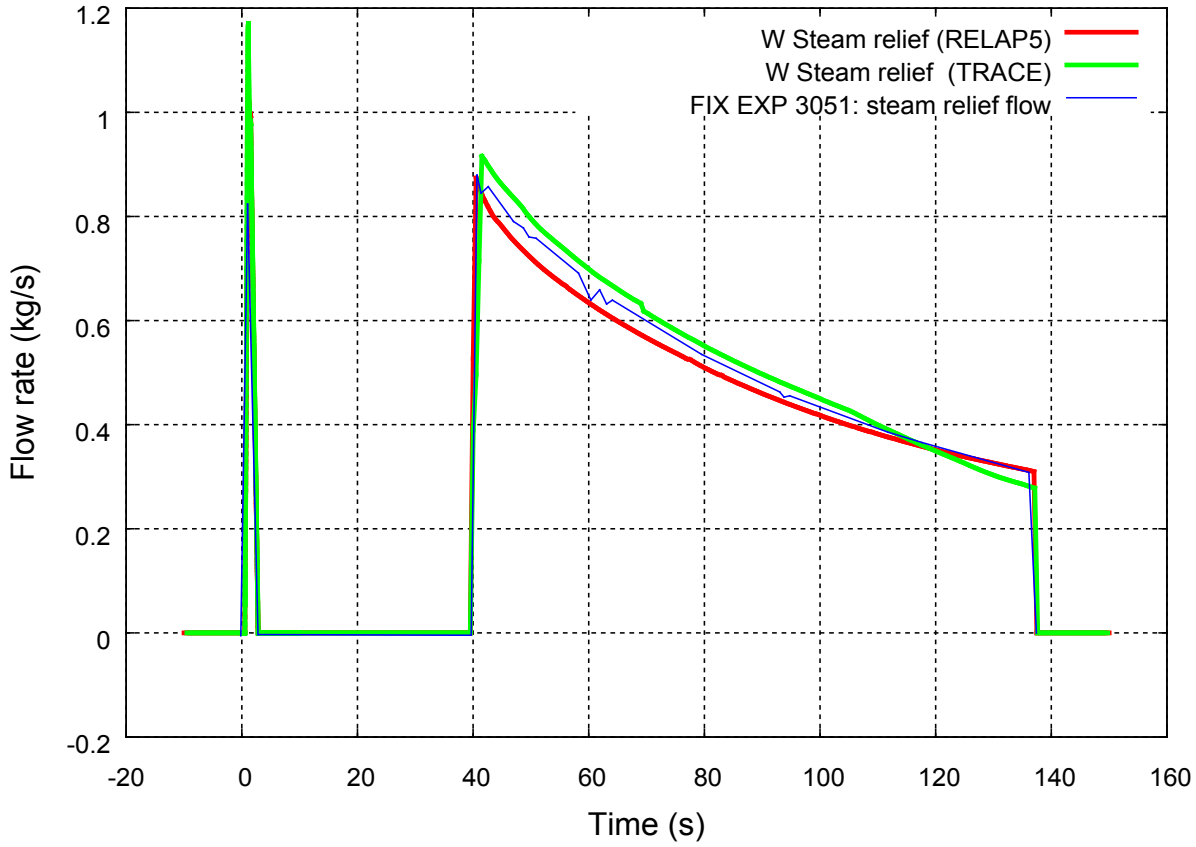

Figure C-3 Mass flow rate of steam through orifice meter K6 in the steam relief valve.

The steam relief valve (flow area 0.94 cm^2) started to open at 0.5 s, and closed soon after that, at 39.6 s it was opened again, and remained so for the rest of the test. A maximum mass flow rate of 0.83 kg/s was obtained in the experiment.

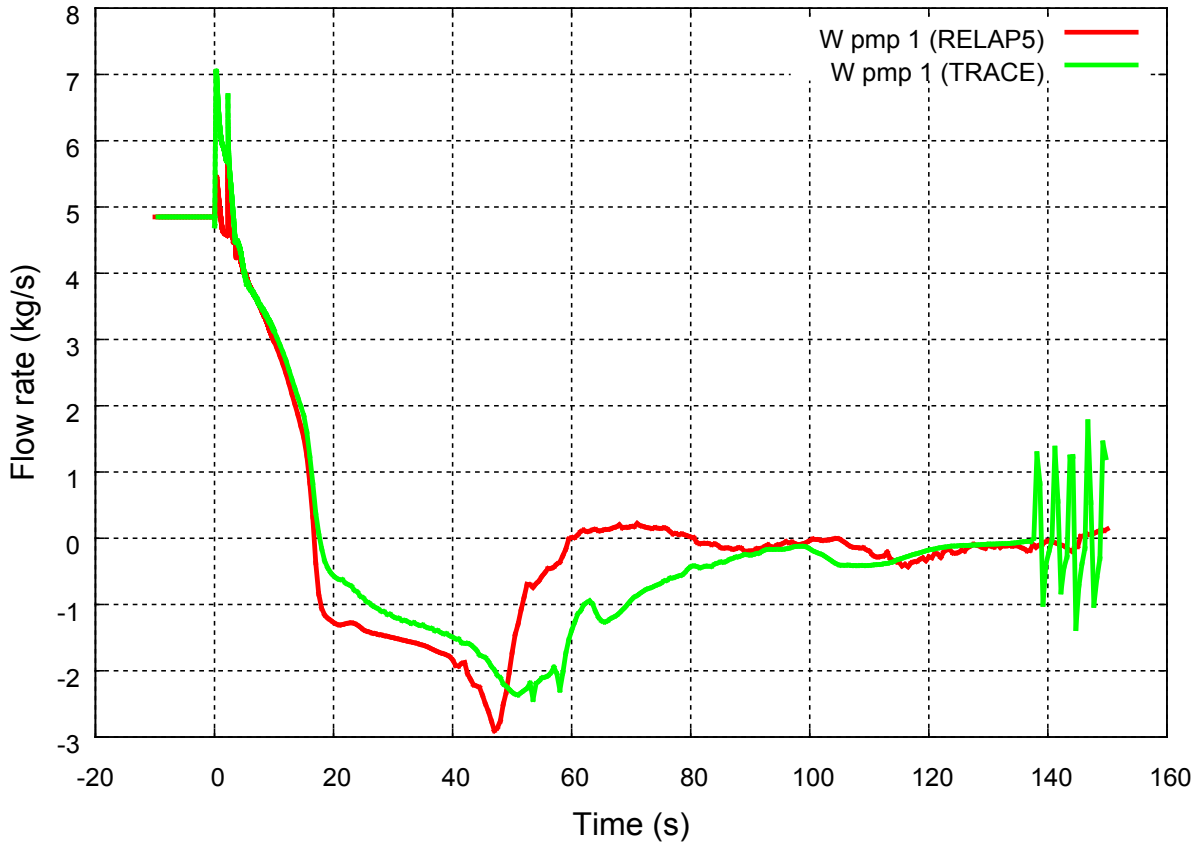

Figure C-4 Mass flow rate through pump 1 in the intact loop.

4.85 kg/s in steady state. The speed of the main recirculation pump P1 is controlled by the control system to reproduce the measured mass flows.

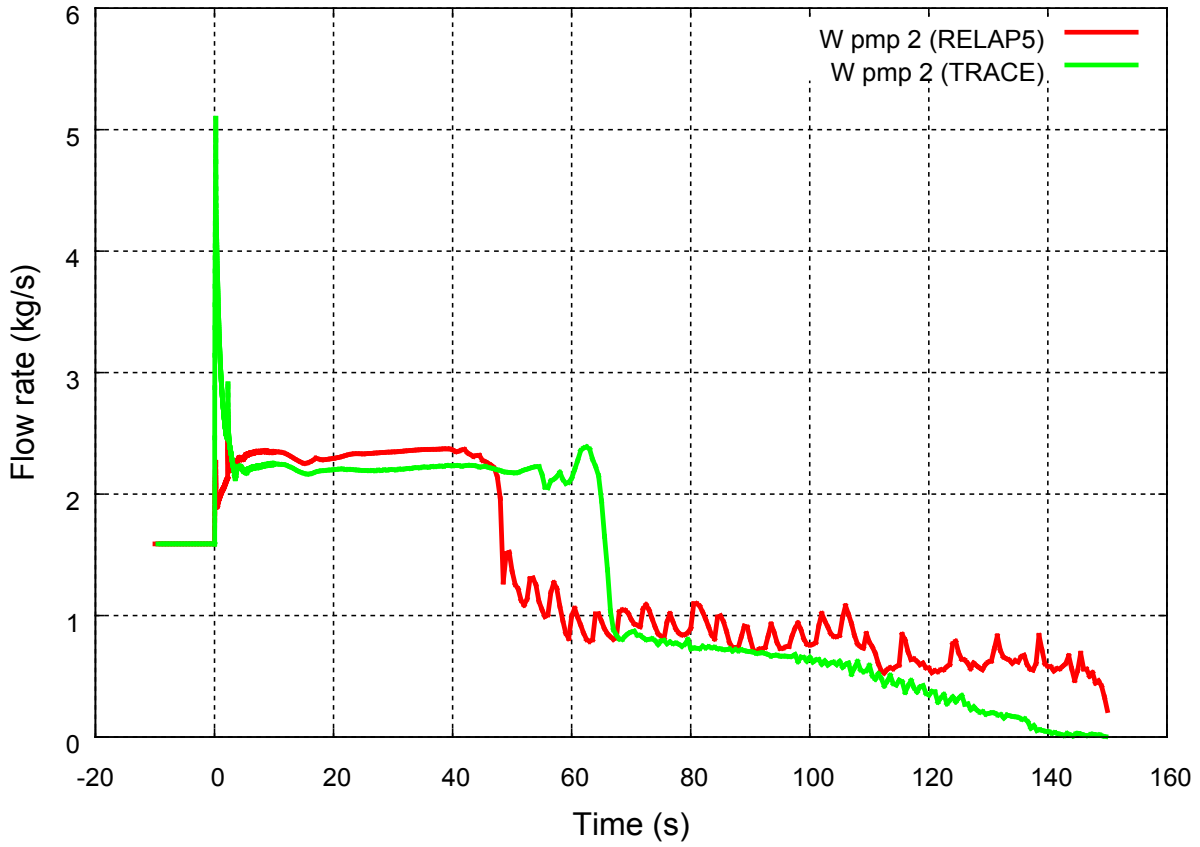

Figure C-5 Mass flow rate through pump 2 in the break pipe line.

1.59 kg/s in steady state. The speed of the main recirculation pump P2 is controlled by the control system to reproduce the measured mass flows.

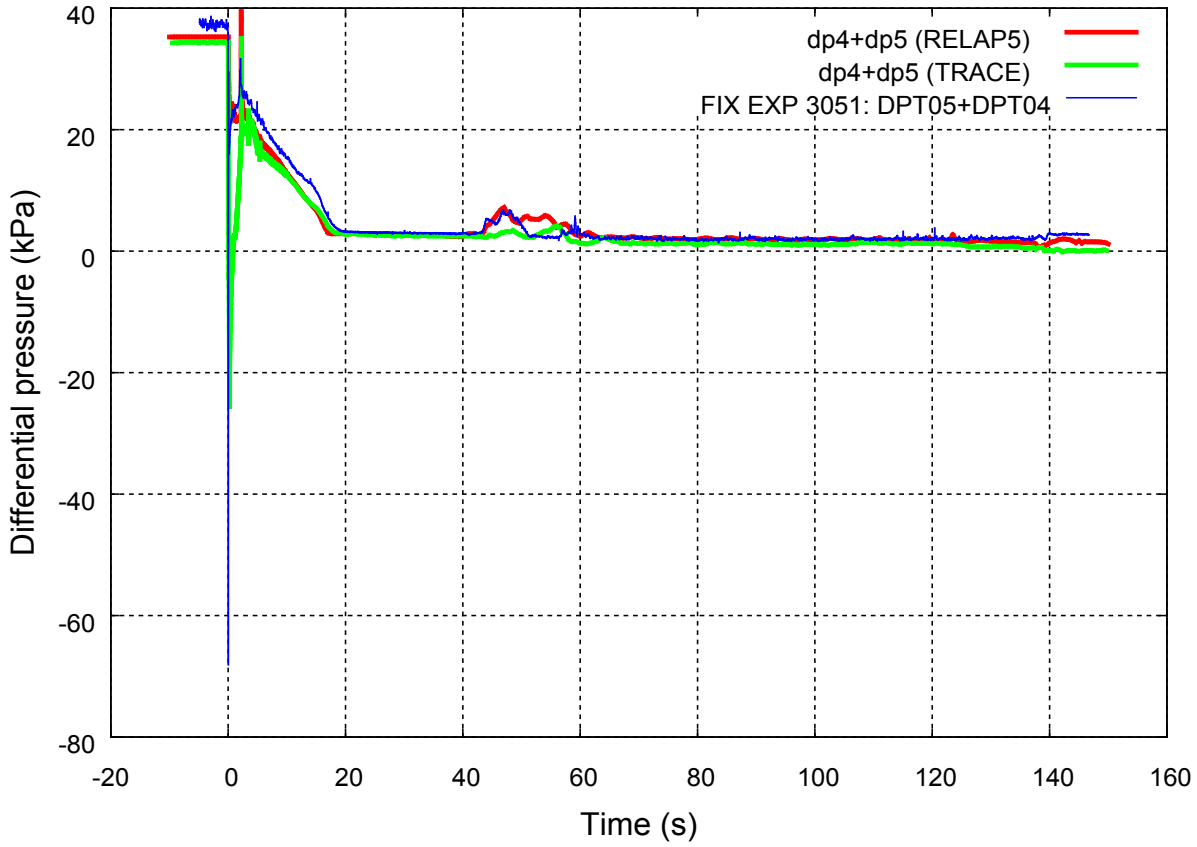

Figure C-6 Differential pressure over the bundle inlet restriction.

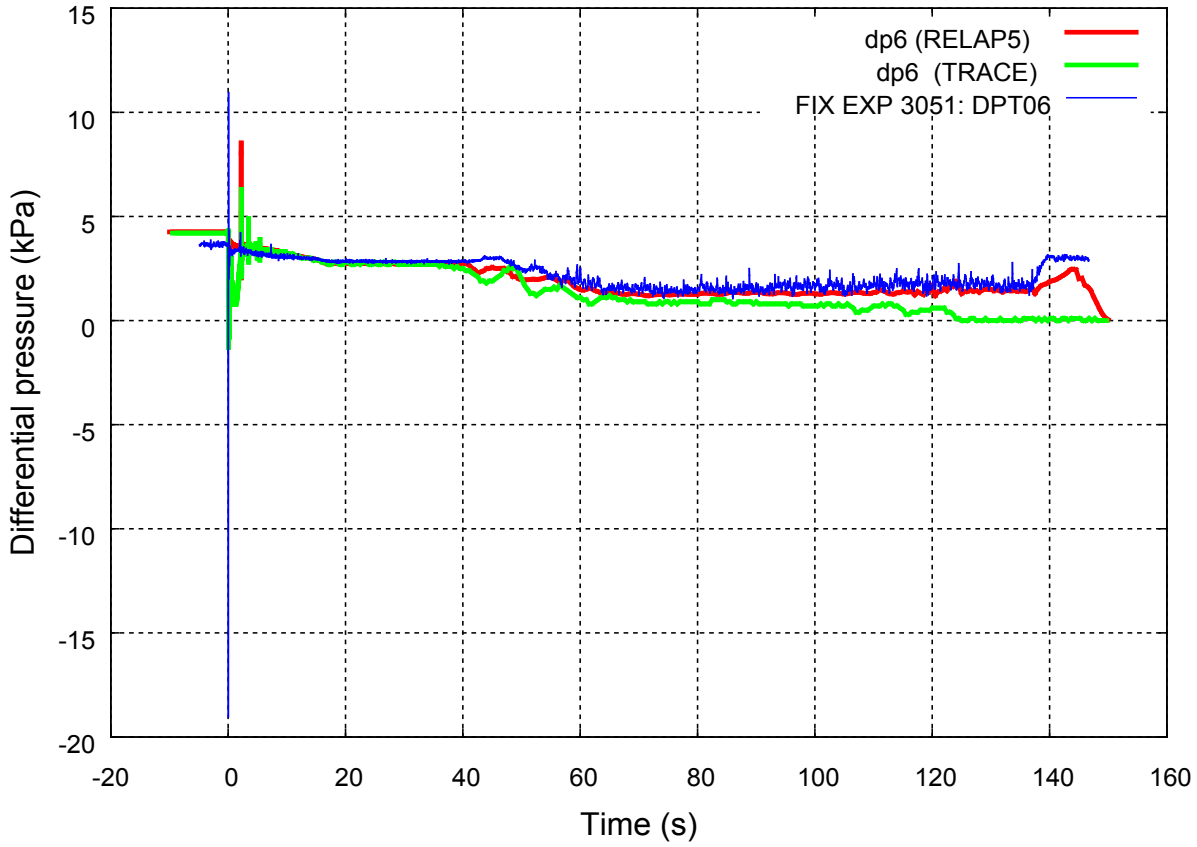

Figure C-7 Differential pressure over subdivisions in the lower part of the bundle.

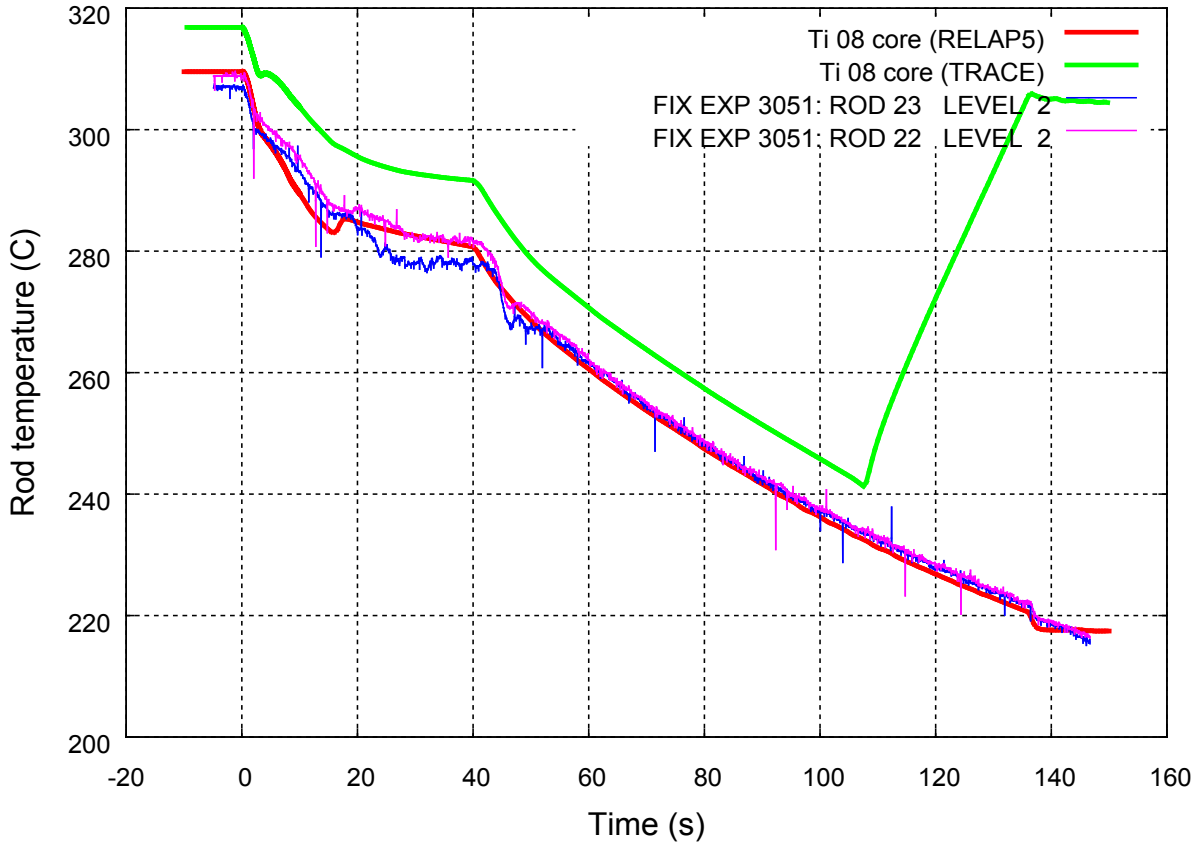

Figure C-8 Rod temperature at cell 8 level.

The heated rod is divided into 46 cells, cell 1 is at the bottom level and cell 46 is at the top of the core.

Since the total loss of water was comparatively small there was never any uncovery of the rod bundle during the blowdown period in the experiment and consequently no heat up of the rods. The RELAP5 could predict the rod temperature profile very well, while the TRACE got somehow slightly higher temperature already at steady state and predicted even a dry out along the whole rod length in the core during the last period of the transient. The reason is described in chapter 4.3.

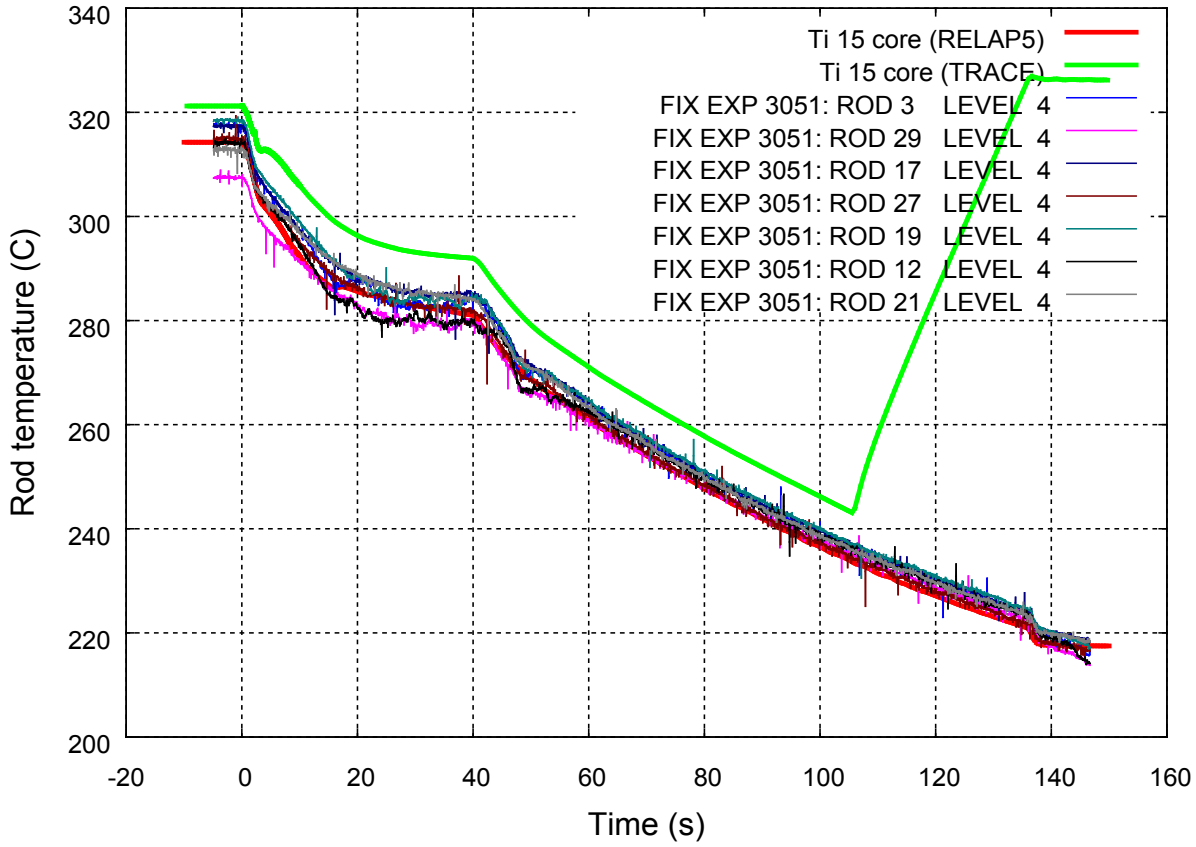

Figure C-9 Rod temperature at cell 15 level.

The heated rod is divided into 46 cells, cell 1 is at the bottom level and cell 46 is at the top of the core.

See comments in Figure C-8.

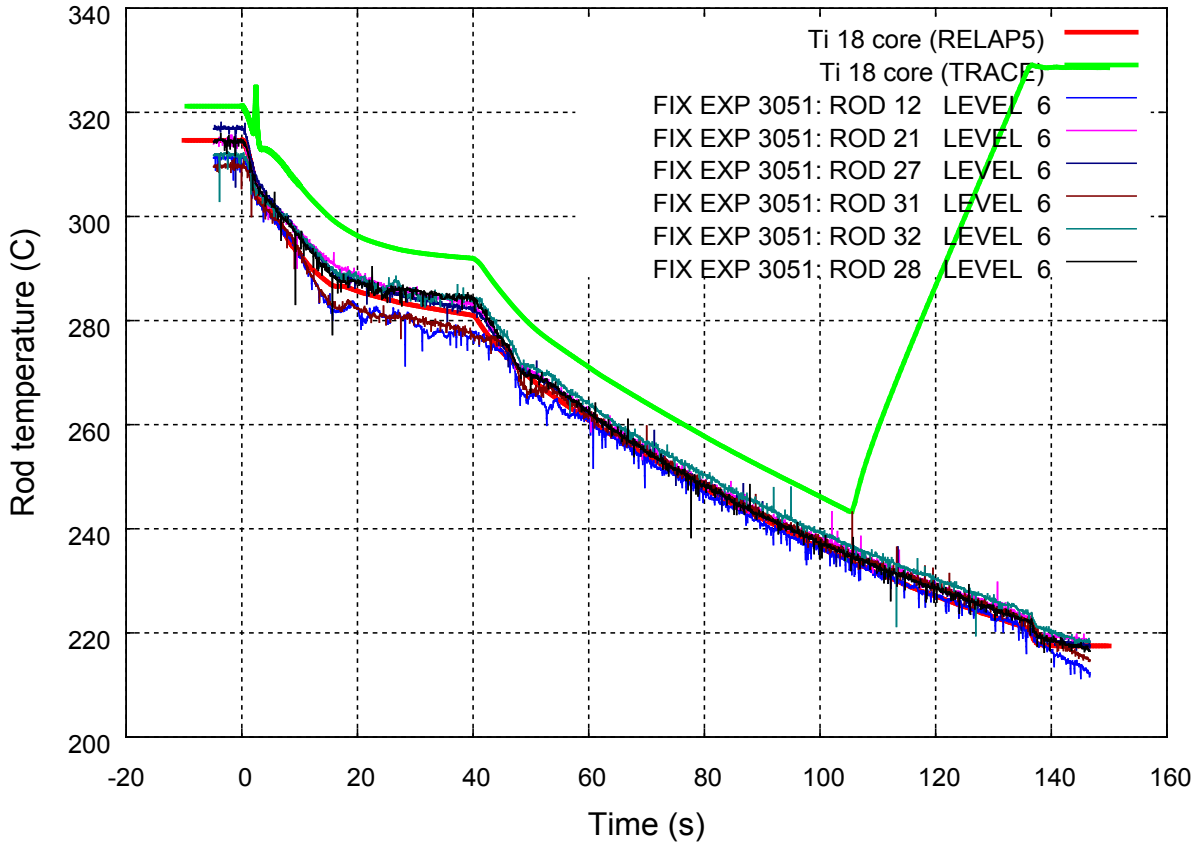

Figure C-10 Rod temperature at cell 18 level.

The heated rod is divided into 46 cells, cell 1 is at the bottom level and cell 46 is at the top of the core.

See comments in Figure C-8.

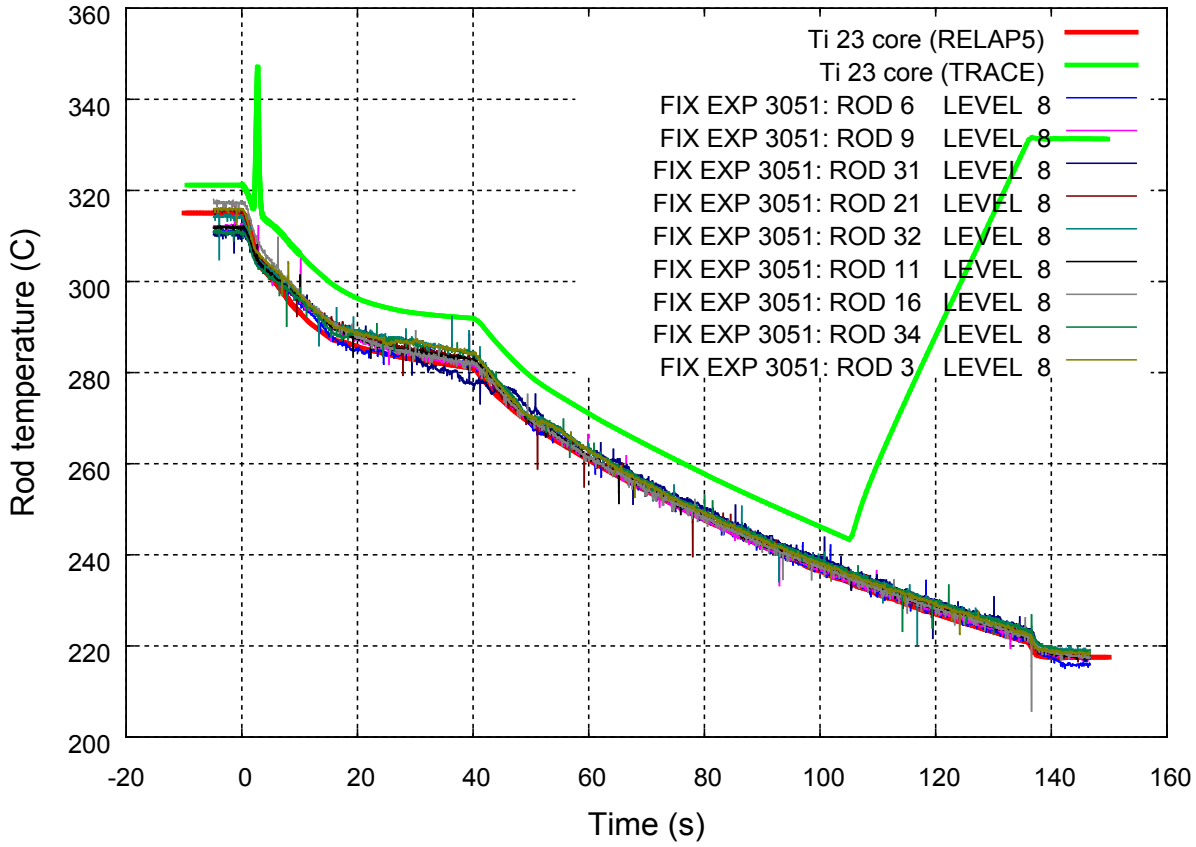

Figure C-11 Rod temperature at cell 23 level.

The heated rod is divided into 46 cells, cell 1 is at the bottom level and cell 46 is at the top of the core.

See comments in Figure C-8.

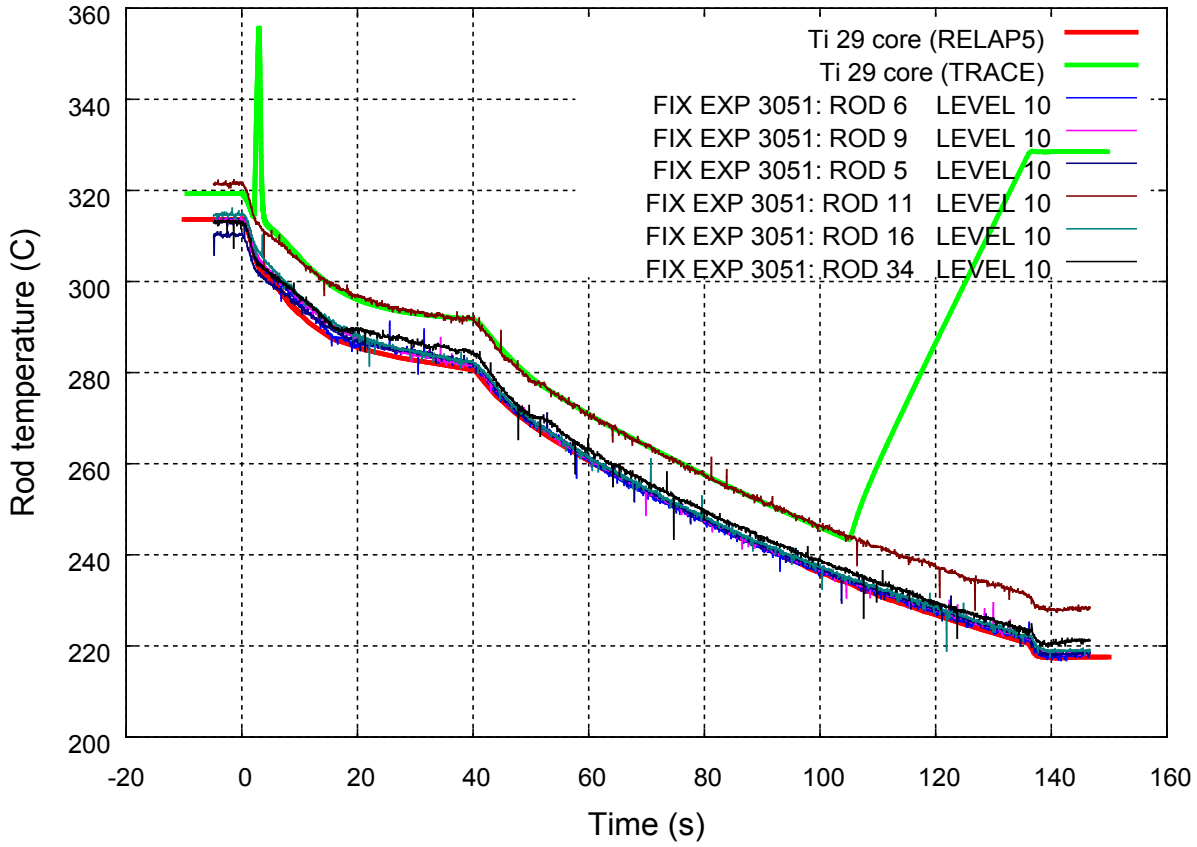

Figure C-12 Rod temperature at cell 29 level.

The heated rod is divided into 46 cells, cell 1 is at the bottom level and cell 46 is at the top of the core.

See comments in Figure C-8.

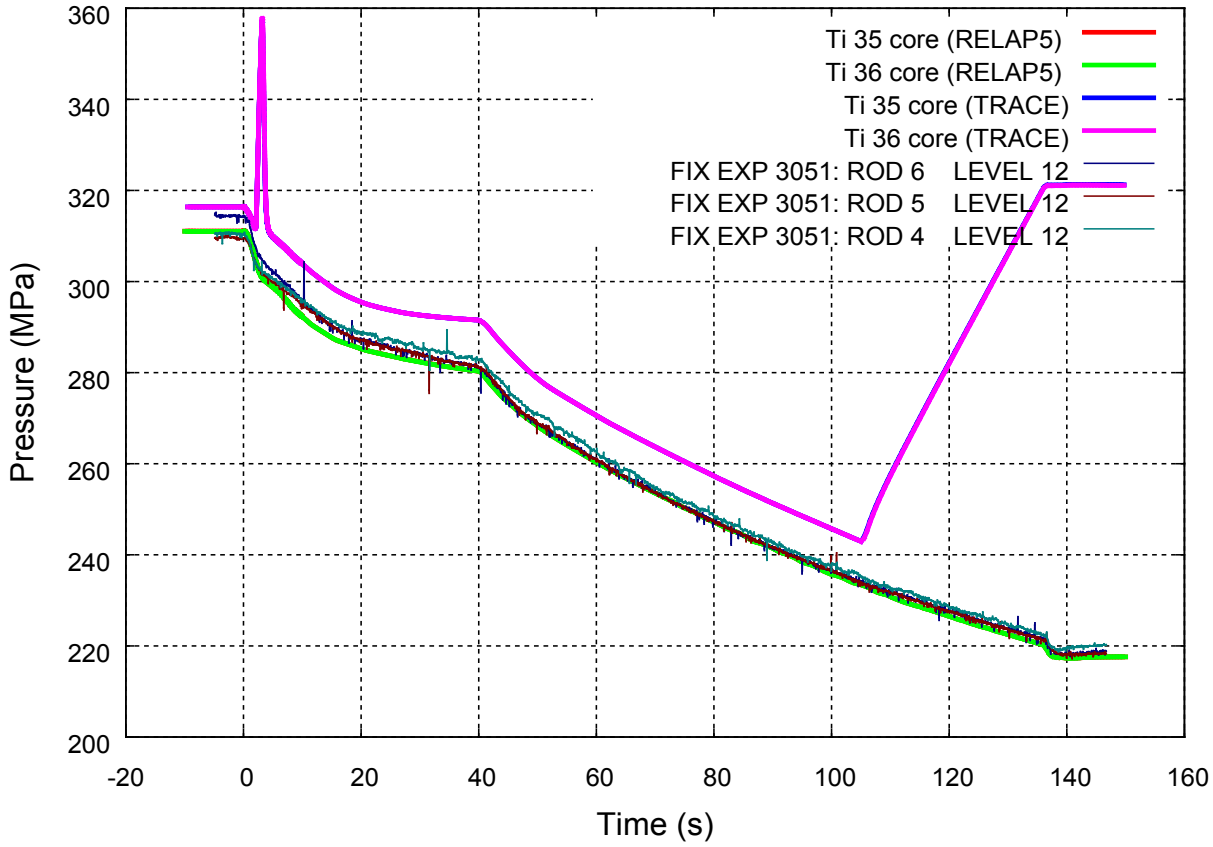

Figure C-13 Rod temperature at cell 35, 36 levels.

The heated rod is divided into 46 cells, cell 1 is at the bottom level and cell 46 is at the top of the core.

See comments in Figure C-8.

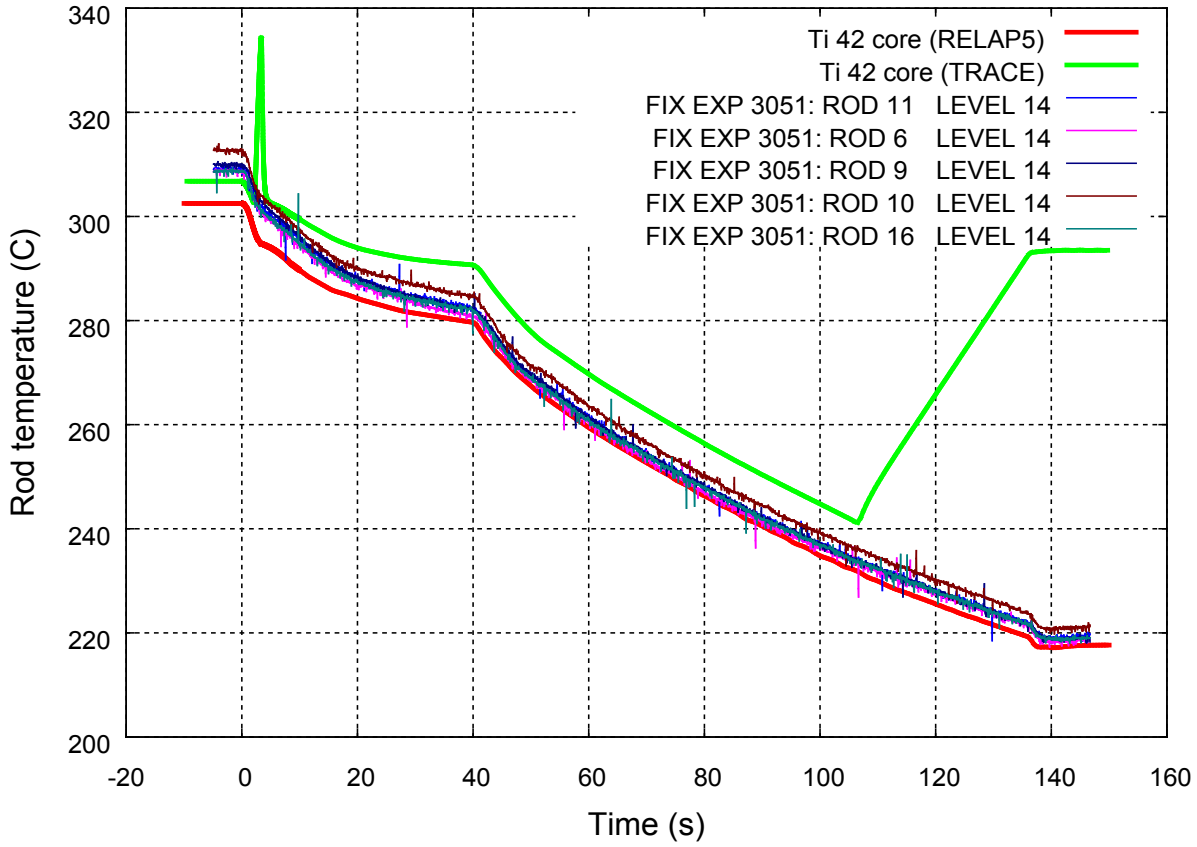

Figure C-14 Rod temperature at cell 42 level.

The heated rod is divided into 46 cells, cell 1 is at the bottom level and cell 46 is at the top of the core.

See comments in Figure C-8.

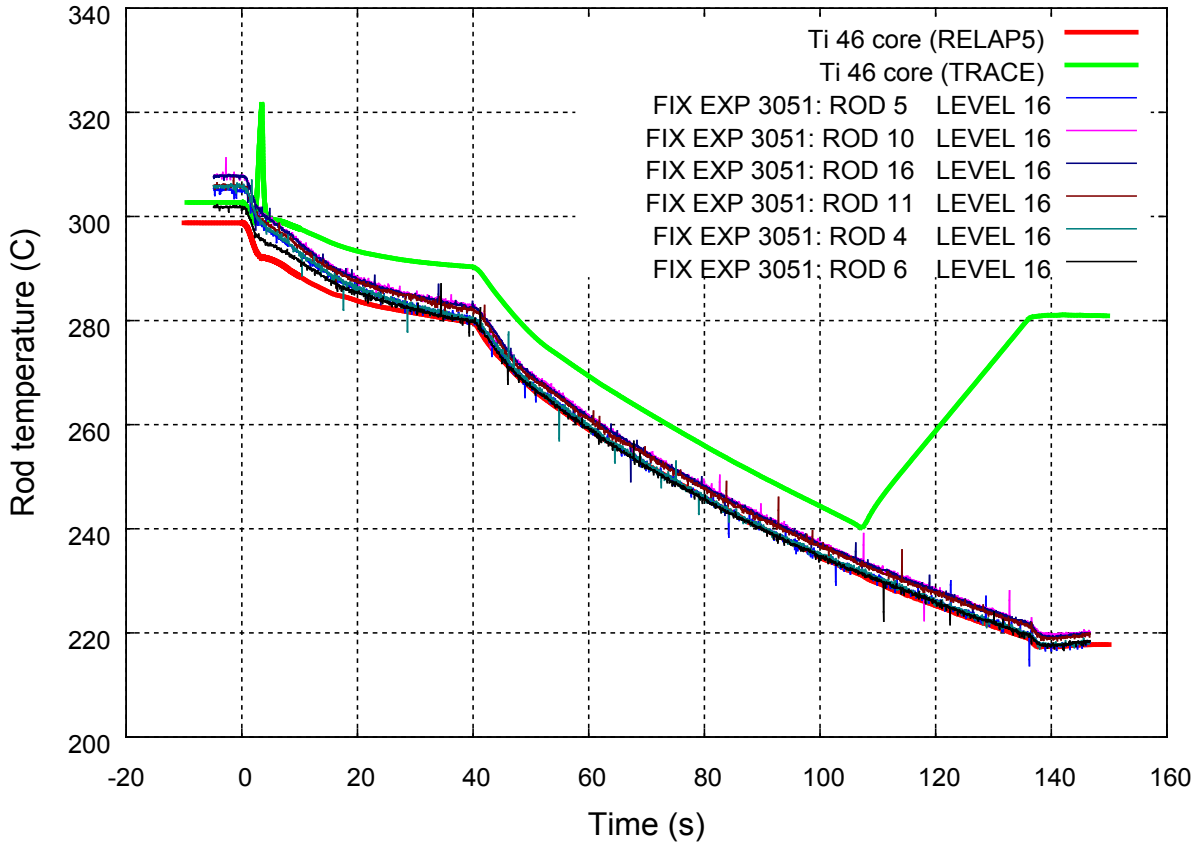

Figure C-15 Rod temperature at cell 46 level.

The heated rod is divided into 46 cells, cell 1 is at the bottom level and cell 46 is at the top of the core.

See comments in Figure C-8.

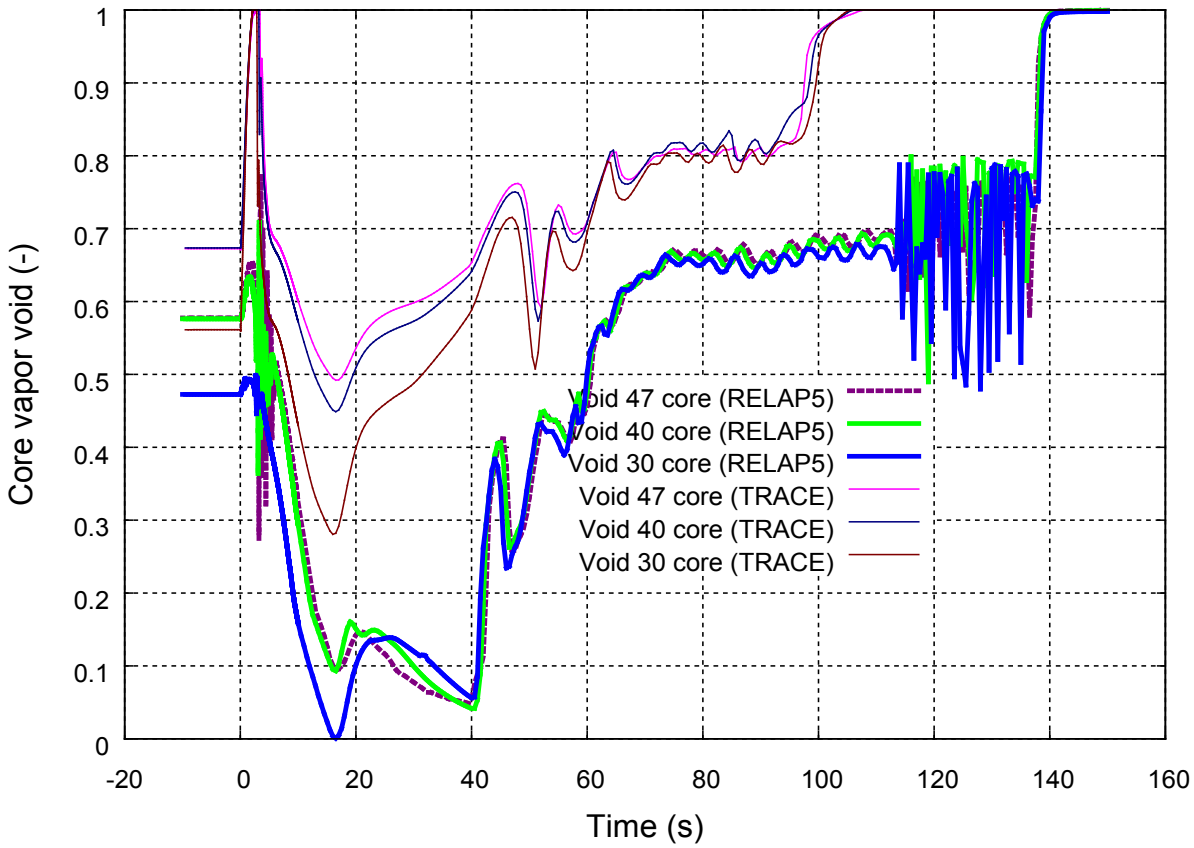

Figure C-16 Void distribution along the core at nodes 30, 40, 47.

The core is divided into 47 nodes, node 1 is at the bottom level and node 47 is at the top of the core.

TRACE analysis showed a more significant void increase along the whole length of the core in comparison to the RELAP5 results, and this is one of the reasons why TRACE predicted the rod dryout.

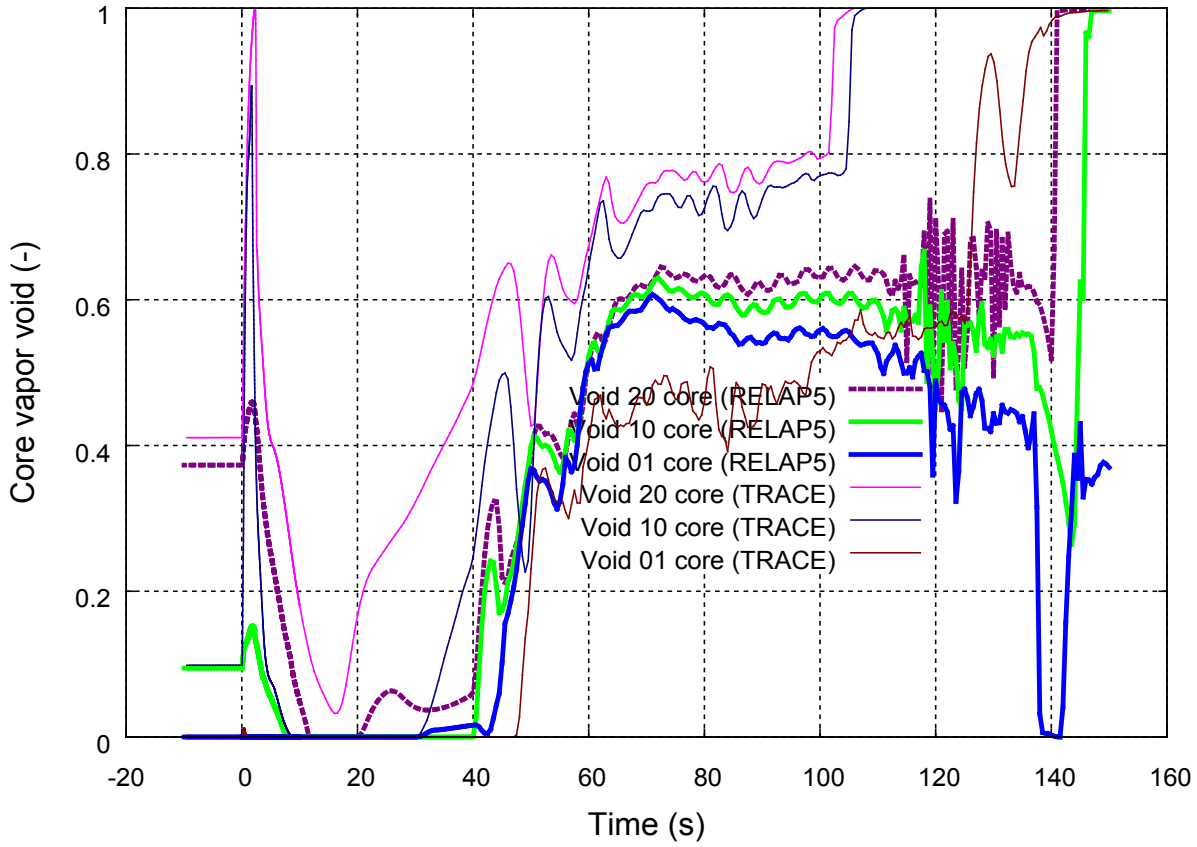

Figure C-17 Void distribution along the core at nodes 01, 10, 20.

The core is divided into 47 nodes, node 1 is at the bottom level and node 47 is at the top of the core.

TRACE analysis showed a more significant void increase along the whole length of the core in comparison to the RELAP5 results, and this is one of the reasons why TRACE predicted the rod dryout.

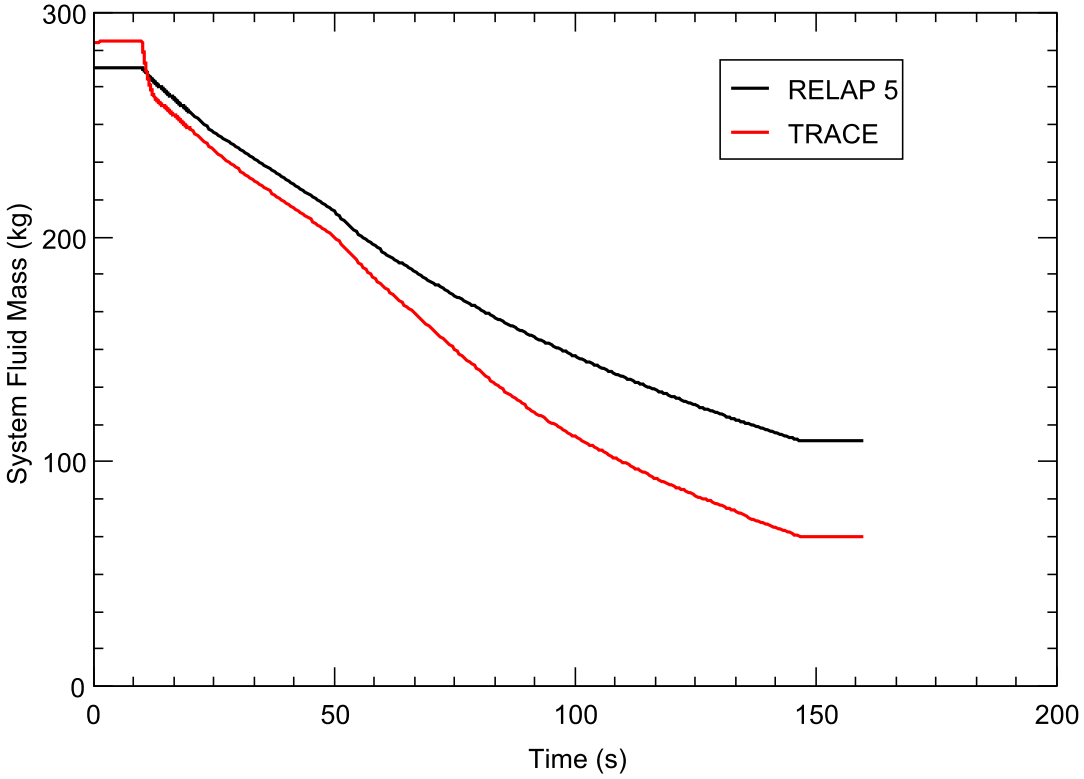

Figure C-18 The total fluid mass in the whole system.

TRACE predicted more mass inventory during the steady state, and it also lost more mass through the break and the steam relief line compared to the RELAP5 results. This is one of the reasons why TRACE predicted a higher rod temperature and even a dryout.

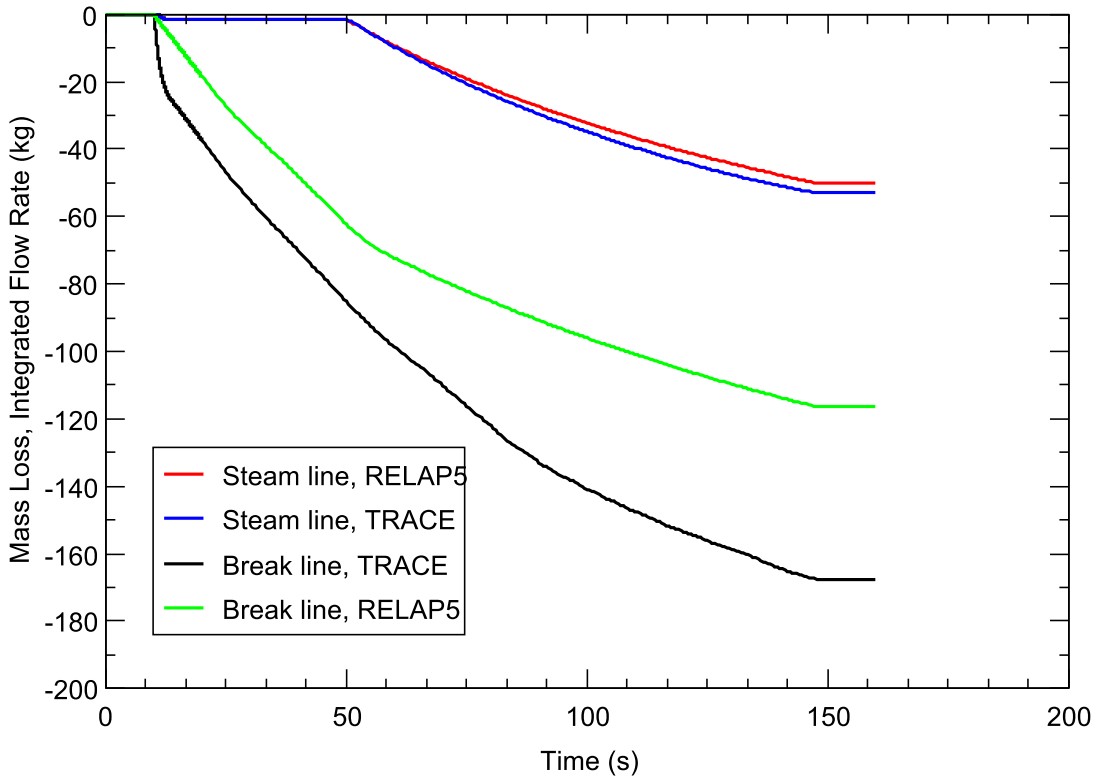

Figure C-19 The total fluid mass loss through the break and the steam relief line.

TRACE results showed that more mass was lost through the break and the steam relief line compared to the RELAP5 results. This is one of the reasons why TRACE predicted a higher rod temperature and even a dryout.

NRC FORM 335
(12-2010)
NRCMD 3.7

U.S. NUCLEAR REGULATORY COMMISSION

BIBLIOGRAPHIC DATA SHEET

(See instructions on the reverse)

1. REPORT NUMBER
(Assigned by NRC, Add Vol., Supp., Rev., and Addendum Numbers, if any.)

NUREG/IA-0415

2. TITLE AND SUBTITLE

TRACE (V 5.0 Patch 2) validation based on the RELAP5-calculation of FIX-II LOCA experiments No. 5052, 4011, 3051

3. DATE REPORT PUBLISHED

MONTH	YEAR
October	2014

4. FIN OR GRANT NUMBER

5. AUTHOR(S)

S. ChunHong Sheng

6. TYPE OF REPORT

Technical

7. PERIOD COVERED (Inclusive Dates)

8. PERFORMING ORGANIZATION - NAME AND ADDRESS (If NRC, provide Division, Office or Region, U. S. Nuclear Regulatory Commission, and mailing address; if contractor, provide name and mailing address.)

Studsvik Nuclear AB
SE-61182 Nyköping
Sweden

9. SPONSORING ORGANIZATION - NAME AND ADDRESS (If NRC, type "Same as above", if contractor, provide NRC Division, Office or Region, U. S. Nuclear Regulatory Commission, and mailing address.)

Division of Systems Analysis
Office of Nuclear Regulatory Research
U.S. Nuclear Regulatory Research
Washington, DC 20555-0001

10. SUPPLEMENTARY NOTES

11. ABSTRACT (200 words or less)

The purpose of this project is to (i) evaluate the functionality of the SNAP capability to convert RELAP5 input files to corresponding TRACE input, and (ii) to validate the TRACE code against selected FIX-II experiments where the blowdown phase of large and small break LOCA is the main focus.

More specifically, the TRACE Version 5.0 Patch 2 code is validated against the FIX-II experiments, where the input is obtained by converting a legacy RELAP5 FIX-II model by means of SNAP, possibly accompanied by additional manual adjustments. All FIX-II components in the RELAP5 model are retained after being converted to TRACE. Three transients (FIX 5052, 4011 and 3051) are analyzed. The TRACE analysis results are compared with experimental data and with previously obtained results from analyses made with the RELAP5/MOD3.3 Patch 03 model.

This work has been performed with financial support from the Swedish Radiation Safety Authority.

12. KEY WORDS/DESCRIPTORS (List words or phrases that will assist researchers in locating the report.)

SNAP
RELAP5
TRACE
LOCA
Swedish Radiation Safety Authority
Studsvik
Swedish BWR Oskarshamn 2
Code Applications and Maintenance Program (CAMP)
SSM

13. AVAILABILITY STATEMENT

unlimited

14. SECURITY CLASSIFICATION

(This Page)
unclassified

(This Report)
unclassified

15. NUMBER OF PAGES

16. PRICE

Federal Recycling Program

UNITED STATES
NUCLEAR REGULATORY COMMISSION
WASHINGTON, DC 20555-0001

OFFICIAL BUSINESS

NUREG/IA-0415 TRACE (V 5.0 Patch 2) Validation Based on the RELAP5-Calculation of FIX-II LOCA Experiments NO. 5052, 4011, 3051 October 2014